Addis Ababa University
Addis Ababa Institute of Technology

School of Graduate Studies
School of Civil and Environmental Engineering

Assessment of Climate Change Impact on Surface Water Resource Availability of Sibilu River Catchment,Upper Abbay Basin, Ethiopia.

By: Alemayehu Mamo Burayu

Advisor: Yilma S. (Professor)

A Thesis Submitted to the School of Civil and Environmental Engineering of AAiT in Partial Fulfillment of the Requirements for the Degree of Master of Science in Hydraulic Engineering

June, 2024

The undersigned have examined the thesis entitled “Assessment of Climate Change Impact on Surface Water Resource Availability of Sibilu River Catchment, Upper Abbay Basin, Ethiopia” presented by Alemayehu Mamo Burayu, a candidate for the degree of Master of Science, and hereby certify that it is worthy of acceptance.

Professor. Yilma Seleshi		
Advisor	**Signature**	**Date**
Interna Examiner	**Signature**	**Date**
External Examiner	**Signature**	**Date**
Chairperson	**Signature**	**Date**

CERTIFICATION

I, the undersigned, certify that I read and hear by recommend for acceptance by Addis Ababa University a thesis entitled “Assessment of Climate Change Impact on Surface Water Resource Availability of Sibilu River Catchment, Upper Abbay Basin, Ethiopia” in partial fulfillment the requirement for the degree of Master Science in Civil Engineering (Major Hydraulic Engineering).

Professor Yilma Seleshi (Advisor)

DECLARATION

I, **Alemayehu Mamo Burayu**, declare that this thesis is my own original work and that it has not been presented and will not be presented to any other University for a similar or any other degree award.

Signature _____

ACKNOWLEDGMENT

First and foremost, praises and thanks to the God, the Almighty, for letting me through the difficulties and his showers of blessings throughout my research work to complete the research successfully. Next, I would like to forward my heartfelt thanks to those helped me at different stages of my present MSc work. I would like to express my sincerely gratitude to my advisor Yilma Seleshi Professor of Water Resource Engineering, for his ongoing mentorship and never-ending guidance throughout my thesis work. His humble approach to research and science is an inspiration and also invaluable guidance and support through my master's program is a paramount in success of this thesis. I am grateful to ESSA Project and Oromia Agricultural Research Institute, for providing me with the opportunity to conduct my thesis and for all the resources and supported them provided.

I am extremely gratefully to my parents for their love, prayers, caring and sacrifices for educating and preparing me for my future. Without their encouragement and motivation, I would not have been to complete this milestone journey. My special thanks go to my mother Dinqitu Biftu for their endless love, support and prayers and your prayer for me was what sustained me this far. Additionally, Melkam Tesfaye for your love, encouragement, and support along my life will have impact for successfulness of my thesis work. My special thanks go to Minister of Water and Energy, particularly for staff members under the Department of Hydrology and GIS and Ethiopian National Metrological Agency (ENMA) for providing me both hydrological and meteorological data of free charge.

I would also thank to Dr. Biru Yitaferu (Coordinate of EARCS), and my colleagues Chala Chimdessa (Associate Researcher of Irrigation Engineering at Sinana Agricultural Research Center), Tesfaye Gragn Associate Researcher of Irrigation Engineering, at Bore Agricultural Research Center), for their keen interest shown to complete this thesis successfully.

Finally, I would like to extend my sincere gratitude to all of the participants in my study. Their willingness to share their experiences and insights has been invaluable to my research and has helped to make this thesis.

DEDICATION

Dedicated to my mother, **Dinqitu Biftu**, and my father **Mamo Burayu** and my brother **Diriba Mamo,** for nursing me with affection, love, and for their dedicated partnership in the success of my life.

ABSTRACT

Understanding the effects Climate change impact on Surface water resource availability is the key point for sustainable management of natural resource. These changes would happen through changes in rainfall patterns, temperatures, and stream flow. The Coordinated Regional Downscale Experiment (CORDEX) was applied. Two Representative Concentration Pathways (RCP4.5 and RCP8.5) scenario for two future periods of 2050 (2031-2060) and 2080 (2061-2090) was used for climate projection. The projected maximum and minimum temperature will increase under both RCP4.5 and RCP8.5 scenario for near-term and long-term future periods by 1.9 ^{0}C, 2.8 ^{0}C, 2.2 ^{0}C, and 4.1 ^{0}C, and 1.9 ^{0}C, 2.9 ^{0}C, 2.5 ^{0}C, and 4.5 ^{0}C respectively. The projected potential evapotranspiration will increase by 6.3% to 8.6% for RCP4.5 scenarios and 6.7% to 11.4% for RCP8.5 scenarios under future periods. The projected the rainfall projection during the rainy season decreased by -5.8% to -1.2% for RCP4.5 scenarios and -3.7% to -0.4% for RCP8.5 scenarios under future periods as a result of increased projected temperature and potential evapotranspiration. HBV-Light model was used to simulate stream flow from 1985-2002 periods for calibration and 2003-2011 for validation periods. The model performance showed with R^2=0.91, NSE=0.88, and PBIAS=13.43% for calibration and with R^2=0.85, NSE=0.77, and PBIAS=15.07% for validation. Future simulated stream flow of the Sibilu River showed a decreasing trend during the rainy season, which has a significant impact on the surface water resource availability of the catchment. The reduction in stream flow volume directly related to decreasing rainfall would be attributed due to climate change impacts.

Key Words: Climate change, GCM, HBV-Light, Catchment, CORDEX, RCPs

TABLE OF CONTENTS

LIST OF TABLES

LIST OF FIGURES

LIST OF TABLES IN THE APPENDIX

LIST OF FIGURES IN THE APPENDIX

LIST OF ACRONYMS

AET	Actual Evapotranspiration
AOGCM	Atmosphere-Ocean General Circulation Models
CORDEX	Coordinated Regional Downscaling Experiment
CV	Coefficient of Variation
CMIP5	Coupled Model Intercomparison Project Phase 5
CMhyd	Climate Model data for Hydrological Model Tool
DD	Degree Decimal
DEM	Digital Elevation Model
EARCS	Ethiopian Agricultural Research Council Secretariat
ECRGE	Ethiopian Climate Change Resilience Green Economy
ENMSA	Ethiopian National Meteorological Service Agency
ESSA	Environmental Sustainability for Sub-Africa Agro-pastoral
ET	Evapotranspiration
FAO	Food and Agricultural Organization
FC	Field Capacity
GCM	General Circular Model
GHG	Green House Gas
GIS	Geographical Information System
GGU	Global Guidance Unit
HBV	Hydrologiska Byråns Vattenbalansavdelning
HEC-HMS	Hydrological Engineering Center Hydrological Modeling System
m.a.s.l.	Mean above Sea level
IPCC	Intergovernmental Panel on Climate Change
ITCZ	Inter-Tropical Convergence Zone
LULC	Land Use Land Cover
LS	Linear Scaling
MoWE	Minister of Water and Energy
NSE	Nash and Sutcliffe Efficiency
OARI	Oromia Agricultural Research Institute
PBIAS	Percentage of Bias

PET	Potential Evapotranspiration
PT	Power Transformation
RCD	Regional Climate Development
RCP	Representative Concentration Pathway
RCM	Regional Climate Model
SDV	Standard Deviation
SRES	Special Report on Emission Scenario
SMHI	Swedish meteorological and Hydrological Institute
SNHT	Standard Normal Homogeneity Test
TGICA	Task Group Impact and Climate Assessment
WCRP	World Climate Research Program
WMO	World meteorological Organization

1. INTRODUCTION

1.1. Background

The effects of climate change on water resources are currently a major global concern and it may be a case corn for all stake holders [1]. One essential natural resource that all others rely on is the climate and it affects the availability of energy, water, and food production in different ways. Climate change is the term used to describe variations in the mean and or variability of the climate's attributes that last for a long time, usually decades or longer, as a result of either natural variability or human activities are highly intensified [2].

Changes in climate may occur due to internal processes and or external forces. Some external influences, such as changes in solar radiation and volcanism, occur naturally and contribute to the natural variability of the climate system. But some other external changes such as: change in the composition of the atmosphere that associated with Industrial Revolution, are the result of human activities. The component of hydrological cycle and availability of water resources were influenced by variations in temperature and precipitation trends [3]. This translates to a future balance of hydrological cycle under pressure as a result this weather changes. As a consequences of warmer climate change, leading the hydrological will hasten and results of more intense and unpredictable rainfall patterns [4]. This implies that due to a shift of precipitation away from their usual water sources in amount and timing of storm runoff.

Nowadays there is strong scientific evidence that indicates the average temperature of the earth's surface is increasing due to greenhouse gas emissions. The average global temperature has increased by about 0.6^0C since the late 19^{th} century and the latest IPCC (Intergovernmental Panel on Climate Change) scenarios indicated that, the project temperature rises from 1.4-5.8^0C, and simultaneously the seal level rises of 9-99 cm by 2100 [5]. The East and Horn Africa were the worst countries that are impacted by climate change in the medium and long-term century and henceforth the prolonged droughts, desertification, flash floods, and land degradation were an effect of environmental changes [6]. Because water is essential to every natural system as well as every socioeconomic system in the country, the effects of climate change on the hydrological cycle in general and on water resources in particular are highly significant [7]. However, it is

anticipated that climate scenarios will differ significantly over time and place, impacting climatic and meteorological variables in a variety of ways depending on the region and having a significant effect on human systems and local natural habitats. However, variations in the mean worldwide temperature will impact both the temporal and spatial distribution of precipitation. Hence that, hydrological cycles, water balances, and the consequent availability of water resources will all be impacted by this event for both short and long term conditions. According to the Intergovernmental Panel on Climate Change (IPCC), Ethiopia will probably be more susceptible to climatic change because of its particular climatic, hydrologic, and economic circumstances.

Climate change poses significant economic and environmental risks worldwide following by alters the ecosystem and livelihood of the community those relied. Since the Ethiopian economy mainly depends on agriculture, and which in turn largely depends on available water resources, the country has a fragile highland ecosystem that is currently under stress due to increasing population pressure and land degradation. According to the [1] report, the population at risk of increased water stress in Africa is projected to be 75- 250 and 350- 600 million people by the 2020s and 2050s, respectively. This means that future water resources could face a double threat in demanding to the increased population. Moreover, apart from these threat yields from rainfed agriculture could be reduced by up 50% in countries that mainly rely on rain-fed agriculture. Among the parts of Africa including Ethiopia has warmed over the past century and human-induced climate change will bring extraordinary rates of warming over the next century as implication of ECRGE (Ethiopian Climate Change Resilience green economy) vision. According to the vision, Ethiopia will see additional warming in all seasons by the 2020s, ranging from 0.7°C to 2.3°C, and by the 2050s, from 1.4°C to 2.9°C. This warming is probably going to be accompanied by heat waves and increased evapotranspiration.

Predicting future rainfall changes across sub-Saharan Africa is difficult, especially for Ethiopia which is locating in East Africa with having complex landscapes and their reliance on rain-fed agriculture is particularly concerning. In these regards, for examples Sululta districts have already faced challenges due to delayed and shortened rainy seasons and this highlights how agriculture of country is vulnerable to changing weather patterns. Due to variable rainfall patterns the country shows of an increase in overall and extreme rainfall events, especially in the

highlands based on downscaled climate projection [8]. Climate change's impact on Ethiopian's water resources has been extensively studied, particularly in the Upper Blue Nile basin. Previous research has focused on various aspects, including: stream flow hydrology- this research examines how water flows through rivers and streams in the basin [9], Land use and climate change- studies have investigated how changes in land use practice, combined with climate change will affect water runoff in specific watershed like Gilge Abbay [10], and hydrological responses-researches have analyzed how entire watersheds, like Gumara, react to changes in climate patterns [11].

Several studies have attempted to evaluate the impacts of climate change in Ethiopia [12], [2], [13], and not much research has been seen on the Sibilu River catchment studies done with climate change impact on water resource availability at the catchment scale. Investigating climate change at the local level gives an insight to defining the degree of vulnerability of local water resources and planning an appropriate adaptation measure must be taken ahead of time. Unfortunately, this gives time to consider the possible future risks in all phases of water resource development projects at the local scale. Current predictions of climate change and anthropogenic impacts on the hydrological regimes of rivers suggest an increase in the variability of river discharge (an increase in high flows and a decrease in low flows) for about one-third of the global land surface area [14]. Projection of climatic variables globally is performed with General Circulation Models (GCM), which provide projections at larger spatial scales. Hoverer, such large-scale climate projections must then be downscaled to obtain smaller-scale hydrologic projections using appropriate linkages between the local climates. Climate change caused by the increase in greenhouse gases in the atmosphere has significantly distressed water resources through temperature, rainfall, and evapotranspiration changes [15].This fluctuations leads to unstable hydrological cycle and put pressure in resources as a whole which will foresee in upcoming periods .

In climate change impact studies, hydrologic models are necessary to replicate sub-grid size processes; these models require similar-scale input data. Typically, these data are produced by transforming the results of the general circulation model (GCM) into trustworthy regional hydrologic time series at the chosen catchment scale. Using methods referred to as "downscaling," GCM outputs were translated into local meteorological variables [16] and [17].

Using General Circulation Models (GCM), a number of climate research organizations projected future world temperatures in the 1950s. However, these models are not as good at estimating climate change at the local scale because of their low spatial resolution [18]. Consequently, in order to offer a uniform framework for assessing and enhancing regional climate downscaling (RCD) methods, the World Climate Research Programme (WCRP) launched the Coordinated Regional Climate Downscaling Experiment (CORDEX) program in 2009. CORDEX offers local-scale data to the community of climate modelers and consumers of climate information [19]. CORDEX-Africa, which is a CORDEX domain, was created experimentally for researchers, especially on the effects of climate change across Africa. Several RCMs were used and created in CORDEX-Africa to assess any justification for Projections uncertainty and to provide rationalized, predictable variations in local climates [20]. Therefore, climate projections with high geographical and temporal resolutions at the local level are important as a basis for providing sufficient information on climate adaptation. Local climate projections are being analyzed using RCM [21]. Recently, simulations based on Coupled Inter-comparison Project Phase 5 (CMIP5) datasets, which have many Global Climate Model (GCM) outputs, showed improvements compared to the previous version of climate models [22]. In turn, CMIP5 downscaled as an ensemble means at the Coordinated Regional Climate Downscaling Experiment Africa domain (CORDEX-Africa) [23] with a new emission scenario called Representative Concentration Pathway (RCP), which overcomes the shortcoming of previous scenarios for climate change impact studies in Africa [24] , [25] , [26] , and [27].

Following the intensification of climate change on hydrological patterns as a result extreme events like droughts and flood might have negative effect on the agriculture sector and the economy as a whole [28]. Therefore, the projection of climate change impact on water resources of the catchment is a case concern for the future development plan. In this regard, it is extremely important to conduct research on the impacts of climate change on water resources so that people and society can foresee and respond to tentative future challenges either by mitigating the worst condition that are likely to happen in future or at least be well prepared and resilient to face the possible challenges.

1.2. Statement of the Problem

Assessment of water resources at the basin, regional, or national scales is essential for finding sustainable solutions for water-related problems that results from adverse consequences of climate change on the hydrological regime of the river. The population has been increasing exponentially, bringing along an increase in water demand. In the last century, water use has increased at more than twice the rate of the world population; simultaneously freshwater resources are steadily being depleted due to pollution and climate change.

Accurate information on the condition and trend of a country's water resources, including surface water and groundwater, quantity, and quality is required to support sustainable economic and social development while addressing the maintenance of environmental quality. Considering the above baseline information, the Sibilu river catchment, which is a tributary of Muger River that eventually discharges into the Abbay River, is found in Sululta districts, Oromia region, and it is a very important area connection with its water resource. Of course, the area has plenty of topography and is currently center for economic development potential in the industrial zone.

The need for water throughout the entire catchment for irrigation, food and energy production, and water supply is growing due to driving factors like economic development and population growth. This could have an effect on the availability of water resources, which could be followed by the effects of climate change. Additionally, the increase in agriculture and the construction of additional dams are altering the catchments' spatial and temporal uses. Water supplies and the environment will be under pressure as resource demand rises in the near future, matching newly established industry and rapid population expansion. According to Nestle Waters Ethiopia, the Sululta plain is facing catchment degradation due to poor land management, wetland loss, and pollution. Addis Ababa's water demand is high, with previous gap of 40%-50% being addressed by projects like the Sibilu and Gerbi dams according to AAWSA report. Additionally, supplies water to Sululta town, Mijan, and Chanco possible put pressure on the future water availability with growing population and industries. Because of the intricate relationships that exist between freshwater ecosystems, climates, the biophysical system, and the socioeconomic system, any adjustments we make to one will inevitably affect the others. Because of the above mentioned integral problem, the Sibilu river catchment's need effective water resources management.

The majority of the results of earlier studies carried out in the basin are based on the out-of-date climate scenarios (SERS), despite the fact that a few studies were carried out in the Sibilu river catchment using various research climate scenarios, particularly based on GCM and RCM models, through downscaling of the GCM output to catchment level. Previous research on these antiquated climate scenarios shows that socioeconomic emission scenarios are exclusive and do not take any strategies to mitigate climate change into account [29]. Because of this, the most recent scenarios have the capacity to address the SRES issue. It is crucial to use this current RCP emission scenario in tandem with other recently generated scenarios to increase the validity and reliability of effect assessments.

For these studies, the hydroclimatic data of CORDEX-Africa RCMs was downscaled from different GCMs from the CMIP5 simulation under different RCP scenarios (RCP 4.5 and RCP 8.5) were used for the catchment. Then the data was be used as an input to the hydrological model (HVB-Light) to simulate the effect of climate change on the hydrological regimes and analyses the future water availability in the region.

No previous study has used to evaluate how climate change may affect the water resources of the Sibilu river basin. Consequently, this study can be valuable in helping policymakers and decision-makers plan for the consequences of climate change on the catchment's water supplies by providing knowledge and understanding of such effects.

1.3. Research Questions

To attain the specific and general objectives of the research the following questions has to be answered:

- What are the projected changes of maximum temperature, minimum temperature and precipitation scenarios in the future compared to the present condition as well as their interlinking to the catchments?
- How water balance of the catchment responds to climate change scenarios?
- Which future climate scenario has impact on water resource of the catchment?

1.4. Objectives of the Study

1.4.1. General Objectives of the Study

The Primary objective of this study is to assess the impact of Climate Change on Surface Water Resource Availability of Sibilu River Catchment, Upper Abbay Basin, Ethiopia.

1.4.2. Specific Objectives of the Study

For a full accomplishment of the work and achievement of general objective, the following specific objectives are set for major long span of the study area**.**

- To assess future changes in precipitation and temperature compared to the current condition of Sibilu River catchment.
- To evaluate the effects of climate change on water resource of Sibilu River catchment.
- To simulate water balance component of Sibilu River catchment using HBV-Light hydrological model.

1.5. Limitations and significance of study

As a significance, the contribution of this research is to address valuable information on the projected climate change impact in the Sibilu River catchment and assess future water resource availability using recent techniques of RCM (Regional Climate Model) from the two emission scenario projection, RCP 4.5 and RCP 8.5, that will serve water resources planning and management efficacy, subject to capturing inherent uncertainties stemming from climatic and hydrological inputs and models. Water availability is critical in reservoir operation and water allocation decision-making, fundamentally contains uncertainties arising from assumed initial conditions, model structure, and modeled processes. Furthermore, understanding the impact of climate change assessment, which is alarmingly increasing from time to time due to the global warming problem, will pay great attention and tackle the consequences for a sustainable, well planned natural ecosystem. At the same time, simulation model results can provide an excellent platform for evaluating various options for water and environmental planning. Such information is crucial for policymakers, decision-makers, implementing agencies, and practitioners to quantify different types of threats to water and environmental security, design policies and programmes, and devise strategies for better allocation, utilization, and management of freshwater resources as well as environmental protection for the country's prosperity.

As a limitation, the CORDEX-Africa relies on data from Global Climate Models (GCM), which themselves have limitation in capturing small-scale processes and atmospheric factors like aerosols. Even if with multi-model ensembles, there is inherent uncertainty in future climate predictions due to factors like greenhouse gas emission scenarios. Lastly, it might not fully represent important processes like mesoscale convective systems (MCSs) that significantly impact African weather.

Similarly, as a limitation HBV-Light model is being a conceptual model, it offers a simplified representation of real-world hydrological processes. This can miss the spatial variations in precipitation, temperatures, and other factors occurs a complex landscape with high elevation differences. The model not fully account for the way topography affects factors like wind speed, radiation exchange, and precipitation patterns. This can lead to an overestimation of precipitation of melt water runoff in certain areas of watershed.

In reality, during climate projection, there is uncertainty raised by climate models and hydrological models at times of downscaling. However, the results of this study should be taken with care and be representative of the likely future rather than accurate predictions. In the meantime, the study should not consider land use and land cover change in the analysis and simulations. The climate projections were based on a single Regional Climate Model (RCM) for assessment of future water resource availability, and other climatic variables like wind speed, relative humidity, and sunshine hours were considered constants through the simulation period; in the real world all these variables were changed and would have an impact on the analysis of future water resource availability in near-term and long-term periods in the Sibilu river catchment.

2. LITERATURE REVIEW

2.1. Climate Scenario

A climate scenario is a plausible representation of future climate that has been constructed for explicit use in investigating the potential impacts of anthropogenic climate change. Climate scenarios often make use of climate projections (descriptions of the modeled response of the climate system to scenarios of greenhouse gas and aerosol concentrations by manipulating model outputs and combining them with observed climate data. Over time, different scenarios have been used in climate research, from SA92 used in IPCC's, first assessment report to the Special Report on Emission and Scenarios (SRES) used in third and fourth assessment report. And recently, the new scenarios, the so-called Representative Concentration Pathways (RCP), were developed and used for preparing fifth assessment report (AR5) of IPCC released in 2015.

Scenarios for climate change are needed to understand how the earth's system might react to human activities, how different anthropogenic contributions could of effect affect climate change, or evaluate the future possible impacts of our current actions. All these efforts to forecast future scenarios are driven by the will to adapt to imaginable fatal situations, however, this is not an easy task for complex socio-economic, technological, and environmental conditions [30] and [31].

Decision- makers and resource managers require information regarding future changes in climate average and variability to better anticipate the potential impacts of climate change. Since then, future climate patterns are difficult to predict, particularly the future radioactive forcing from greenhouse gases is difficult to quantify since the emission of these gases depend on many assumptions and uncertain factors such as population growth, the use of carbon fuel as an energy source, technological development, policy, and attitudes towards the [32] and [33]. In this case, climate scenarios have been developed to investigate the potential consequences of anthropogenic climate change.

2.1.1. Representative Concentration Pathways (RCP)

RCPs are time and space dependent trajectories of concentrations and emission of greenhouse gases and pollutants resulting from human activities, including changes in land use. RCPs provide a quantitative description of concentrations of the climate change pollutants in the

atmosphere over time, as well as their radioactive forcing in 2100. RCP is the latest generation of scenarios that provide input to climate models in climate research. The RCPs were developed by combined efforts of the researchers from different disciplines involved in climate research [34].

There are four RCP (RCP2.6, RCP4.5, RCP6.0 and RCP4.5) which is defined by their level of the total radiative forcing pathway in the year 2100, and are representative for existing literature about emission scenarios.

RCP2.6 was developed by the IMAGE modeling team of the PBL Netherlands Environmental Assessment Agency. The emission pathway is representative of scenarios in the literature that lead to very low greenhouse gas concentration levels. It is a "peak-and-decline" scenario; its radiative forcing level first reaches a value of around 3.1 W/m2 by mid-century, and returns to 2.6 W/m2 by 2100. In order to reach such radiative forcing levels, greenhouse gas emissions (and indirectly emissions of air pollutants) are reduced substantially, over time [15].

RCP4.5 was developed by the GCAM modeling team at the Pacific Northwest National Laboratory's Joint Global Change Research Institute (JGCRI) in the United States. It is a stabilization scenario in which total radiative forcing is stabilized shortly after 2100, without overshooting the long-run radiative forcing target level [35].

RCP6.0 was developed by the AIM modeling team at the National Institute for Environmental Studies (NIES) in Japan. It is a stabilization scenario in which total radiative forcing is stabilized shortly after 2100, without overshoot, by the application of a range of technologies and strategies for reducing greenhouse gas emissions [36].

RCP8.5 was developed using the MESSAGE model and the IIASA Integrated Assessment Framework by the International Institute for Applied Systems Analysis (IIASA), Austria. This RCP is characterized by increasing greenhouse gas emissions over time, representative of scenarios in the literature that lead to high greenhouse gas concentration levels [37].

2.2. Bias Correction

Most of the time, GCM or RCM-modeled data are not directly used because of their bias, as natural phenomena cannot be predicted accurately. Furthermore, this uncertainty and bias were developed during the advancement of circulation models by scientists due to a lack of an

absolute and strong concept about the nature of atmospheric circulation [38]. GCM models may not necessarily estimate variables to reduce the differences, and there is always a deviation between observed and simulated variables, even if the difference is insignificant. Accordingly, it is important to count on bias correction methods to remove bias from GCM and RCM outputs for predicting climate change impacts over the world's climate regions [39] and [38]. The application of appropriate and suitable bias correction methods to the climate model enables researchers to be more confident in the hydrological model's outcome as large errors are expected to be removed.

There are several bias correction methods to remedy the various problems with biased RCM output. The well-known bias correction methods are linear scaling, the delta change approach, local intensity scaling, power transformation, variance scaling, and distribution transfer mapping. Among the methods being employed, some are used for one parameter meant either for temperature or precipitation, whereas others are used for both parameters and further information [40].

Often, the outputs of regional climate models cannot be directly used for impact assessment as the computed variables may differ systematically from the observed ones. Bias correction is therefore applied to compensate for any tendency to overestimate or underestimate the mean of downscaled variables. A bias correction factors are computed from the statistics of observed and simulated variables. Bias correction methods are assumed to be stationary i.e., the correction algorithm and its parameterization for current climate conditions are assumed to be valid for future conditions as well. A method that works well under the current circumstances is probably going to work better under altered circumstances than a method works poorly under the existing conditions through providing explanation and pointing out that method [7].

The correction techniques used in this study were the linear scaling method (LS) for bias correction for downscaled temperature and power transformation (PT) for precipitation, where both methods are the most straightforward bias correction employed in several studies and which are aimed at perfectly matching the monthly average of corrected values with observed ones.

2.3. Previous Related Studies in the Study Area

At the Sibilu River catchment scale, only a few studies have been conducted. In this case, there is considerable literature; those done past in the catchment are largely highlighted at Sululta Town and Nestle Water Bottling JV Company. Besides the above consideration, the government with the aid of the African Development Bank group also carried out a more detailed hydrological study of the Gerbi and Sibilu catchments, including reservoir sedimentation, a detailed assessment of the groundwater potential, supervision of boreholes, and the geotechnical inspections of the dam sites. Apart from Sibilu river catchment, more studies are done at basin scales specifically on the upper Blue Nile basin. Some of the studies are summarized as follows:

[41] Did research on numerical groundwater flow modeling for sustainable groundwater resource development in the Sibilu River, and the studies pass through methods like quantitative and qualitative/descriptive statistics and broadly divided these methods into three major steps. The first category illustrates how secondary data is collected and organized for the ease of work. Similarly, the second category illustrates field investigation and primary field data collection. Lastly, data integration, analysis, interpretation, and result output has been done using ArcGIS routine, SWAT, and MODFLOW modeling software. This phase will define the groundwater flow system and intimately, based on the results of the calibrated Groundwater flow model, steady state scenarios were created for further analysis of groundwater movement. While conducting the research studies, the following data types are used from various sources. This data includes:

- Climate Forecast System Reanalysis (CFSR).
- Existing boreholes with well drilling completion history, hand dug wells, Cold Springs, Geophysical survey data, Vertical Electrical Sounding data, and water quality and population data.
- Soil maps, land cover maps, and DEM from MoWE.
- Geological, hydrological, and hydrogeological investigations and maps.

At the end, the finding of the studies revealed that there is a significant ground water level drop on average of 31.3 meters for 50% abstraction rate increment and 19.31 meters for a 10% recharge reduction. Additionally, a subsequent reduction in the base flow of the Sibilu River was observed.

[41] Under Project analysis II, conducted a reconnaissance survey and determined that the Sibilu catchment had the capacity to supply water to Addis Ababa through regional resources, and Seureca (1991) carried out a feasibility analysis of the Sibilu and Gerbi rivers dams in addition to the initial plan.

[42] Carried out studies on groundwater potential and Evaluations of Sululta catchment. Various study techniques are helpful in providing information about hydrochemistry and the evaluation of groundwater potential of the catchment. Among techniques used are the following:

- Interpretation of aerial photos, field geological and in hydrogeological studies, and other pertinent data compilations and revisions of books and articles.
- Examination of the drainage map of a 1:50,000 topographic maps.
- Creating of geological map that uses information from published studies and the site investigation.
- Site analysis to map the soil and various maps of land use and cover.
- GPS to locate various water points for the purpose of mapping and spatial distribution
- Conducting vertical electrical surveys at various catchment areas.
- Gathering hydro meteorological, soil, land cover, water point inventories, well logs, and pumping ell results.

Accordingly, the classification of the water- bearing formations of the catchment was done based on the aquifer's characteristics. As a result, the region includes the middle section along the fracture lines of the stream with transmissivity greater than 27.4 m^2/day and yield ranging from 2 l/sec to 4 l/sec. Aquifer yields in the range of 0.5 l/sec to 1 l/sec and acidic lava flows of Entoto Ridge with transmissivity values ranging from 1.12 m^2/day to 4.49 m^2/day were also mapped as low productive or permeable zones, and the remaining areas with transmissivity ranging from 4.49 m^2/day to 27.4 m^2/day were identified as a moderate permeable or productive zone. The resistivity investigation conducted in the catchment during that study revealed that ground water extends down to a depth of 120 meters and the worn and/or broken basaltic lava flow that was the recognized main aquifer. The groundwater potential of the watershed was found to be more confined to the weathered and fractured portions of the rocks during that investigation.

[43] Conducted a geotechnical and engineering geology research of the Sibilu watershed and demonstrated that the majority of the soils and rocks exposed at the dam site, reservoir, and catchment region had geotechnical and engineering geological features that make them appropriate for the proposed surface water damming.

[44] Studied the Groundwater Dynamics in the Upper Awash River Basins and Left Bank Catchments of the Middle Blue Nile, Central Ethiopia. Based on the δ18O and δD signature data gathered from shallow aquifer systems throughout all the sub-basins demonstrate how locally generated precipitation from current events replenishes the aquifer system. Conversely, the inter-basin groundwater flow determined from the evidence-based litho-structural model is supported by the highly depleted waters from deep wells in the Upper Awash and Guder sub-basins, including those situated very close to and along the water divide between the Blue Nile and the Upper Awash basin.

[45] Did GIS-based physical Irrigation Potential Assessment of the Sibilu river catchment and explore suitable sites for irrigation potential. Accordingly, the data categories were used and utilized in the work are: secondary data, which included spatial data (DEM, LULC, and soil), hydrological data (stream flow), and weather data like (rainfall, temperature, relative humidity, and solar radiation). Following the data's consistency check and infill, the suitability model was created by model builder in the Arc tool box and tools from spatial analysis tool sets and then assessing of individual irrigation suitability was performed. Catchment's slope stability was assessed using several slope classifications based on an FAO analysis, and the watersheds were delineated. Finally, an assessment of the Sibilu catchment's irrigation potential was carried out and results were determined. The findings showed that the Sibilu catchment has many qualities that make it a great choice for surface irrigation.

[46] Carried out research on Modeling LULC change assessment and its impact on the hydrology using GIS-RS on Muger catchment. Input data like spatio-temporal; land-use land cover, soil map, and DEM as input for HRU analysis. Land-use land-cover, soil map, and DEM were used as input for HRU analysis. The maximum likelihood supervised land-use land cover classification for the years 1990, 2000, 2010, and 2021 were conducted to get the land-use land-cover data for HRU. The temporal data including metrological and stream flow data were also

used. And finally stream flow data were used for the calibration and validation of the SWAT simulation result. The analysis of land-use land-cover shows that in 1990, forest covered 3.19% of the land, followed by woodland and shrubs in 2000, 2010. By 2021, forest covered 2.15%, woodland 6.88%, shrubs 8.10%, cropland 73.33%, grasslands 7.10%, bare land 2.14%, and settlement 0.3%. Following the findings, the majority of the catchment was covered by cropland and bare land and settlement were covered small area.

[47] Did a research on modeling the spatial and temporal availability of water potential over Abbay river basin, Ethiopia. The data used at the execution of work are: spatial data like soil, land use land cover, DEM (30*30 m resolution), weather data like rainfall, temperature, relative humidity, wind speed, and sunshine hours and also hydrological (stream flow) used for model simulations. Arc SWAT model were used and the simulation process involves watershed delineation and a multisite evaluation of the Abbay river basin that can divide the basin into upper and lower that are serving as an outlet. The model setup considers the basin as natural condition, allowing for consideration of heterogeneous physical characteristics. Similarly, the Hydrologic Response Units (HRUs) are defined by overlaying soils, land use, and slope classes. The study revealed that the basin has significant regional and temporal variability in rainfall, as seen by the distribution of rainfall. From June to September, three-fourths of the yearly rainfall was contributed. The investigation of the water balance components demonstrated that evapotranspiration is high throughout the basin, accounting for over half (55.20%) of the yearly precipitation. The yearly rainfall is only 21.73% covered by the water yield (WYLD-Qmm).

[48] Conducted a research on modeling the impacts of climate on surface runoff in Fincha sub-basin, Ethiopia and using the data like historical climate and stream flow data, along with watershed parameters like area, mean elevation, land use, and shape, are used to calibrate and validate the SWAT model. Future climate generation was handled using the statistical downscaling model (SDSM). To retrieve climate scenarios, the process involves using climatic output data from General Circulation Models. The SWAT hydrological model was then used to simulate stream flow by using the weather generator to generate daily temperature and precipitation data. To determine the shift brought about by climate change, the outcomes of the future simulations were then contrasted with the baseline period. In order to estimate the efficacy of prospective management techniques in the future, the model was evaluated against a separate

set of measured data. The model was employed for future forecasts under various conditions since its predictive performance was shown to be reasonable throughout both the calibration and validation phases.

The findings of the studies had shown, the watershed's average annual rainfall could decrease by up to 9.84%, 23.29%, and 41.51% in the 2020s, 2050s, and 2080s, respectively. The average annual maximum temperature could rise by 0.25 ^{0}C, 0.60 ^{0}C, and 1.09 ^{0}C, while the average annual minimum temperature could rise by 0.3 ^{0}C, 0.80 ^{0}C, and 0.92 ^{0}C. Consequently, the yearly runoff at the watershed's outlet decreased by 4.29%, 10.62%, 18.07%, and 8.27%, 8.58%, 16.69% for the 2020s, 2050s, and 2080s.

[49] Conducted research on “Estimation of Hydrological Components under and future Climate Scenarios in Guder Catchment, Upper Abbay basin, Ethiopia.” For the execution of work data such as soil, land use land cover, DEM, weather data like precipitation, maximum and minimum temperature, and stream flow are used during the basin.

SWAT model were used and in the process involves watershed delineation and some methods like trend analysis which is conducted by Man-Kendal and Sen’s slope to evaluate and detected changes in statistical time series data. The Regional Coordinate Downscale Experiment (CORDEX) was used to downscale the climate scenarios data for future climate change impacts studies. CMhyd software was used to extract and bias correction purpose for raw climate GCM outputs. The findings the study found that precipitation and air temperature will decrease by 14.4% and 3.2 mm per year under the Regional Climate Model (RCP 8.5) from 2057 to 2086, potentially reducing future basin water yield output and indicating a warmer prediction than RCP 4.5.

[50] Did a research on the “Assessment of Climate change Impacts on the water Resources of Megech River Catchment, Abbay basin, Ethiopia.” During the entire study span data’s like weather data such as daily precipitation, maximum and minimum temperature, hydrological data (stream flow) and potential evapotranspiration were used. For this specific study, the Statistical Downscaling Model (SDSM) version 5.11 was used to statistically downscale the output variables from the Regional Climate Model (REMO) for both the A1B and B1 emission scenarios. The HBV-light model was verified and calibrated using the specified stations'

historical climate data. In order to evaluate the watershed hydrological response to climate change, the HBV-Light model was fed downscaled future scenario 20 ensembles data from both the REMO A1B and B1 scenarios. The climate scenario data (A1B and B1) for this study were taken from the REMO model using a grid resolution of 50 km (0.5º latitude by 0.5º) longitude grid size) based on longitude and latitude. Using a statistical downscaling methodology, the coarser climatic data (REMO output) was further downscaled to the station level. The study revealed that the maximum temperature is expected to exhibit an increasing trend of +0.57˚C, while the lowest temperature shows a decreasing trend of −0.61˚C, based on forecasted climatic data. Precipitation is not showing any discernible trend.

[5] Did a research on Assessment of climate change impacts on the hydrology of Gilgle Abbay Lake Tana Basin, Ethiopia. Data like meteorological (Rainfall, Maximum and minimum temperature, wind speed, sunshine hours and, relative humidity); spatial data such as soil, DEM, land use land cover, and stream flow and HBV-96 was used for calibration and validation of the basin which is pre-defined. Additionally, statistical downscaling model (SDSM) and the HBV hydrological models (Hydrologiska Byråns Vattenbalansavdelning) was used to evaluate the effects of climate change on the inflow to Lake Tana. He discovered that there is a notable variation in the monthly and seasonal flows during IPCC AR4 emission projections and in the 2080s, the A2 and B2 emission scenarios indicated a decrease in the runoff volume during the rainy season of roughly 11.6% and 10.1%, respectively.

[51] Did a research on the impacts of climate change and land use on hydrological response in Gumara watershed, Ethiopia. Besides meteorological (Rainfall, Maximum and minimum temperature, wind speed, sunshine hours and, relative humidity) and hydrological data (stream flow), both spatial (soil, DEM, and land use land cover) and non-spatial (population size and management practice such major crops, planting, harvesting and killing, tillage, and fertilize application data) were used for the study area. SWAT model was used to evaluate the combined impacts of land use and land and climate change hydrological responses in Gumara watershed by examined four land use scenarios from 2015(present) and 2050 (projected) on basis of business as usual trend (BAU), expansion of irrigation crop (EIC), and expansion of forestland (EFL). Accordingly, simulation of climate model were done by utilizing weather Research and Forecasting (WRF) model compared to baseline period (2005-2015) with projected period from

2045-2055 under RCP 4.5 and RCP 8.5 scenarios. The result obtained from the findings revealed that, the simulated steam flow, surface runoff, and evapotranspiration under RCP 8.5 might be increased significantly by 34.3%, 51.8%, and 12.2%, respectively. Similarly, the findings are suggested to intensify the impact of climate change would be greater than land use changes. In expansion agriculture and wetter climate there will be exacerbated flooding else expansion of irrigation and forest offset will increase surface runoff.

[52] Did a research on evaluation of climate change impact on hydrology. A case of Lake Tana, upper Abbay Basin, Ethiopia) using CORDEX and SWAT model. Data like meteorological (Rainfall, Maximum and minimum temperature, wind speed, sunshine hours and, relative humidity); spatial data such as soil, DEM, land use land cover, stream flow, and CORDEX climate are used for simulation and evaluation of the basin which is pre-defined. SWAT version - 12 model was used to simulate stream flow in the basin that aimed to study impacts of climate change on future runoff generated. The model was calibrated and validated for the period of 2001-2006 to 2007-2010, respectively at Kesse river gauging stations.

Accordingly, evaluation of climate change will be conducted on monthly, seasonal, and annual cases for the downscaled climate data likely precipitation, maximum and minimum temperature, and evapotranspiration with that of baseline period.

The findings of the study revealed that, the monthly average rainfall for RCP 2.6 is expected to increase in the future, with maximum increase in December by 95.89% in 2090s and the minimum change in June by 3.8% in 2030s. RCP 4.5 shows an increase in rainfall in 2030s, 2050s, and 2090s, with maximum increase in March by 243.1% in 2090s and the minimum change in July by 0.31% in 2030s. In this case, there is an increasing of monthly average rainfall. The projected mean annual stream flow shows an increasing trend across all RCP scenarios, with increase in runoff for RCP 2.6, RCP 4.5, and RCP 8.5 over the 2030s, 2050s, and 2090s maximum increase in RCP 8.5 with 23.64% to 41.24%.

Seasonal flow data shows increased runoff shows in Belg, Kiremt, Bega, and RCP 8.5 for the 2030s, 2050s, and 2090s, with Belg of 10.1%, 18.3%, and 40.9% increase. Kiremt showing a 7.7%, 12.6%, and 20.3% increase whereas Bega experiencing a 30.7% increase.

Similarly, the projected monthly stream flow for RCP 2.6, RCP 4.5, and RCP 8.5 is expected to increase by 16.1%, 19.9%, and 35.7% in the future, with corresponding increase in 2030s, 2060s,

and 2090s. In respective of future annual maximum flow pattern there is an increasing trend by 21.94% for RCP 2.6, 21.59% for RCP 4.5, and 11.94% for RCP 8.5 in 2035, followed by a decreasing trend in 2036, and a peak flow pattern in 2090s.

2.4. Hydrological Modeling

Hydrological models are mathematical formulations that determine runoff signals that leave a watershed basin from the rainfall signals received by this basin. They provide by means a quantitative prediction of the catchment that may be required for efficient management of water resources. Such hydrological models are also used as by means of extrapolating from available measurements in both space and time into the future to assess the likely impact of future hydrological change. Changes in global climate are believed to have significant impacts on local hydrological regimes, such as in-stream flows that support aquatic ecosystems, navigation hydropower, and irrigation, etc. Hence, hydrological model frames work to conceptualize and investigate the relationships between climate and water resources.

The development of the watershed hydrologic model is for different reasons and therefore has many different forms. However, they are in general designed to meet one or more of the following objectives: To gain a better understanding of the hydrologic processes in a watershed and of how changes in the watershed may affect these phenomena, it is to of generate synthetic sequences of hydrologic data for facility design or for use in forecasting. And they are also providing valuable information for studying the potential impacts of changes in land use or climate.

A model is deterministic if a set of input values will always produce exactly the same output values and stochastic if, because of random components, a set of input values need not produce the same output values [53]. Basically, the deterministic model is further classified into three main categories.

Lumped models: do not vary spatially within the basin, and thus, basin response is evaluated only at the outlet without explicitly accounting for the response of individual sub-basins. Parameters of lumped models often do not represent physical features of hydrologic processes and usually involve a certain degree of empiricism. The impact of spatial variability on model

parameters is evaluated by using certain procedures for calculating effective values for the entire basin. Lumped models are not usually applicable to event-scale processes.

If the interest is primarily in discharge prediction only, then these models can provide just as good simulations as complex physically based models [53]. Deterministic hydrologic models can be classified into three main categories [54].

Semi-distributed models: Parameters of semi-distributed (simplified distributed) models are partially allowed to vary in space by dividing the basin into a number of smaller sub-basins.

There are two main types of semi-distributed models: 1) kinematic wave theory models (KW models, such as HEC-HMS), and 2) probability distributed models (PD models, such as TOPMODEL). The KW models are simplified versions of the surface and/or subsurface flow equations of physically based hydrologic models [53]. In the PD models spatial 20 resolutions is accounted for by using probability distributions of input parameters across the basin.

A distributed model: is one in which parameters, inputs, and outputs vary spatially. Parameters of distributed models are fully allowed to vary in space at a resolution usually chosen by the user. The distributed modeling approach attempts to incorporate data concerning the spatial distribution of parameter variations together with computational algorithms to evaluate the influence of this distribution on simulated precipitation-runoff behavior. Distributed models generally require large amounts of (often unavailable) data for parameterization in each grid cell. However, the governing physical processes are modeled in detail, and if properly applied, they can provide the highest degree of accuracy [55]. The overall classification of hydrological model can be presented in figure below.

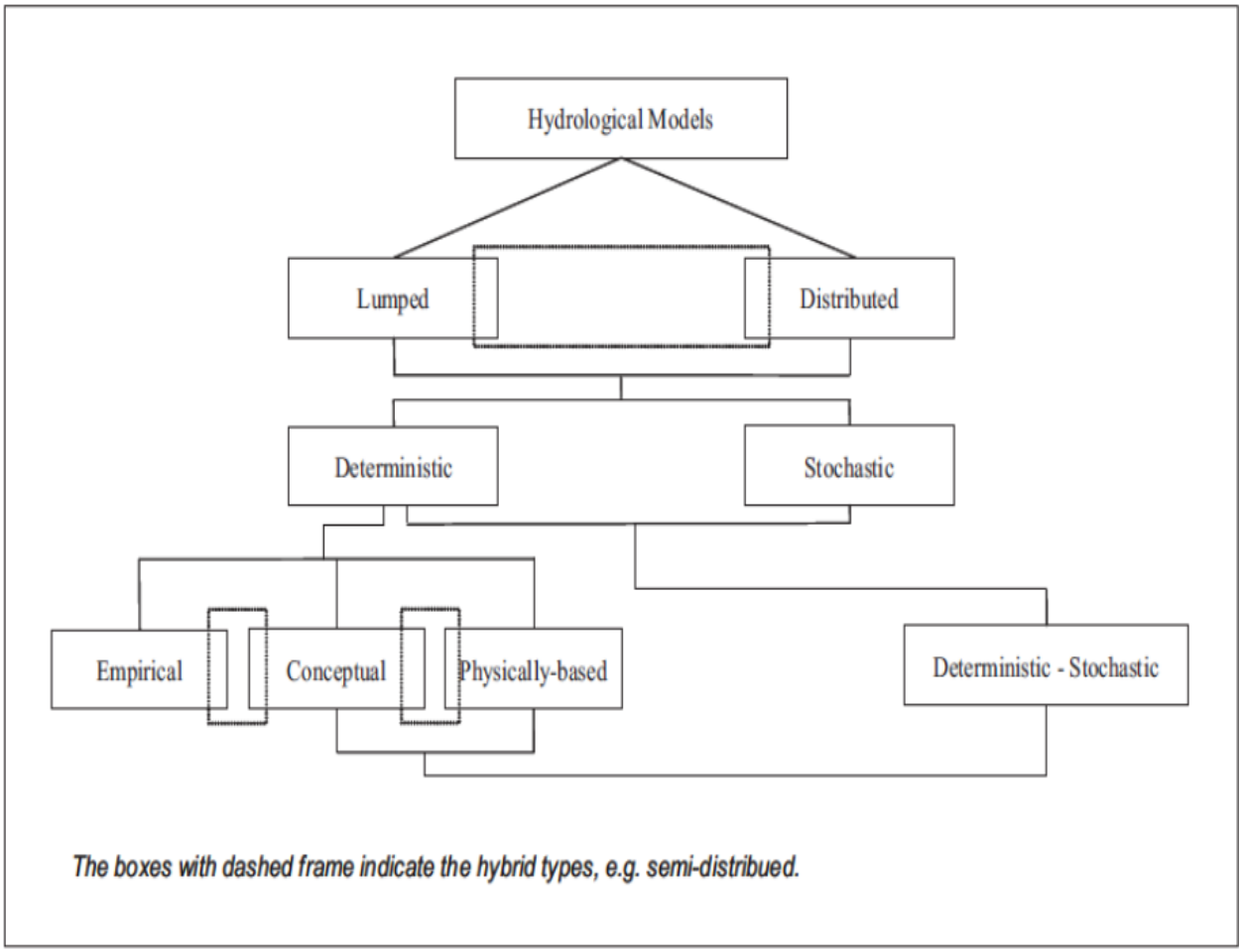

Figure 1: General classification of hydrological models

2.4.1. Common Hydrological Model used for Climate Change Assessment

Today a variety of hydrological model are utilized through the world wide for different reasons, among the reasons they mostly are used for climate change impact studies or assessments at regional or local scales. Some models that are used for climate studies are listed and discussed as below.

SWAT model: A semi-distributed, time-continuous watershed simulator that runs on a daily time step is called SWAT [56]. Due to its semi-physical basis, SWAT's division of the watershed into smaller watersheds enables the simulation of a high degree of spatial variability. In complicated catchments with varied soils, land use, and management conditions over an extended period of time, the model is designed to forecast the effects of land management methods on water, sediment, and agricultural chemical yields. Within a watershed, the HRUs are

used to characterize the spatial heterogeneity in terms of soil type, land cover, and slope class [57]. Relevant hydrologic parameters including evapotranspiration, surface runoff, and runoff peak rate are estimated by the model and also, sediment yield and groundwater flow for every HRUs unit. Accordingly there are four storage volumes hold the water in each HRU in SWAT: snow, soil profile (0–2 m), shallow aquifer (usually 2–20 m), and deep aquifer. The quantity of surface runoff from daily rainfall is calculated using the modified SCS curve number approach, which bases the calculation on the kind of soil, antecedent moisture state, and land usage in the area. Forecasts of peak runoff are predicated on a tweaked version of the Rational Formula [58]. Manning's formula is used to determine the watershed concentration time while accounting for both channel and overland flow.

HEC-HMS: The Hydraulic Engineering Center-Hydrologic Modeling System (HEC-HMS) was created by the US Army Corps of Engineers to model the processes involved in precipitation and runoff [59]. The semi-distributed conceptual hydrological model would be effective tool for modeling catchments and analyzing the long-term effects of climate change on water resources. The Hydrologic Models System (HEC-HMS) is designed to simulate the complete hydrologic processes of dendritic watershed systems and linked into a dendritic network in simulation of runoff processes. It is a numerical model that provides a variety of models to simulate watershed hydrological parameters like runoff, infiltration losses, and river routing to predict runoff and snow [60]. In this scenarios, the model required physical data to anticipate hydrologic simulation that requires detailed and more complex parameterization to compare the lumped conceptual model, which requires minimal input data. Additionally, the model contains components like basin models, Metrologic models, control specifications, and input data. Available elements within the model are sub basin, reach, junction, reservoir, source, and sink that are proceeds from upstream into a downstream direction.

VIC model (Variable Infiltration Capacity model): Is a semi distributed grid based hydrologic model which uses both energy and water balance equations. The model required inputs such as precipitation, minimum and maximum daily temperature, wind speed, and allows many land cover types within each model grid. It includes processes like infiltration, runoff, base flow and others that are based on various empirical relations. In this regards, the surface runoff is generated by infiltration excess runoff (Hortonian flow) and saturation runoff (Dunne flow). The

model simulates saturation excess runoff by taking account soil heterogeneity and precipitation. Of the 3 layers, the top layer allows a quick soil evapotranspiration, the middle layer represent dynamic response of soil with rainfall events, and the lower is used to characterize the behavior of soil moisture. Through a time an improvised VIC model has included both excess runoff and saturation excess runoff and also the effects of variability of soil heterogeneity on surface runoff characteristics. Hence forth, it can deal with the dynamics of surface and water interactions and calculate ground water table [61] and applied for cold climate. Apart from effects of variability of soil heterogeneity on surface runoff characteristics, the model now day applied to a number of river basins and helps in predicting climate changes studies.

WaSiM-ETH: the model is a grid-based, spatially distributed hydrological watershed model, which is developed at the Swiss Federal Institute of Technology in Zurich and used for runoff forecasting or modeling of substance transport. The model has two versions in which version 1 uses, the conceptual TOPMODEL-approach in the soil model. This type of approaches describes the flow components between and within the saturated and unsaturated zone by fluxes to and out of several reservoirs. Since the model is a conceptual base it has no physical meaning. The other version 2 uses the RICHARDS-equations to describing the flow of water within the unsaturated zone [62]. The minimum input data are time series are such as: temperature, precipitation, grid information about topography, land use, and soil type [62].

There are numerous studies that use WaSiM-ETH to assess how climate change affects hydrology ([62], [63], [64], and [65]. [66] Reported that the model is a useful tool for simulating lowland catchments' hydrological behavior. According to [67], the model accurately represents the hydrological behaviors of every sub-basin catchment in the Ethiopia's Blue Nile basin. The Volta Basin, a sub-humid catchment in West Africa, has also seen successful use of the model for historical analysis and scenario quantification [68].

HBV-Light model: The HBV (Hydrologiska Byråns Vattenbalansavdelning) model is a conceptual hydrological model that simulates daily discharge using daily rainfall, temperature, and potential evapotranspiration as input. It was originally, developed at the Swedish Meteorological and Hydrological Institute (SMHI) in the early 1970s. Originally the HBV model was developed for runoff simulation and hydrological forecasting.

One of the many versions of the HBV (Hydrologiska Byråns Vattenbalansavdelning) model is the HBV-Light version 3.0 [69], which is a conceptual model that simulates daily discharge using daily rainfall, temperature, and potential evapotranspiration as input.

The HBV model was first applied to catchment runoff simulation more than 30 years ago [70]. The Swedish Meteorological and Hydrological Institute (SMHI) have been developing the HBV-model [70] over the past few decades, and it is now widely used for runoff simulations in Sweden [71]. Additionally, the model has been used in about 30 nations, occasionally in modified variants.

The primary goal of HBV-light's development was to offer a user-friendly Windows version for teaching and research. Jan Seibert (at Uppsala University, Oregon State University, the Swedish University of Agricultural Sciences, Stockholm University, and the University of Zurich) developed the initial version of HBV light in 1995 and continued to expand it ever since. HBV light is written in Visual Basic, and Marc Vis (at the University of Zurich) rewrote the code in 2009–2010 to transition from Visual Basic 6 to Visual Basic.NET.

HBV-Light model shines as versatile tool for hydrologists and its strength lies in its ability to be calibrated and validate for specific catchments, allowing it to accurately simulated river runoff in diverse locations around the world, which holds true for Africa [72] and [73], including Ethiopia. This adaptability makes it a valuable asset for understanding and predicting water flow in watershed across the globe. The following section describes the relevance of the HBV-Light hydrological model in some cases and indication of widely accepted model like others models.

Climate change Impact on Lake Tana water storage Using HBV-Light model, upper Blue Nile Basin, Ethiopia [3]**.** Variations in temperature and precipitation trends impact the elements of the hydrological cycle, the accessibility of water resources, and the ensuing changes in the equilibrium of lake water (lake level). The HBV model's performance was assessed through calibration and validation using objective functions (RVE, NSE). For Gumara, Kiltie, Koga, Gilgle Abbay, Megech, and Rib, respectively, the model provided NS of 0.79, 0.63, 0.72, 0.803, 0.68 and 0.797 during calibration and NSE of 0.8, 0.64, 0.7, 0.82, 0.801, and 0.82 during validation. Similarly, for Koga, Gilgle Abbay, Megech, and Rib, the model provided RVE of 3.7%, -1.27%, 1.05%, -0.72%, 8.9%, and -0.68 during validation. This findings revealed that the model to simulate the lake.

Impact of Climate change on Water availability and Comparative study of HBV-Light conceptual hydrological models, Awata watershed, Genale Dawa river Basin, Southern Ethiopia [55] using current climate inputs and observed river flows, the two hydrological models (HBV Light and GR4J) were successfully calibrated (2003-2012) and verified (2013-2017) on the watershed basis. The two models' combined total performances were good, at the monthly time scale; on the GR4J model, calibration (R2=0.86) and validation (R2=0.81) are higher than those on the HBV Light calibration (R2=0.87) and validation (R2=0.85).

Assessment of Climate Change Impacts on the water Resources of Megech River Catchment, Abbay Basin, Ethiopia [13] using current climate inputs and observed river flows of the Megech river catchment, the HBV-Light hydrological model was successfully calibrated (1991–1995) and validated (1998–2000). On a monthly time frame, the model performed well overall for both calibration (NSE = 0.91) and validation (NSE = 0.86).

Additionally, studies on climate change that use the HBV-Light model are [13], Impact Assessment of Climate Change on the Hydrology of Gojeb River Catchment in Western Omo Gibe River Basin, Ethiopia. [50], Downscaling Climate Model Outputs for Estimating the Impact of Climate Change on Water Availability over the Baro-Akobo River Basin, Ethiopia had shown the HBV-Light hydrological model is widely accepted in different parts of the world including Ethiopia.

2.5. Hydrological Model Selection Criteria

Model selection is challenging for practicing a hydrologist because of the complexity and patterns of the hydrologic data; however, the model section is based on the availability of input data, the nature and type of hydrologic process needed to be simulated, and nature of data handling mechanisms. The following factors and criteria are relevant when selecting a model:

- The general modeling objective is, e.g., hydrological forecasting, assessing human influences on the natural hydrological regime, or climate change impact assessment.
- The type of system to be modeled; e.g., a small catchment, a river reach, a reservoir or a large river basin.

- The hydrological element(s) to be modeled are, e.g., floods, daily average discharges, monthly average discharges, and water quality, amongst others.
- The climatic and physiographic characteristics of the system are to be modeled.
- Data availability with regard to type, length, and quality of data versus data requirements for model calibration and operation.
- Model simplicity, as far as hydrological complexity and ease of application is concerned.
- The possible transposition of model parameter values from smaller sub catchments of the overall catchment or from neighboring catchments.
- The ability of the model to be updated conveniently on the basis of current hydrometeorological conditions.

3. MATERIAL AND METHODOLOGY

3.1. Description of the Study Area

3.1.1. Location

Sibilu River catchment is found in the Sululta district, Special Zone, Oromia Regional State, to the north of Addis Ababa on the Fitche highway. It has catchment area of about 61,655.5 hectares (616.555 k m2) in the upper Abbay Basin. Geographically, it is bounded by 9º 5' 8.23''and 9º 27 '26.7'' North latitude and 38º 33' 28.453'' and 38º 49' 55.207'' East longitude. The study area ranges in elevation from 1420 m.a.s.l the downstream of the Sibilu River to 3400 m.a.s.l. at the picks of Cheleleka Mountain [41] and is about 26 km from Addis Ababa.

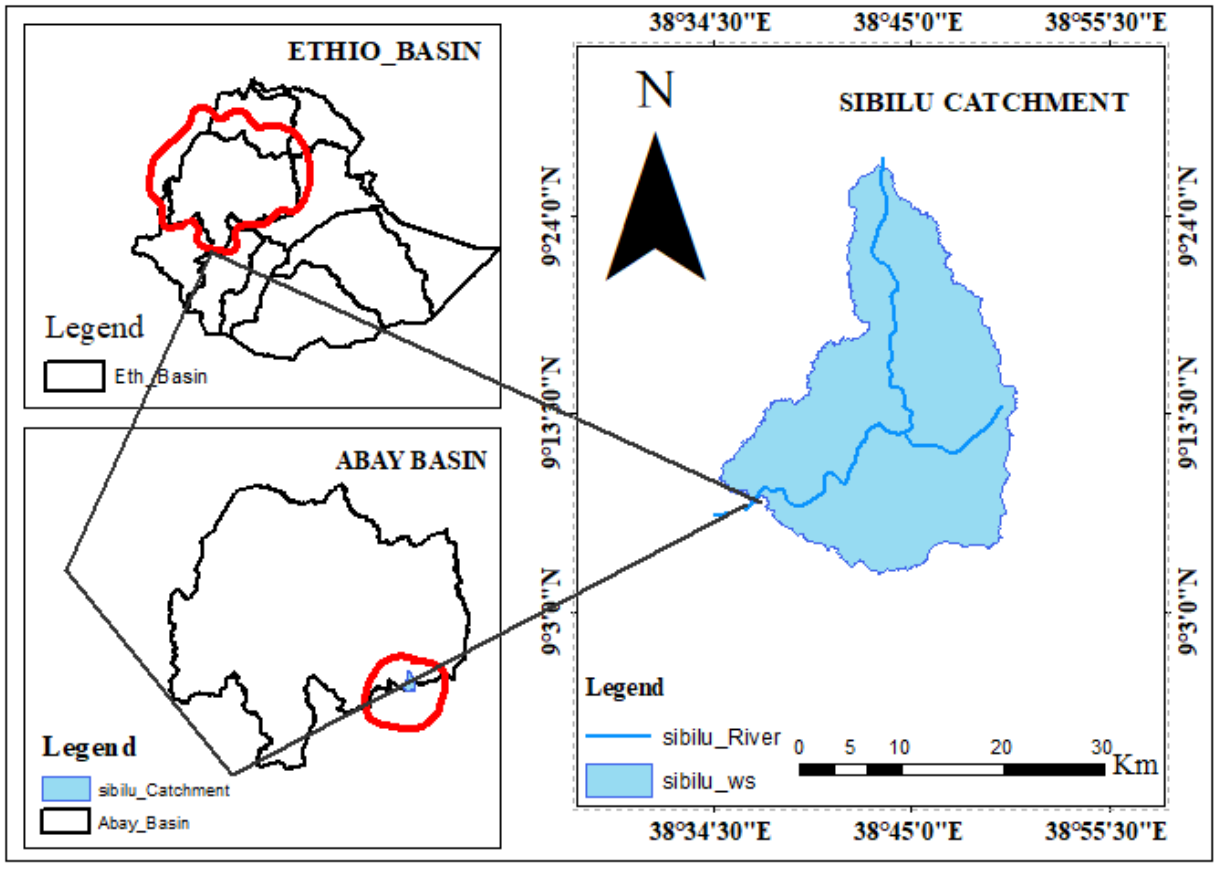

Figure 2: Location Map of Sibilu River Catchment

3.1.2. Topography

Topography is an aspect of land surface and a significant factor in catchment response. The area covers the uppermost catchment of the Abbay basin, which drains into a northerly direction. Predominately, the catchment is composed of flat lands and hill domes, including undulating terrain and river gorges. Sibilu River meanders in the flat area of Sululta Plain and drains in the northwest direction, which is bounded by the Cheleleka Nono mountains in the east, whereas in the south Entoto and undulating terrain of the river gorges in the northwest. Several streams merged and flowed in northeastern and northwestern directions. Finally, the streams formed broad and deep dissected gorges near Chanco and drain to the Muger River, which is the main tributary of the Abbay basin. Five classes of slope classification of the catchment were done based on [74] guidelines. Accordingly, the excessive slope of the catchment lies south as well as at the center and decreases northward. A steep and very steep slope (30-60%) lies northwards. Similarly, a flat and strongly sloppy slope (0-15%) lies at the south, including the center of the catchment, and decreases towards the north.

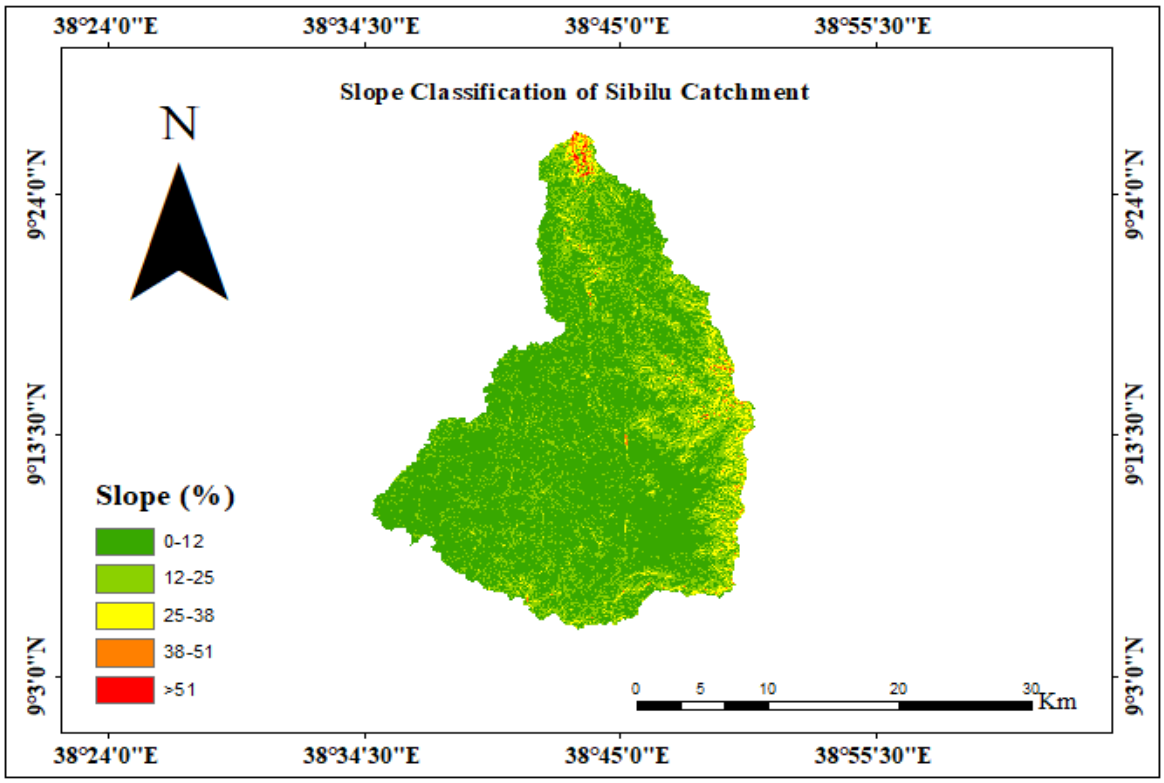

Figure 3: Slope Classification of Sibilu Catchments

3.1.3. Hydrology

The Sibilu River is a perennial river that has a gauge station near Chanco, and its river flow depends on seasonal rainfall variability. Subsequently, the river originated from Entoto mountain chains at an elevation of 3200 m.a.s.l., which is in the southern part of the study area, and falls at 1450 m.a.s.l. in the river length, from which it confluences with the Muger River [41]. Intermittent streams and tributaries such as Weserbi, Dakeye, Deneba, Lega Guda, Shunke, Bori, Roba, and Chanco are the main sources of the Sibilu River on the left and right banks of the catchment. The river flow starts rising in June, reaches its peak in August, and similarly starts slowing down from September to December, as shown in Figure 4.

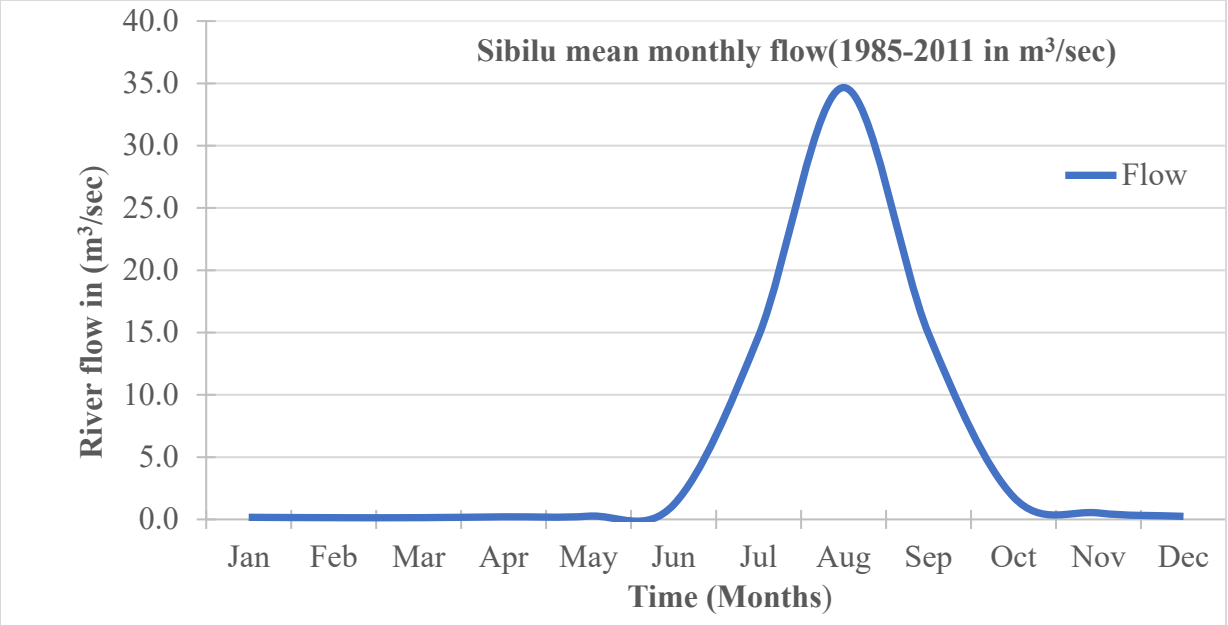

Figure 4: Mean monthly flow of Sibilu River near Chanco outlet (1985-2011)

3.1.4. Climate Condition

According to [75], Ethiopia's climate varies widely due to its varying topography and relative placement. The Inter-tropical Convergence Zone (ITCZ), which is elevated by the convergence of trade winds in the northern and southern hemispheres with that of related atmospheric circulation, controls Ethiopia's climate on a seasonal basis [76]. It has had a significant impact on the country's complicated regional and local geography ever since. Warm temperatures and agro-atmospheric circulation are characteristics of the tropical humid climate zone, which includes the

Sibilu watershed in this instance. Rainfall in the nation varies in quantity and distribution due to the strength, location, and orientation of the aforementioned weather systems, which is relevant to the study.

3.1.5. Rainfall

Rainfall across Ethiopia is very seasonal, and typically there are major rainy seasons (Jun-Sep), which are dominated by major rainfall; Belg (Feb-May), short rain season; and Bega (Oct-Jan), which brings generally dry weather to the central and northern Ethiopia, according to [77]. Rainfall in Ethiopia is predominately controlled by the multi-weather systems of Sub Tropical Jet (STJ), Inter Tropical Convergence Zone (ITCZ), Read Sea Convergence Zone (RSCZ), Tropical Eastern Jet (TEJ), and Somalia Jet [78].

The rainfall of the study area is characterized by two different rainfall patterns, which are called bimodal, as stated by [42]. The main wet season, locally named Kiremt, extends from June to September, while the minor rainy season, which is locally called Belg, contributes moisture to the region from mid-February to mid-April [42]. In this case, the highest rainfall was observed in the months of July and August, respectively. A short rainy season was observed from November to February, followed by the lowest rainfall in the month of December. Based on data from the meteorological stations, of Addis Ababa Observatory, Chanco, Entoto, and Sululta station, the average annual rainfall distribution is about 1327.2 mm.

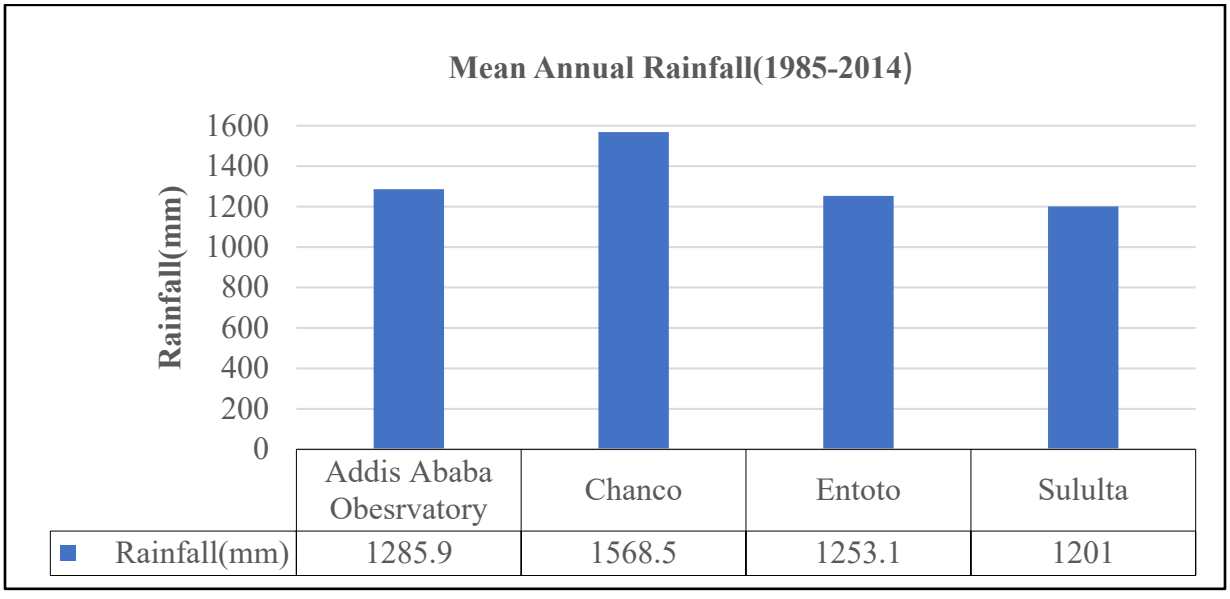

Figure 5: Mean Annual Rainfall Stations of Sibilu Catchments (1985-2014)

The mean maximum and minimum temperature of Addis Ababa Observatory (1985-2014) at an elevation of 2386 m.a.s.l. vary from 21.10 ^{0}C to 25.39 ^{0}C and 8.34 ^{0}C to 12.47 ^{0}C, respectively. The station has a mean annual rainfall of 1285.9 mm, and the rainy season starts from April to October, with a peak in July and August. Among the stations used for the determination of area rainfall, the station has the least contribution of point rainfall since it is outside of the catchment.

The mean maximum and mean minimum temperature of Chanco (1985-2014) at an elevation of 2632 m.a.s.l. vary from 20.5 ^{0}C to 24.16 ^{0}C and 7.71 ^{0}C to 10.64 ^{0}C, respectively. Similarly, the station has the highest amount of areal rainfall, which is about 1568.5 mm, and contributes more as compared to the other stations. The main rainy season starts from May to September and reaches its peak during July and August, followed by September.

The mean maximum and mean minimum temperature of Entoto (1985-2014) at an elevation of 2903 m.a.s.l. vary from 16.14 ^{0}C to 20.55 ^{0}C and 7.52 ^{0}C to 10.04 ^{0}C, respectively. The station has a mean annual rainfall of about 1253.1mm, and it is the second largest next to Chanco station. The Main rain season starts from April to September and peaks in July and August.

The mean maximum and mean minimum temperature of Sululta (1985-2014) at an elevation of 2610 m.a.s.l. vary from 20.12 ^{0}C to 23.59 ^{0}C and 4.46 ^{0}C to 6.42 ^{0}C, respectively. It has about 1201.0mm of mean annual rainfall, and is the third contributing station next to Entoto. The mean maximum and minimum temperature of the Sibilu catchment are 21.6 ^{0}C and 8.6 ^{0}C, respectively. The main season began in June and ended in September, with peaks in July and August. In general, the rainfall and temperature patterns in all stations follow almost all similar trends, as shown in Figure 6.

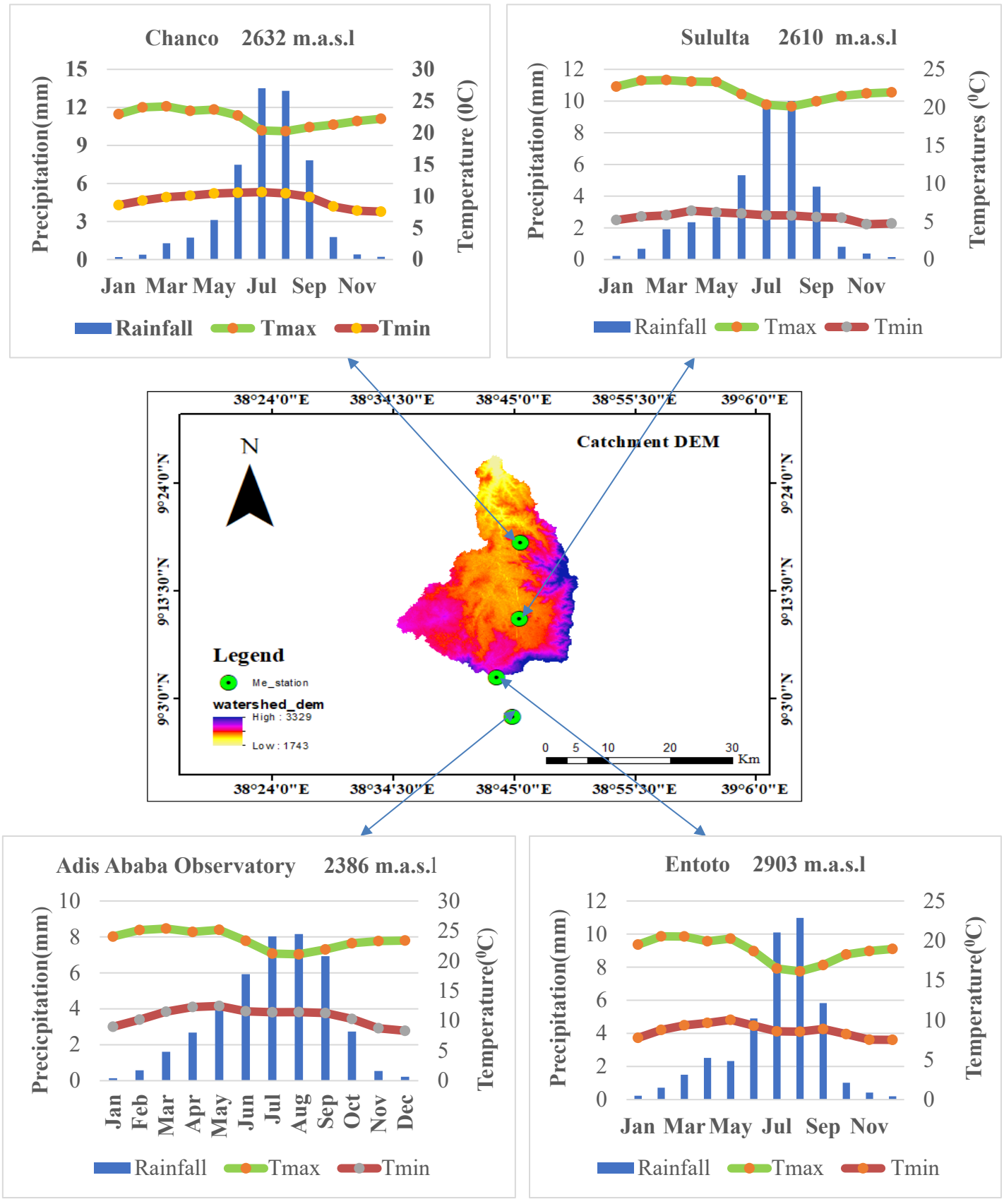

Figure 6: Mean monthly rainfall and temperature of the stations

3.2. Data Types and Sources

Issues to consider in selecting the climatological baseline include the types of data required, the duration of the baseline period, the sources of the data, and how they can be applied in an impact assessment. Relevant and appropriate data are very essential for the simulation of any model to achieve the objective of the research through major milestones. Therefore, the basic and essential task of this study was getting the right data specifically for the model being modeled.

The World Meteorological Organization has recommended 30 years as a minimum for searching for evidence of climate change in hydroclimate time series [79]. Based on these criteria, four stations were identified both in and near the study area. The data applied for climate impact studies were gathered from ministry, regional, and local- level data sources, and most of them were made available using climate and hydrological models.

3.2.1. Meteorological Data

Metrological data in this study was mainly used for two purposes. First used for hydrological modeling to simulate the hydrological process of the catchments. Second, it was used as input for CORDEX-Africa data.

Accordingly**,** the long-term records of daily metrological data for 30 years **(**1985-2014) were gathered from the Ethiopian National Meteorological Service Agency (ENMSA) Head Offices. Daily data like rainfall, maximum and minimum temperature, relative humidity, wind speed, and sunshine hour's data can be collected from the four selected metrological stations (Addis Ababa Observatory, Chanco, Entoto, and Sululta). Other than Addis Ababa Observatory, all the stations record mainly rainfall and temperatures since they are classes three and four. Though Addis Ababa Observatory records fully rainfall, minimum, and maximum temperatures, relative humidity, wind speed, and sunshine hours, there is still a huge gap of missed data on relative humidity, Wind speed, and Sunshine hours that were not filled by the data filing method like rainfall, maximum and minimum temperatures.

Table 1: List of station name, location and meteorological variables

Station Name	Lat (DD)	Long (DD)	Elev (m)	Rain	Tmax	Tmin	RH	WS	SH
A.A.Observatory	9.01891	38.7475	2386	✓	✓	✓	✓	✓	✓
Chanco	9.303	38.759	2632	✓	✓	✓			
Entoto	9.08366	38.725	2610	✓	✓	✓			
Sululta	9.179	38.758	2903	✓	✓	✓			

Source: Ethiopian National Meteorological Station

(Lat= Latitude, Lon= Longitude, DD= Degree Decimal, Elev= Elevation, Tmax= Maximum Temperature, Tmin= Minimum Temperature, RH = Relative Humidity, WS= Wind Speed, SH= Sunshine hours).

All stations listed above contain daily rainfall and temperature data for overlapping period of 30 years. Therefore, all stations were used for hydrological model development and used for as input for CORDEX data. As it can be seen from fig 7, Chanco, Entoto and Sululta are located within the watershed whereas Addis Ababa Observatory is out of the watershed. Sululta station was used as reference station for the study area.

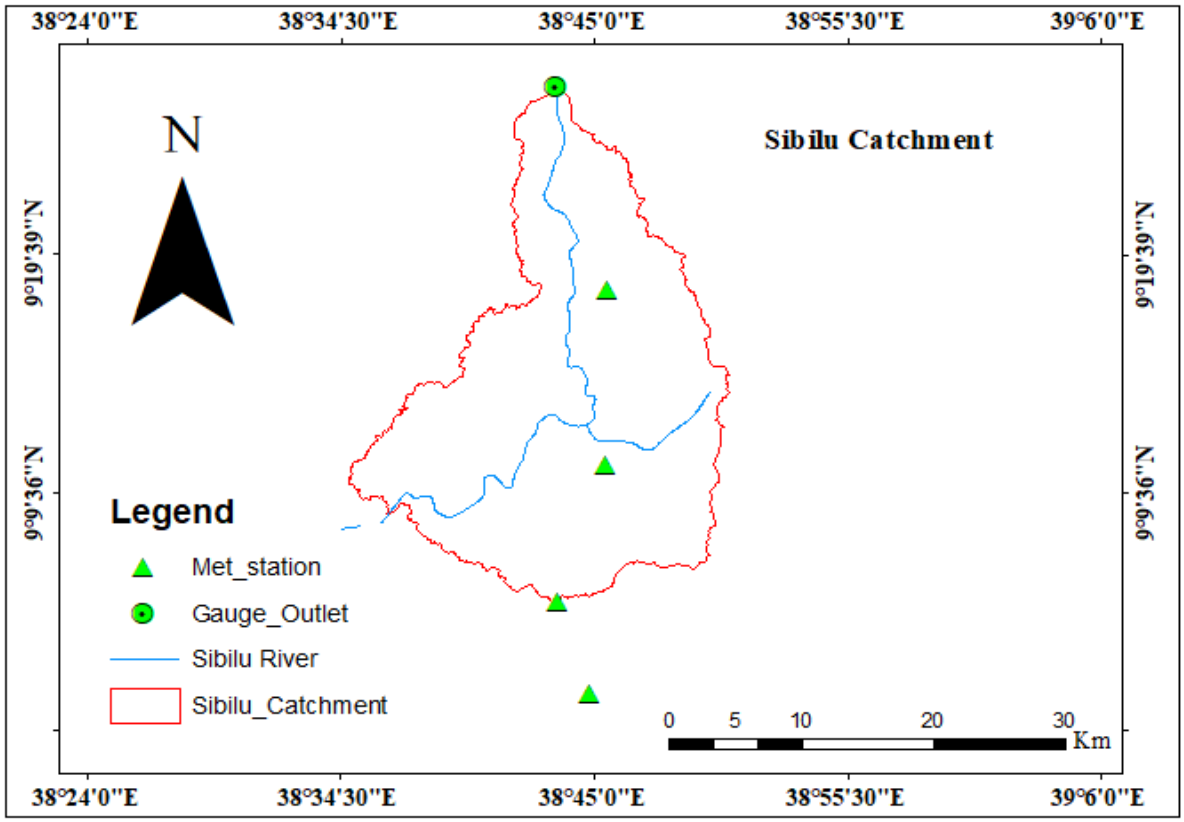

Figure 7: Location of Meteorological and Outlet of Sibilu Watershed

3.2.2. Hydrological Data

The stream flow data of the Sibilu river catchment is required for calibrating and validating the models. The gauging station, which is found at Chancho gauging station, is used. The daily and average monthly stream flow discharge data for 27 years (1985-2011), which has a continuous record for relatively long period, was collected from the Minster of Water and Energy (MoWE).

3.2.3. Digital Elevation Model (DEM)

For this study area, (DEM) Digital Elevation Model was used having 30 * 30m resolution which is collected from Ministry of Water and Energy (MoWE. DEM map of the area was processed using Arc-GIS to delineate the catchment and analyze the drainage pattern of the land surface terrain. Elevation of the area generally drops to the northwest direction which varies from 1420 m.a.s.l at the downstream of Sibilu river to 3400 m.a.s.l at the picks of Cheleleka mountain [41].

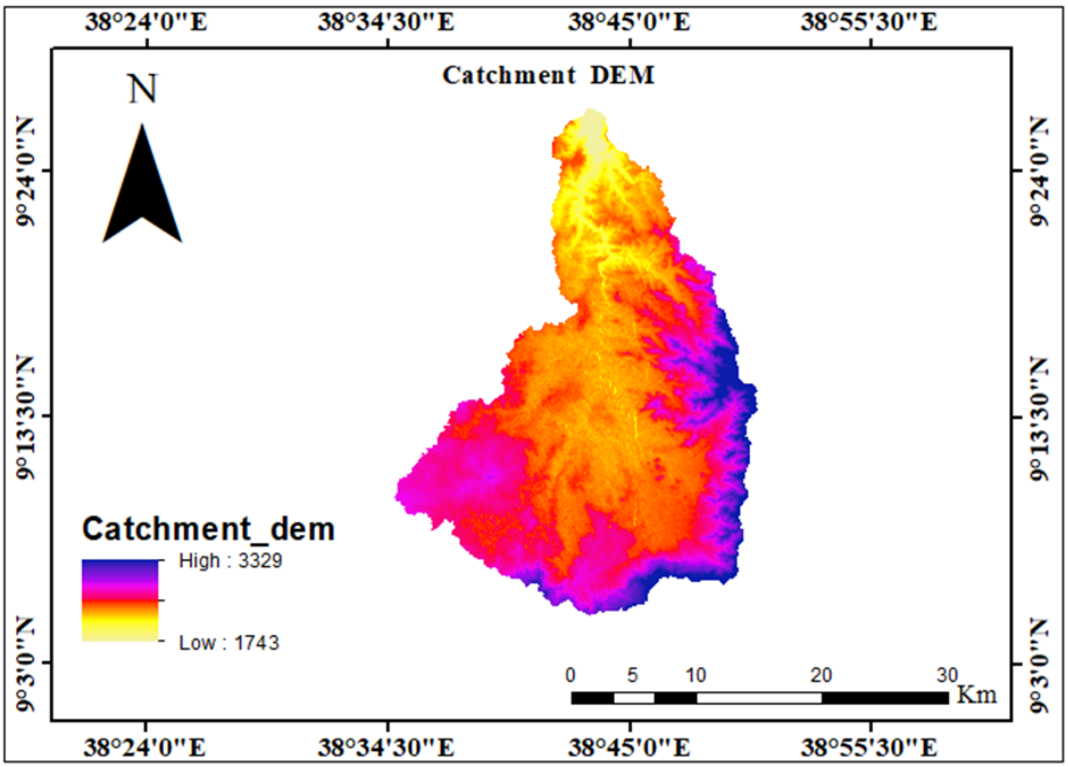

Figure 8: DEM map of Sibilu Watershed

3.2.4. Soil, Topographic map and LULC data

3.2.4.1. Soil

Soil data that are used for characterizing soil of the study area and also data used for preparing a topographic map as well as the LULC (Land use land cover), which is an attribute of the condition of the LULC of the area collected from the Ministry of Water and Energy (MoWE) for manipulation in Arc GIS software. Soils are one of the largest world's natural resources, and hence a soil map is a spatial representation of these resources. Therefore, the preparation of soil maps is fundamental and should be the turning point since it affects the water balance of the catchments. Accordingly, there are five major soil groups in the catchments. The Catchment's soils are Luvisols, Cambisols, Vertisols, Leptosols, and Nitosols, which can be classified into five soil units: the Chromic Luvisols, Eutric Cambisols, Eutric Vertisols, Eutric Leptosols, and Haplic Nitosols respectively. Chromic Luvisols are dominant soil type found in the catchments, covering about (21.32%). Eutric Cambisols are the second most of common soil type covering about (21.07%). Eutric vertisols cores about (18.99%) which is the third soil most common type

followed by Eutric Leptosols, which is about (6.38%) and Haplic Nitosols which cover about (1.44%) respectively. Soil map of Sibilu catchment is shown in figure 9 below.

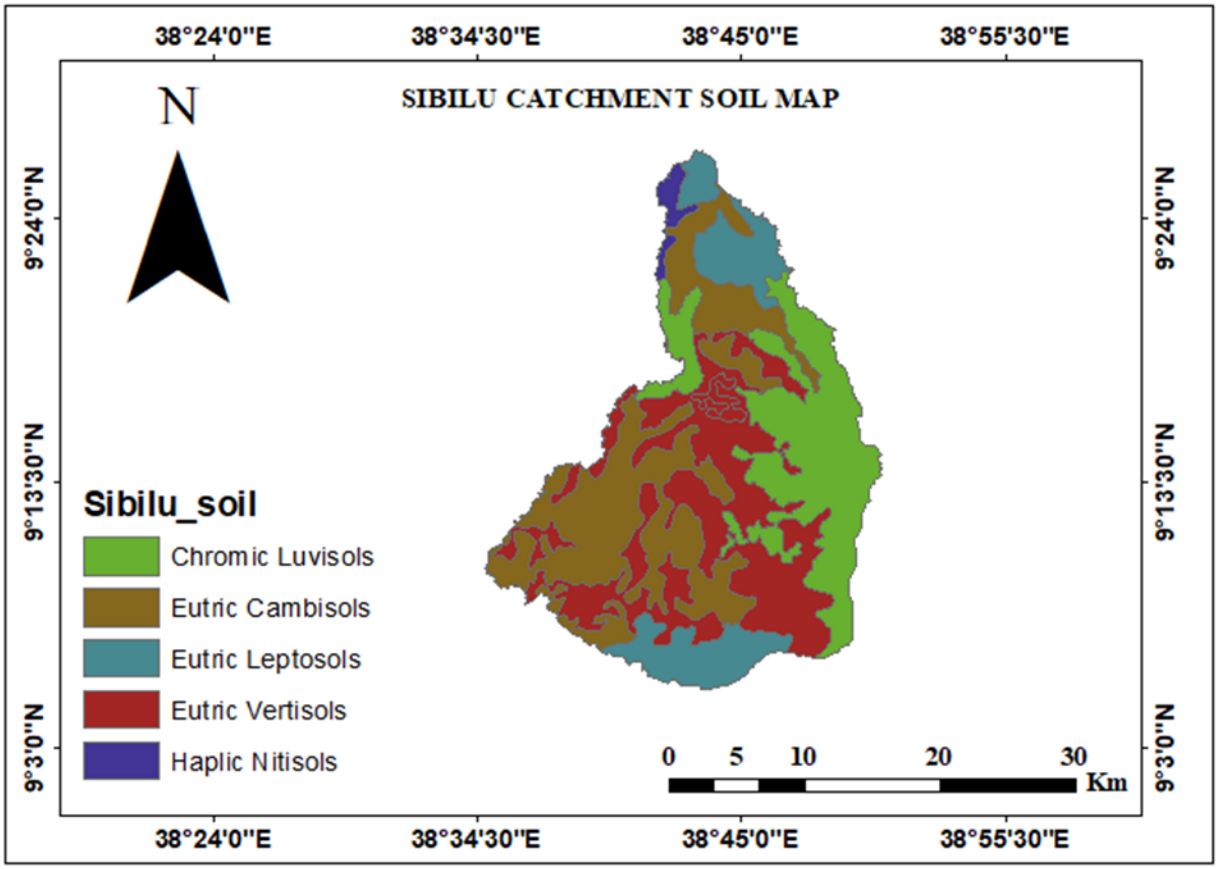

Figure 9: Soil map of Sibilu Catchment

3.2.4.2. Land Use Land Cover

The 2013 classification of land and land cover were obtained from the Ministry of Water and Energy. Land use/Cover of the Sibilu catchment of Land use and land cover are an important aspect for modeling and understanding the catchment process and are key parameters for assessing the climate change impact related to water resource management activities. The Land cover of the catchments is driven by topography, Climate, and ecological conditions that typically influence the hydrological properties of the entire catchment. Based on the LULC map of the catchment's study area, it is covered with cultivation. And also, the catchments constitute wetlands, settlements, open grass, bare soil, and dense forest. The LULC map of the Sibilu catchment is shown in figure 10 below. The information regarding on LULC extent plays

significant role in characterizing LULC of the study area and easily understand catchment importance for future aspects as a whole.

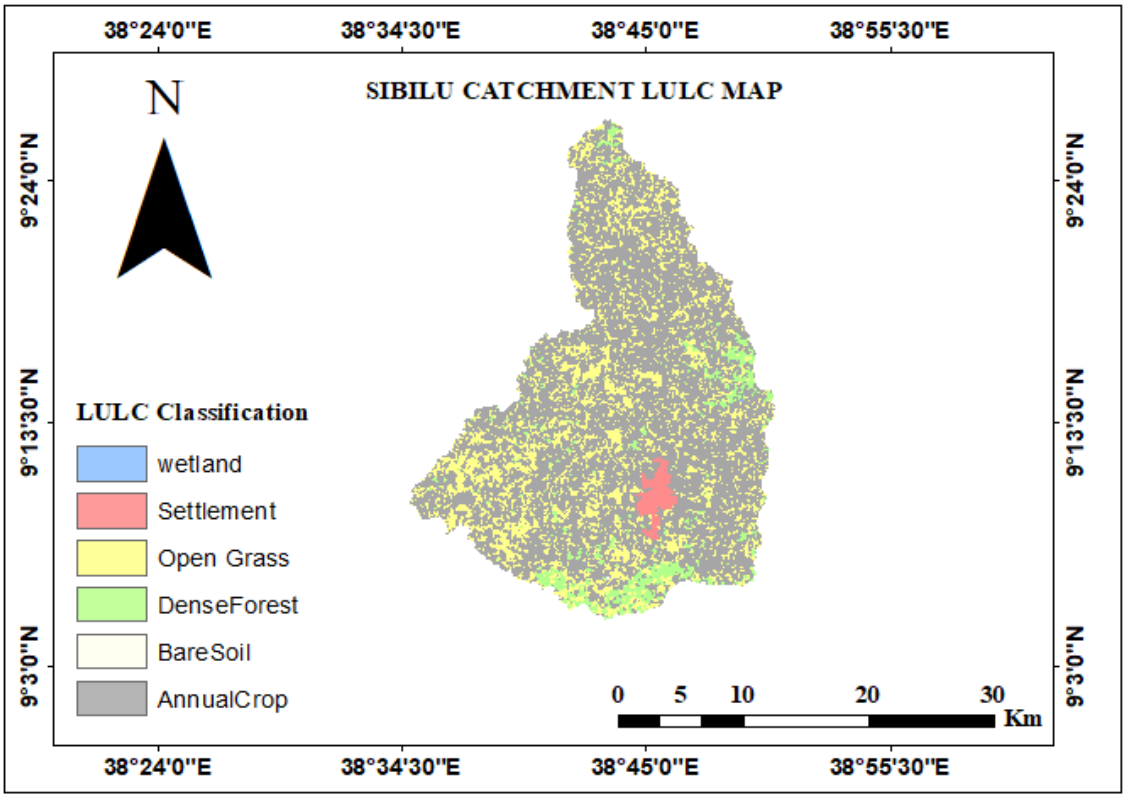

Figure 10: Land use /Land cover of map of Sibilu Catchment

3.2.5. Major Socio-economic Activity

The main economic activity in the study area is agriculture, dairy farming, trade, manufacturing, Agro-industry, water production, construction materials like quarrying, agricultural crop production, and commerce. Dairy farming is the main duty of households engaged in agriculture since the plain is endowed with grass. As a result, it is the main source of animal feed in the area due to the water logging problem for crop production. In a nutshell, crops such as pulses and minimal oil seeds are found to be socio-economic activity in the area [80].

3.3. Software and Models used

3.3.1. Software

In order to attain the desired goal of this study, software has an accounted value. In this case, software such as ArcGIS version 10.4 was utilized for acquiring the spatial, hydrological, and physical characteristics of the catchment. XLSTAT 2019 was applied for homogeneity test of rainfall data. Spread sheet excel was used for preparing meteorological and hydrological data (stream flow) in suitable formats. Mule date convertor aimed to arrange stream flow and meteorological data in the vertical direction. Medeley desktop was applied for referencing the citations from different sources. Google earth used to find and at the same time to check the coordinate and elevation with providing a clear view of the catchment. CMhyd tools is used for both extraction and bias correction of dynamically downscaled climate data (Rainfall, maximum, and minim temperatures).

3.3.2. Models Used

For achieving the goal of the study area, the output RCM was selected in the frame work of CORDEX-Africa project for studied the future climate change impact assessment. Due to the three reasons, Africa was chosen as the CORDEX target. In line with [23], they were highly vulnerable to climate change, relatively low adaptive economy capacity, and substantial changes in rainfall and temperature patterns. HBV-Light hydrological model was used for formulating water resource availability of the Sibilu river catchment. The model was selected due to its simplicity, less input data requirement, availability, and widely accepted which were used for assessing climate change from simple regional to catchment scale, widely catchment to large watershed and wide global accepted [69].

3.4. Data Quality Control and Adjustment for Model Input

3.4. 1. Data Quality Checking and Control

Missing data is one of the most important tasks in a weather station and of the foremost complications that are frequently come across in climate research analysis. This may be due to the absence of an observer or short disturbances in observations due to different causes. The most frequent problems of the breakage, malfunction, and calibration problem of instruments during a certain time period. There are different methods used to fill in the missing data from

weather stations. These are: arithmetic mean, normal ratio methods, inverse distance weighing methods and Linear programming methods.

3.4.1. 1. Arithmetic mean method

The missing precipitation P_X can be determined using arithmetic average, if the normal annual precipitation at target stations is within 10% of the normal precipitation at target station, X as follows:

$$P_X = \frac{1}{m}(P_1 + P_2 + \cdots, + P_n) \quad (1)$$

3.4.1. 2. Normal ratio method

If the normal precipitations vary considerably then P_X is estimated by weighting the precipitation at target stations at neighboring station is above 10% of normal annual precipitation and calculated as follows:

$$P_X = \frac{N}{m}\left[\frac{P_1}{N_1} + \frac{P_2}{N_2} + \cdots, + \frac{P_m}{N_n}\right] \quad (2)$$

This method is based selecting m (m is usually 3) stations that are near and approximately evenly spaced around the station with the missing record.

Where, P_X is the daily rainfall or temperature with missing records, P_1, P_2, P_3, n_x are recorded daily rainfall or temperature, N_1, N_2, N_3, ...N_m are recorded normal annual precipitation or temperature and m is the number of observations for estimation.

3.4.2. Filling of Missing Data

Normal annual rainfall at each neighboring station was above ten percent of normal annual precipitation at the target station since the data were filled by the normal ratio method (equation 2), as recommended by WMO, and then the data was used to test for consistency and homogeneity as well. Similarly, the method was used for selected stations of Addis Ababa Observatory, Chanco, Entoto, and Sululta.

3.4.3. Consistency test of time series

Before plotting a cumulative rainfall curve, it were necessary to understand the best methods used. Checking the consistency of rainfall recorded is an important concept for producing

reliable information for hydrological investigation. Double mass curve analysis is the common method used for check for inconsistency in a rain gauged record. The curve is a plot of cumulative rainfall of one or more gauges in the region that has been subjected to similar hydrometeorological occurrences and is known to be consistent [15]. An inconsistent record may result from a number of reasons, shifting of the rain gauge to a new location, undergoing marked change of neighboring stations, changes in the ecosystem due to calamities, and the occurrence of an observational error from a certain date. In this case, a constant slope was observed, but if a change in slope is significantly evident, then the record of station X needs to be adjusted by multiplying the record values of rainfall by the ratio of slopes of the straight lines before and after a change in the environment. Finally, the corrected precipitation was adjusted by the following relationship.

$$Y2 = \frac{S2}{S1} * Y1 \quad (3)$$

Where: Y_2= corrected precipitation at station X

Y_1= Original recorded precipitation at station X

S_2= Slope of double mass curve to be corrected

S_1= Original slope of double mass curve

Accordingly, the double mass curve was plotted by using the total annual cumulative rainfall of the base station as an ordinate while average annual total of neighboring stations as an abscissa and found to be linear for all the considered stations. Since is no significant change were observed in the regime of the curve, unfortunately all the selected stations used in the study were consistent, hence there was no need for further correction as shown in Figure below (11).

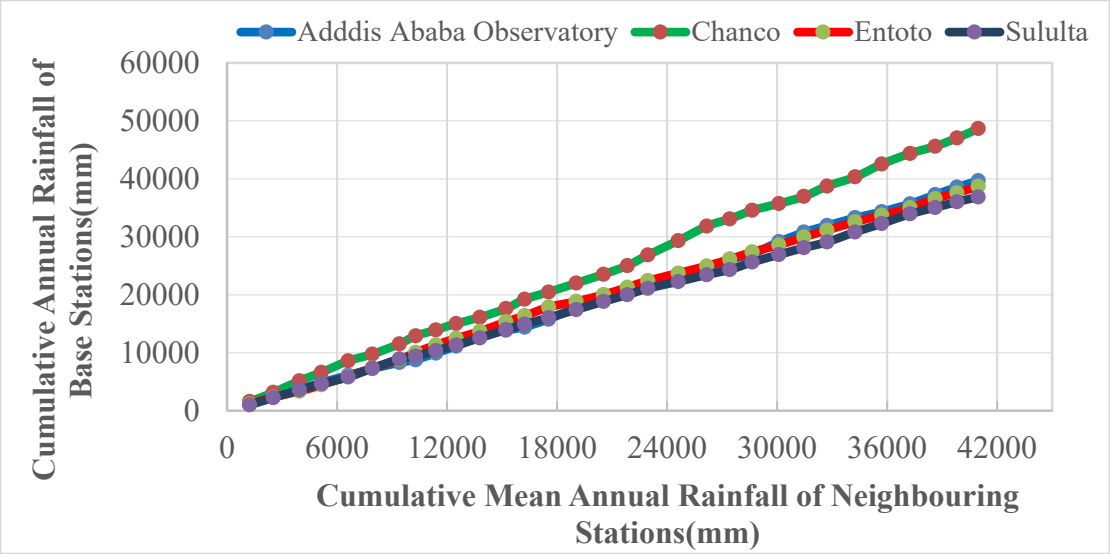

Figure 11: Double mass curve of rainfall stations nearby the catchments

3.4.4. Homogeneity test of time series

The homogeneity of the annual rainfall for all the stations (Addis Ababa Observatory, Chanco, Entoto, and Sululta) was analyzed by XLSTAT version 2019 statistical software using standard Normal Homogeneity Test Method (SNHT). At the time of analysis the P-value has been computed using Monte Carlo simulations at a 95% confidence interval. The result revealed that the P-value was greater than the significant level alpha value (α=0.05), hence all rainfall data at the station were homogenous since we cannot reject the null hypothesis (H0). The sample test homogeneity of annual rainfall for meteorological stations (Addis Ababa Observatory, Chanco, Entoto, and Sululta) is graphically presented below (Fig .12).

Table 2: Summary statistics of homogeneity test

S. No	Station Name	Variable	Obs.	Mean	SD	T0	alpha	P-value
1	AA Obs	Prec.	30	1285.88	414.9	4.217	0.05	0.393
2	Chanco	Prec.	30	1568.50	381.8	2.478	0.05	0.719
3	Entoto	Prec.	30	1253.11	166.9	3.078	0.05	0.563
4	Sululta	Prec.	30	1201.01	264.1	2.941	0.05	0.623

Where; T0= Statistic derives, Prec= precipitation, Obs= Observation, SD= Standard deviation

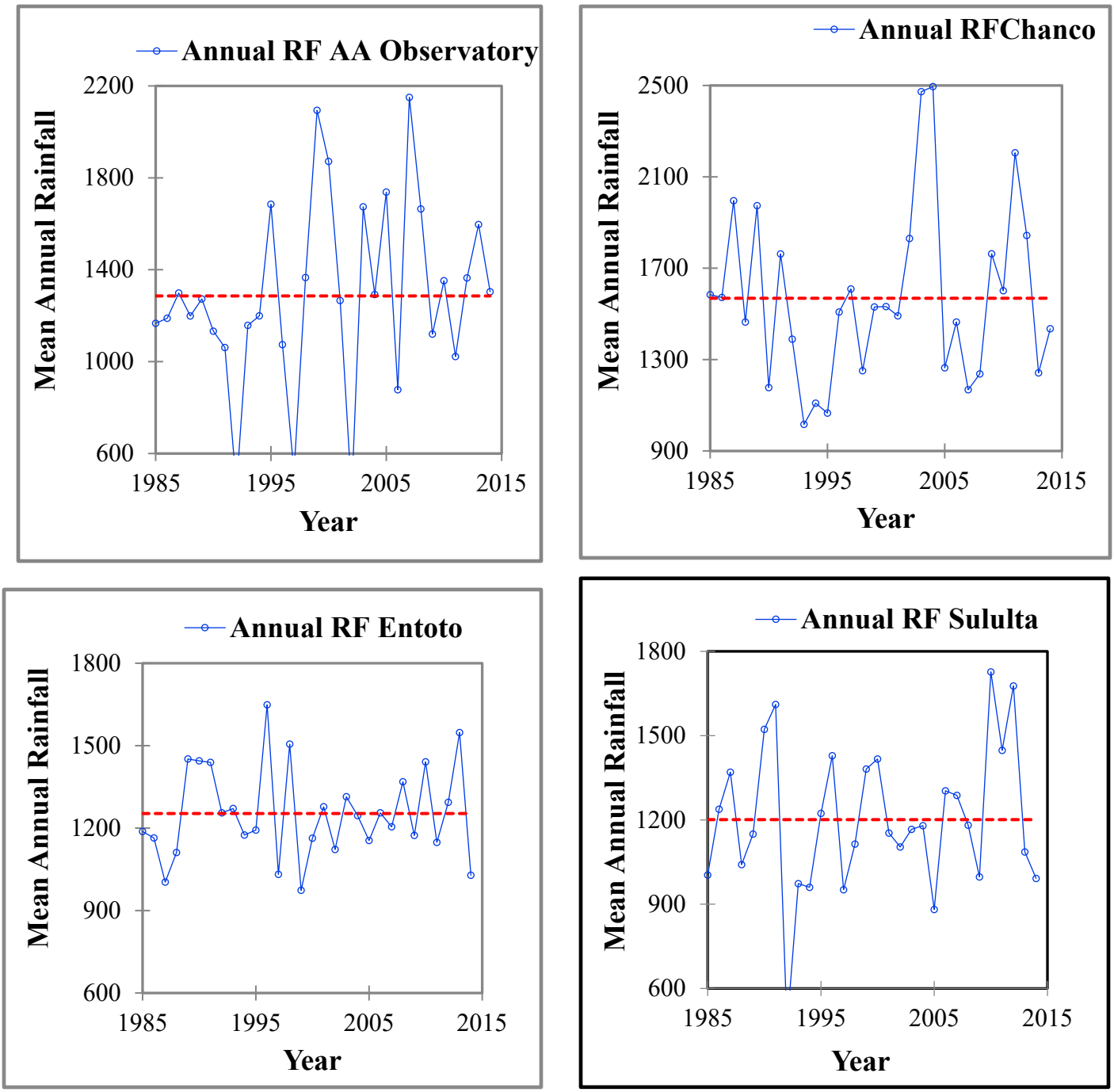

Figure 12: Rainfall homogeneity test for all stations

3.4.5. Test for Outliers

3.4.5.1. Grubbs-Beck (G-B) Test

An outlier is a rainfall observation that deviates from the rest of the data for various causes. High and low outliers have different effects on the analysis of rainfall data [81]. The following formulas are used to determine the X_H and X_L values.

$$X_H = EXP(\bar{X} + KN * S) \quad (4)$$

$$X_L = EXP(\bar{X} - KN * S) \quad (5)$$

Where $\bar{X}$ and S are the sample's natural logarithms of mean and standard deviations, and X_H and X_L are the upper and lower outliers, respectively. At 10% significant level K_N is determined by the following formula.

$$K_N = -3.62201 + 6.28446N^{1/4} - 2.49835N^{1/2} + 0.491436N^{3/4} - 0.037911N \quad (6)$$

Where N=Sample size and 5≤ N≤ 150. In this case, N=30

Values in the sample that are higher than X_H are regarded as high outliers, whereas values that are lower than X_L are regarded as lower outliers. Therefor data series bigger than X_H and smaller than X_L are flagged as an outlier data [82]. For Addis Ababa station:

$$KN = -3.62201 + 6.28446 * 30^{\frac{1}{4}} - 2.49835 * 30^{\frac{1}{2}} + 0.491436 * 30^{\frac{3}{4}} - 0.037911 * 30$$

$K_N == -3.62201+14.70782-13.68403+6.299527+1.13733$

$K_N = 22.14 - 17.30 = 4.84$

K_N =2.56

Then after calculating statistical parameters the next step is determining upper and lower limits.

Mean=3.81

Standard deviation =0.18

K_N= 2.56

Upper Limit

$X_H = EXP(\bar{X} + KN * S)$

$X_H = EXP(3.81 + 2.56 * 0.18)$

$X_H = EXP(4.84)$ =71.52 mm

Lower

$X_L = EXP(\bar{X} - KN * S)$

$X_L = EXP(3.73 - 4.84 * 0.23)$)

$X_L = EXP(2.62)$ = 28.50 mm

The results show that for annual maximum daily rainfall data 28.50 mm is smallest and 71.52 mm is the largest value, which means the values outside these ranges should be studied or care shall be taken. But in case of Addis Ababa Observatory Rainfall station there were no outliers. For Chanco station:

Mean =3.77

Standard deviation =0.36

$K_N = KN = -3.62201 + 6.28446 * 30^{\frac{1}{4}} - 2.49835 * 30^{\frac{1}{2}} + 0.491436 * 30^{\frac{3}{4}} - 0.037911 * 30$

K_N=2.56

Then after calculating statistical parameters the next step is determining upper and lower limits.

K_N=2.56

Upper Limit

$X_H = EXP(\bar{X} + KN * S)$

$X_H = EXP(3.77 + 2.56 * 0.36)$

$X_H = EXP(4.69)$ =108.85 mm

Lower

$X_L = EXP(\bar{X} - KN * S)$

$X_L = EXP(3.77 - 2.56 * 0.36$)

$X_L = EXP(2.85)$ =17.29 mm

The results show that for annual maximum daily rainfall data 17.29 mm is smallest and 108.85 mm is the largest value, which means the values outside these ranges should be studied or care shall be taken. In case of Chancho Rainfall station there is upper outlier in the year 2012 and the magnitude is 123.0mm. For Entoto station:

$K_N = KN = -3.62201 + 6.28446 * 30^{\frac{1}{4}} - 2.49835 * 30^{\frac{1}{2}} + 0.491436 * 30^{\frac{3}{4}} - 0.037911 * 30$

K_N=2.56

Then after calculating statistical parameters the next step is determining upper and lower limits.

Mean =3.80

Standard deviation =0.23

K_N=2.56

Upper Limit

$X_H = EXP(\bar{X} + KN * S)$

$X_H = EXP(3.80 + 2.56 * 0.23)$

$X_H = EXP(4.39)$ =80.6 mm

Lower

$X_L = EXP(\bar{X} - KN * S)$

$X_L = EXP(3.80 - 2.56 * 0.23)$

$X_L = EXP(3.2)$ =24.53 mm

The results show that for annual maximum daily rainfall data 24.53 mm is smallest and 80.60 mm is the largest value, which means the values outside these ranges should be studied or care shall be taken. But in case of Entoto Rainfall station there were no outliers. For Sululta station:

$KN = -3.62201 + 6.28446 * 30^{\frac{1}{4}} - 2.49835 * 30^{\frac{1}{2}} + 0.491436 * 30^{\frac{3}{4}} - 0.037911 * 30$

K_N == -3.62201+14.70782-13.68403+6.299527+1.13733

$K_N = 22.14 - 17.30 = 2.56$

K_N = 2.56

The next step is calculating the upper and lower limits.

Then after calculating statistical parameters the next step is determining upper and lower limits.

Mean = 3.73

Standard deviation = 0.23

K_N = 2.56

Upper Limit

$X_H = EXP(\bar{X} + KN * S)$

$X_H = EXP(3.73 + 2.56 * 0.23)$

$X_H = EXP(4.32)$ =75.19 mm

Lower

$X_L = EXP(\bar{X} - KN * S)$

$X_L = EXP(3.73 - 2.56 * 0.23)$)

$X_L = EXP(3.14)$ =23.10 mm

The results show that for annual maximum daily rainfall data 23.10 mm is smallest and 75.19 mm is the largest value, which means the values outside these ranges should be studied or care shall be taken. 75.19 were outside of this range which means that there was a flood with a rainfall depth of magnitude of 75.19 mm. But there was no value greater than the 75.19 mm and in the sululta rainfall station, there were no outliers.

3.5. Application of Thiessen Polygon for Areal Rainfall Determination and PET

For this particular study, the determination of areal rainfall at each station was computed by the Thiessen polygon. The computation was done by manipulating of Arc GIS version 10.4 software at the catchment level. This is done by gauge weights developed for the catchment multiplied with rainfall gauging stations in and around the catchment; hence, the transformed area rainfall is done with the aid of ArcGIS itself. The transformed area rainfall map and the resulted gauge weight area are shown in figures (13) and table (4) below, respectively.

Table 3: Thiessen gauge weight for Sibilu catchment

S. No.	Station Name	Area(km^2)	Gauge Weight (%)
1	AA. Observatory	3.94	0.64
2	Chanco	245.9	39.9
3	Entoto	276.5	44.8
4	Sululta	94.2	15.3

Monthly PET was estimated from the four meteorological stations (Addis Ababa Observatory, Chanco, Entoto, and Sululta). The Hargreaves method is recommended as a sole for temperature-based PET estimation for the definition and procedure used [83]. Due to the inadequacy of meteorological data such as; solar radiation, relative humidity, and wind speed are missed; they should be estimated using Hargreaves methods.

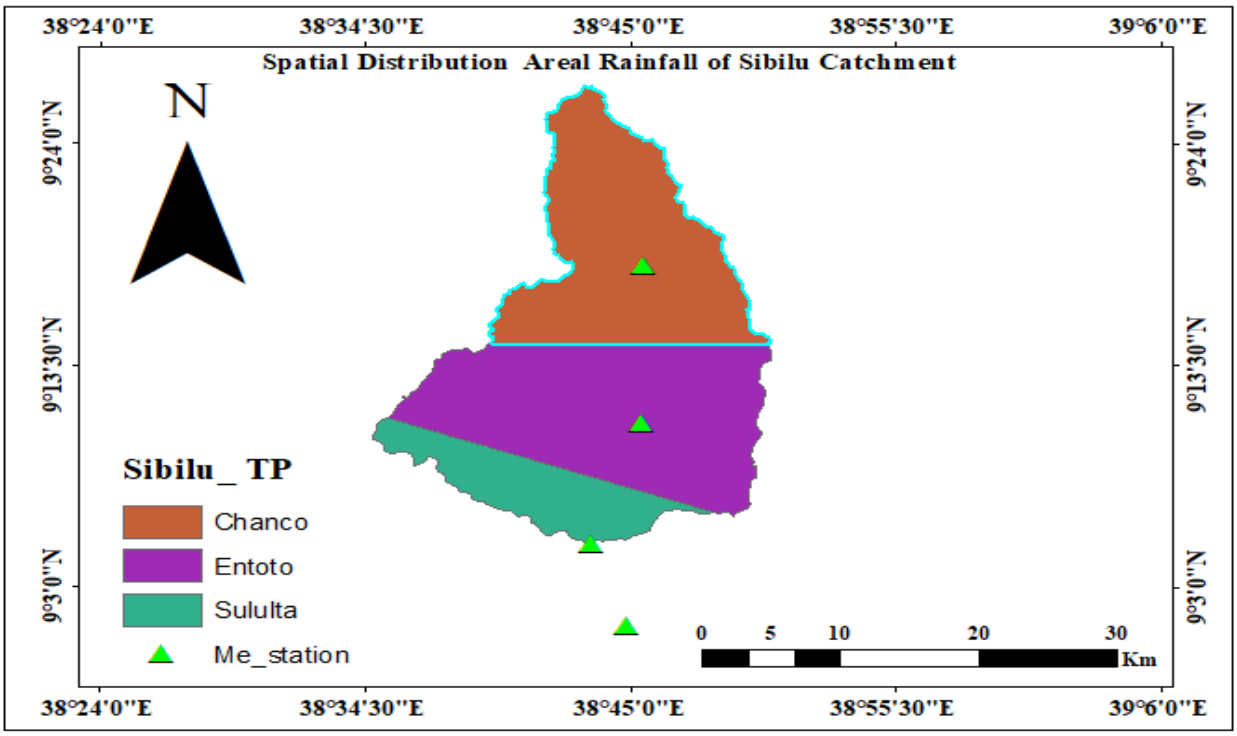

Figure 13: Thiessen Polygon developed for Sibilu Catchment

3.6. HBV-Light Model and Input Data

The HBV-Light software is freely available and can be downloaded from http://www.geo.uzh.ch/en/units/h2k/hbv-model. From the beginning guiding principles in the development of the HBV-Light software were on the core model. A user –friendly graphical user interface (GUI), the possibilities to perform uncertainty analyses and making the software available for research and educational use. The model consists of different routines and simulates catchment discharge, usually on a daily time step, based on time series of precipitation and air temperature was well as estimates of monthly long-term potential evapotranspiration rates. In this case, in the snow routine snow accumulation and snow melt are computed by a degree-day method. Whereas for a soil routine, the groundwater recharge and actual evapotranspiration was simulated as a function of actual water storage. Similarly, runoff was computed as a function of water storage in the response routine. Eventually, a triangular weight function is used to simulate the routing runoff to the catchment outlet in the routing routine.

The model uses a warm-up period during which state variables evolve from standard initial values to their appropriate values according to meteorological conditions and parameter values. Precipitation is considered to be either snow or rain, depending on whether the temperature is above or below a threshold temperature.

Besides running a single model simulations there are a few additional simulation tools available that are important features of the GBV-Light software. Batch simulations can be used to run the model for a list of predefined parameter sets. In addition to this, there are two different tools available for automatic calibration of the model, Monte Carlo simulation and generic Algorithm and Powell optimization (GAP).Monte Carlo simulations can be used run a large number of simulation based on randomly selected parameter sets (within user-defined parameter) boundaries. HBV-Light is primary useful for education, because the user-friendly interface makes the use of the model intuitive and little time is needed to learn how to run the model.

The HBV-Light model is selected for this study due to the following possible reasons:

- The required input data is moderate or low.
- Simulation of the major hydrological processes at catchments.
- The model is tested for the impact of climate change on a hydrological study in different parts of the world, including Ethiopia.
- The availability of the model.

The model has four routines for discharge simulation:

(i) The “snow routine” is a threshold melting temperature (TT usually in 0 °C) and a parameter

CMELT that reflects the equivalent melted snow for the difference of temperature.

(ii) The “soil routine” is a process where rainfall goes to the root zone and to groundwater as recharge depending on the relationship between field capacity (FC [mm]) and moisture content in the root zone (SM [mm]), (Equation.6), and actual evaporation is estimated depending on soil moisture availability using the relation between SM and FC (Equation. 11).

(iii) The "response routine" is for computing runoff from upper (SUZ*mm+) and lower (SLZ [mm]) groundwater boxes as the sum of two or three linear outflow equations depending on a threshold parameter, UZL [mm] (Equation.15).

(iv) The "routing routine" is used to transform runoff to simulated runoff *mm/day+ (Equations. 16 and 17) using a triangular weighting function defined by the parameter MAXBAS [55].

The following central equations are used in the formulation of HBV-Light model which are given below.

$$melt = CFMAX(T(t) - TT) \quad (7)$$

$$refreezing = CFRCMAX(TT - T(t) \quad (8)$$

$$\frac{Recharge}{P(t)} = (\frac{(SM(t)^{BETA}}{FC}) \quad (9)$$

$$QGW(t) = K2SLZ + K1SUZ + Komax(SUZ - UZL, 0) \quad (10)$$

$$\left(P_{(h)}\right) = P_o \ + (1 + \frac{P\ CALT(h-h_o)}{10000}) \quad (11)$$

$$E_{Pot}(t) = (1 + C_{ET}(T(t) - T_m))E_{Pot,M} \quad (12)$$

$$(T(h) = T_o \ - \frac{T\ CALT(h-h_o)}{100}) \quad (13)$$

$$E_{act} = E_{pot}\min(\frac{SM(t),1)}{PC,LP}) \quad (14)$$

$$Q_{WT}(t) = K_2SLZ + K_1SUZ + K_0max(SUZ - UZL, 0) \quad (15)$$

$$Q_{Sim}(t) = \sum_{i=1}^{MAXBAS} C(i)Q_{WT}\ (t - i1) \quad (16)$$

Where:

$$C(i)A = \int_{i=1}^{i} \frac{2}{MAXBAS} - |U - \frac{MAXBAS}{2}\Big|_{\frac{4}{MAXBAS}} d \quad (17)$$

where P (t) is the precipitation at time t, FC is the field capacity, BETA is a parameter that determines the relative contribution to runoff from rain or snow melt, E_{act} is the actual

evapotranspiration, E_{pot} is the potential evapotranspiration, LP is the soil moisture value above which E_{Tact} reaches E_{Tpot}, QGW is the groundwater recharge, Q_{sim} is the simulated runoff, SUZ is storage in soil upper zone [mm], SLZ is storage in soil lower zone [mm], UZL is Threshold parameter [mm], and Ki is the recession constant. A more detailed description of the model can be found in [69].

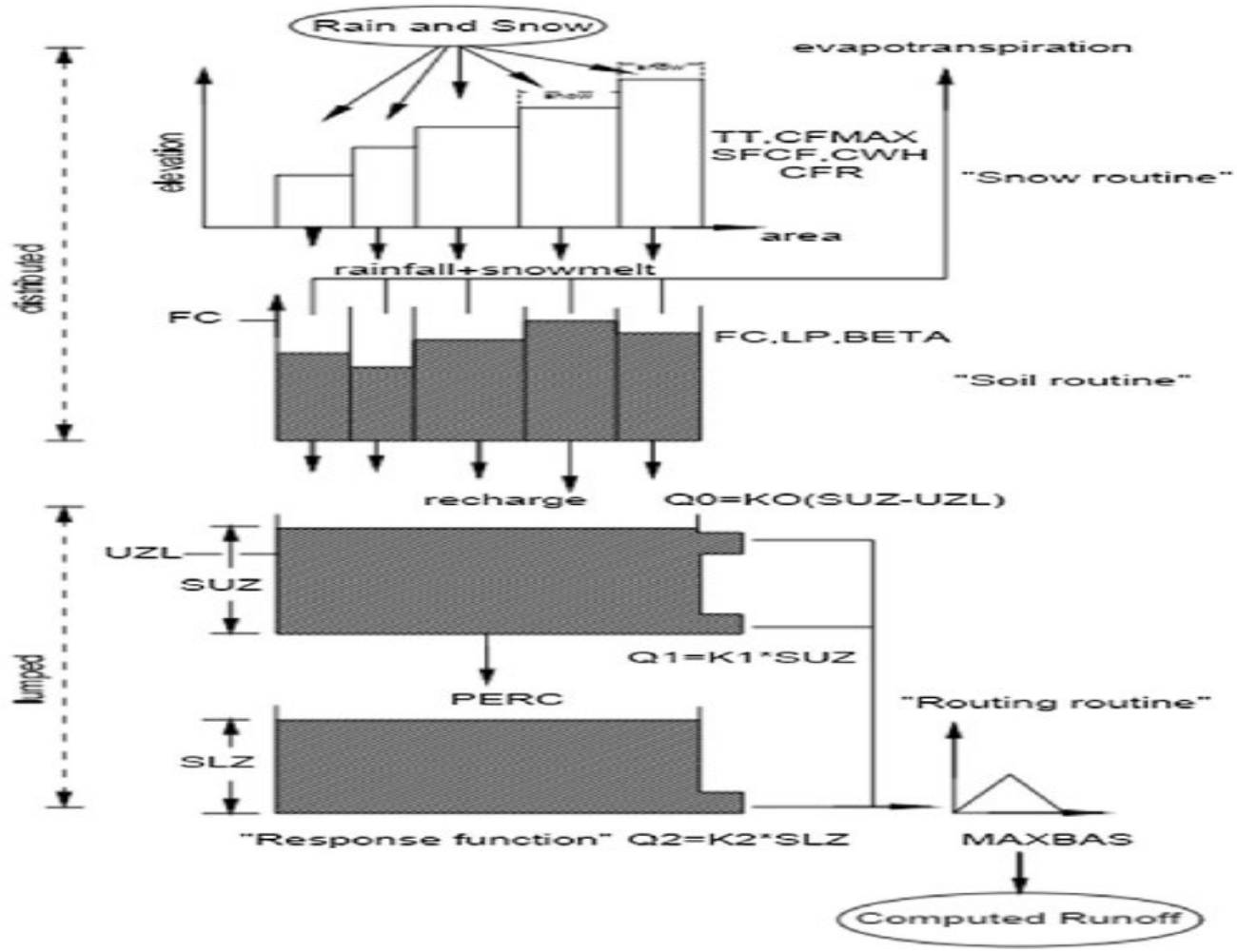

Figure 14: General structure of the HBV-Light model [69].

The conceptual hydrological models called HBV-Light was chosen for the simulation of the study area. In this case, it requires data on daily discharge in mm/day, entered using the model data storage format; daily rainfall; in mm/day entered using the model data storage format; mean temperature in (^{0}c), entered using the model data storage format, and daily and average monthly potential evapotranspiration in mm/day as input.

3.6.1. Application of HBV-Light model

The model can be used for a different purpose based on the intended importance to be utilized. Among the application some are listed out as follows:

- To extend runoff of data series (or filling gaps).
- Used for data quality control.
- For water balance studies.
- For runoff forecasting (flood warning and reservoir operation).
- To compute design floods for dam safety.
- To investigate the effects of changes within the catchment.
- To simulate discharge from ungagged catchment.
- For climate change effects.

3.6.2. Determination of Areal Depth of Precipitation

Areal rainfall depth was computed using the Thiessen polygon to identify the representative rainfall stations that contributed to the entire catchments. Basically, the method is based on a good network of representative rain gauges. Hence, rainfall data for the period of thirty years (1985-2014) was prepared for four meteorological stations in and around the catchment area. Therefore, to determine the mean area rainfall of the stations, the rainfall amount of each station was computed by multiplying the rainfall by the weight of each station considered by the area of the polygon, and the sum of these products was divided by the total area of the catchment. If P_1, P_2, Pn are the rainfall magnitudes recorded by the stations 1, 2, n, respectively of A_1, A_2,A_n areas of Thiessen polygon, then the average rainfall in catchment P is given by:

$$P_{avg} = \frac{P_1 A_1}{A_1} + \frac{P_1 A_1}{A_1} + \cdots, + \frac{P_n A_n}{A_n} \quad (18)$$

$$P_{avg} = \sum_{i}^{n} \frac{A_i}{A} \quad (19)$$

Were, $\frac{A_i}{A}$ Weight factor for each station

Table 4: Location of rainfall station and their respective area for Sibilu Catchment

No	Station	Area (Km^2)	Location (DD)	
			Easting	Northing
1.	Addis Ababa Observatory	3.93	38.745	9.018
2.	Chanco	245.91	38.759	9.303
3.	Entoto	276.68	38.758	9.179
4.	Sululta	94.16	38.725	9.083

3.6.3. Potential Evaporation (PET)

Evapotranspiration is the major component in the hydrologic cycle, next to precipitation. There are a number of methods to estimate evapotranspiration, and these methods vary based on the climatic variables required for calculation. For instance, the temperature-based method uses only air temperature and sometimes day length; the radiation-based method uses net radiation and air temperature; and some other formulas like Penman-Monteith require a combination of the above, including net radiation, air temperature, wind speed, and relative humidity.

FAO Penman-Monteith method is globally accepted and performs well in many climatic conditions that determine reference evapotranspiration when standard meteorological variables, including air temperature, relative humidity, and sunshine hours, are available [84]. In this case, the limitation for widely using FAO Penman-Monteith is that numerous data points are required that are not available, especially those is valid for Sibilu catchments. Therefore, the Hargreaves method, which is temperature based and that has linked to solar radiation, is selected for the computed catchment evapotranspiration of the study area. For this study, the long-term baseline period (1985-2014) was computed by Hargreaves methods. The Hargreaves method to estimate ETO is given by the equation (20) as follows: -

$$ET_O = 0.0023Ra(T_{mean} + 17.8)(\Delta T)^{0.5} \quad (20)$$

Where: Ra= is extra-terrestrial radiation [(MJ/m^2/day

G_{sc} is solar constant which is 0.0820 [(MJ/m^2/day]

Ra is a function of latitude f (G_{sc}, dr, δ, φ, ω).

ω is sunset hour in [radians]

$\boldsymbol{\varphi}$ is latitude in [radians]

δ is solar declination[radians]

T_{mean} = Mean air temperature [^{0}c]

ΔT is a temperature difference (mean monthly temperature minus mean monthly temperature(^{0}c)

J is number of days in the year (i.e., 1 for January 1, 365 for December 31) at a leap year.

dr is inverse relative distance earth-sun

The following equation expressed the parameters which is listed above and calculated accordingly by equating different variables.

$$Ra = \frac{24/60}{\pi} * Gsc * dr[\omega \sin(\varphi)\sin(\delta) + \cos(\varphi)\cos(\delta)\sin(\omega)] \quad (21)$$

$$dr = 1 + 0.033\cos(\frac{2\pi J}{365}) \quad (22)$$

$$\omega = arccos[(-\tan(\varphi)\tan((\delta)] \quad (23)$$

$$\delta = 0.409\cos(\frac{2\pi J}{365} - 1.39) \quad (24)$$

$$\varphi(rad) = \frac{\pi}{180} * latitude \quad (25)$$

$$Tmean = \frac{Tmax+Tmin}{2} \quad (26)$$

Equivalent evapotranspiration in mm/day=0.408*(Ra)[(MJ/m^2/day] (27)

Lastly, the corresponding equivalent evaporation in mm/day is obtained by multiplying the Ra by correction factor of 0.408.

3.7. Modeling Approach and Method of Data Analysis

While modeling and analyzing climate data, different modeling approaches is used. As indicated in figure (11), the modeling approach used in case of study area was divided into two broad classes. The first broad class was the climate change modeling approach, and the second class was the hydrological modeling approach. To conduct this spatio-temporal data were used. Spatial data such as land use, land cover, soil map, and DEM were manipulated using Arc GIS, which characterized the attributes of the catchment. The temporal data of base period climate and

stream flow data were used as input for the HBV-Light hydrological model that has been collected from the Ethiopian National Meteorological Agency and Minister of Water and Energy that is used to calibrate and validate the HBV-Light model. Thereafter, model parameters have been computed from catchment parameters, observed flow, and climate data. The overall procedure applied in the study area is represented by a flow chart. Basically, there are two categories of climate downscaling, namely dynamic and statistical downscaling [16].

Dynamical downscaling: refers to the use of RCM driven by a GCM to simulate regional climate by extracting local-scale information by developing and using limited-area models (LAMs) or regional climate models with a GCM as a boundary condition. Furthermore, it uses complex algorithms, on an affine-grid scale to; describe atmospheric processes nested within GCM outputs this results in limited-area models or regional climate models (RCM), but computational costs are high, as cited by [85]. RCMs have been recently developed that can attain horizontal resolution in the order of tens of kilometers or less over selected areas of interest. Compared with GCMs, the resolution of these RCMs is much closer to that of distributed parameter hydrological models and that even makes coupling of such models possible.

Statistical downscaling: is based on the assumption that there are significant relationships between local and large-scale climates [86]. It is unknown whether present-day statistical relationships between large-scale variables will be upheld in the future climate system. From this point of view, regional or climate information is derived by first determining a statistical model that relates large-scale climate variables or predictors to regional and local variables (predictand). Then the large-scale output of an AOGCM simulation is fed into this statistical model to estimate the corresponding local and regional climate characteristics [87]. The overall procedure applied in the study area is represented by a flow chart.

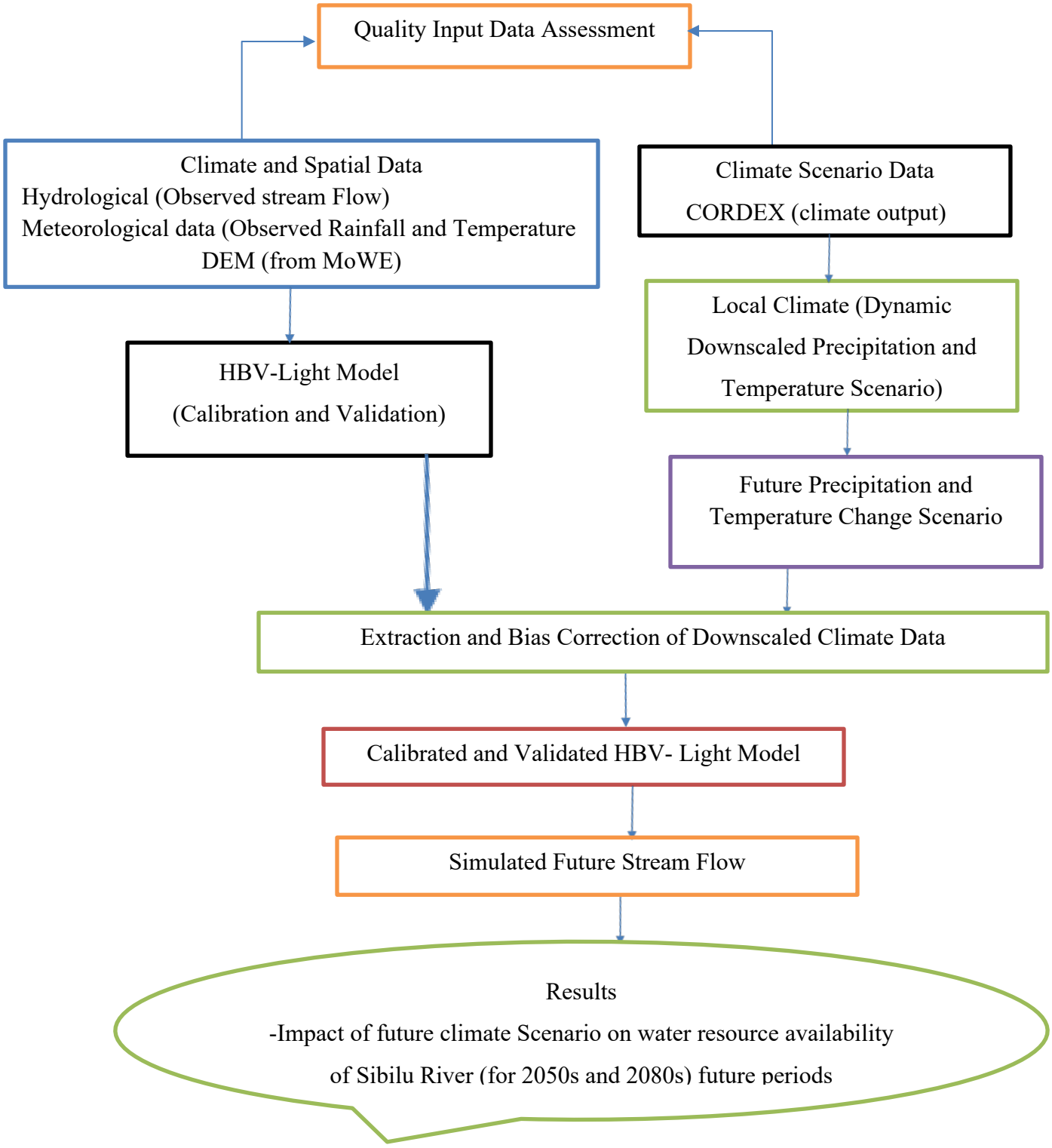

Figure 15: General Modeling and Methodology of flow chart of the study area

Obviously, watershed models are often used to simulate the impact of future climate conditions on hydrologic processes. [40] State that simulation of temperature and precipitation often show significant biases as a result of errors occurring while averaging within grid cells and systematic modeling or discretization. Therefore, a bias correction procedure is used to minimize the model discrepancy between observed and simulated climate variables on a daily time step. In this case, hydrological simulations driven by corrected simulated data match the simulated observed climate as well. CMhyd is a tool that can be used to extract and bias correct data obtained from global and regional climate models, so it is highly recommended to apply an ensemble approach as stated by [88], [40].

The output of coarser climate data (GCM) is downscaled into interest of the study area by using CMhyd software. These downscaled climate data have not been directly used as input for the model since they introduce model uncertainty and cause bias. Therefore, bias correction techniques are applied before being used to assess the future climate change impact on the water resource availability of the catchment. At the end, the output of the models was analyzed, summarized, and presented as graphs and tables. The general procedure for working in the CMhyd software is summarized in the following flow chart.

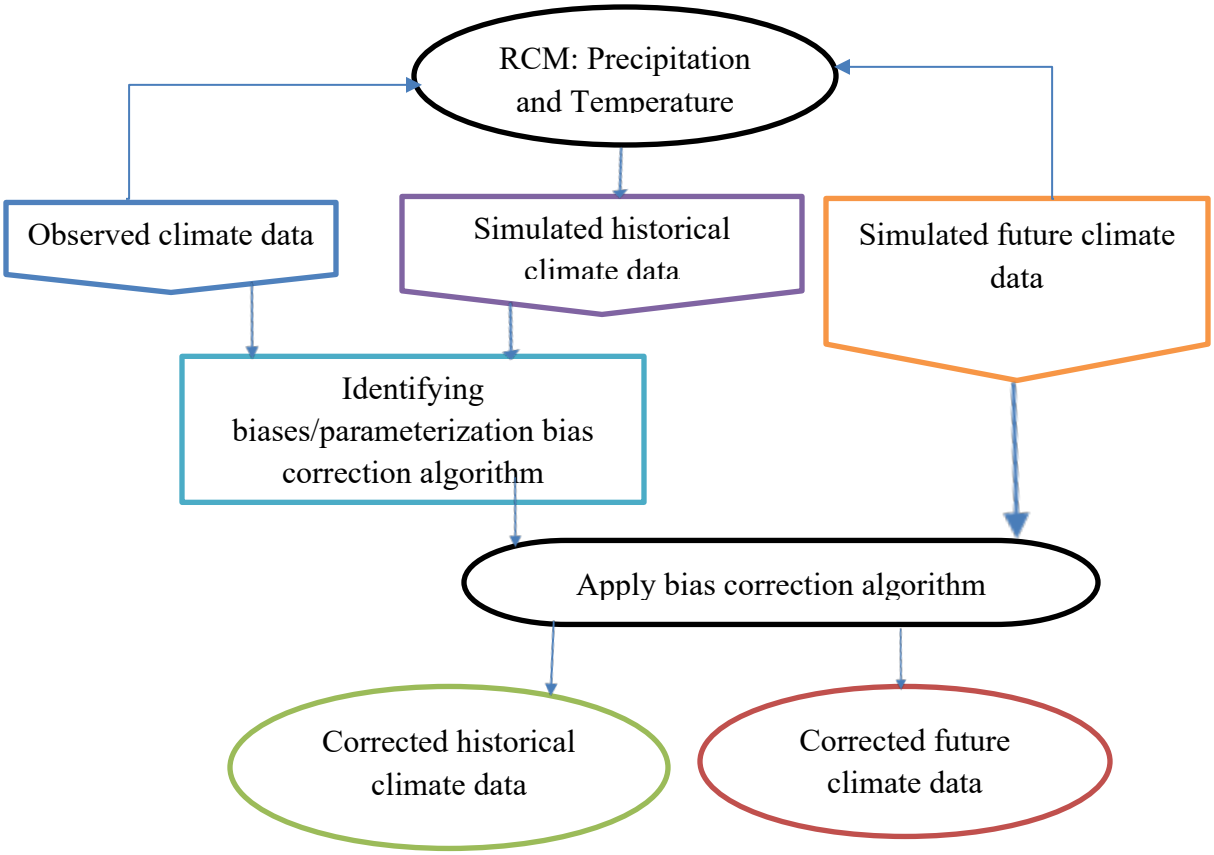

Figure 16: Bias Correction frame work

3.7.1. CORDEX Climate Model Data

For this study, results of CORDEX-Africa ensemble RCMs simulations for historical (1985-2005) and future (2006–2100) climate projections downscaled from different GCMs under RCP4.5 and RCP8.5 with a spatial resolution of 50 km are used. The climate data contains daily values of precipitation, maximum and minimum temperature but the other climate variables were assumed to be constant for the future time period. The selected two RCPs are medium-low and high radiative forcing scenarios, respectively. The two RCPs use radiative forcing values of 4.5 and 8.5 W/m−2, respectively.

As the WMO states that for climate change impact analysis, a period of 30 years is recommended as a standard averaging period in climatological studies. For consistency, a uniform analysis period of 1985-2005 was employed across all selected climate models, even though the recreated reference data covered the range of 1951-2005. This period of 21 years was

deemed appropriate for evaluating the performance of the selected models by considering the limited availability of observed data for the study. Studies by [89] and [90] reinforced that this period was adequate for the assessment of the climate models for impact analysis. Though using a multi-model ensemble is superior to using a single model, for such cases, studies reviewed by [91] and [92] revealed that the application of multi-model ensemble retrieval yields superior predictions than those from a single model. Surprisingly, the output from single models is prone to overconfident and causing model uncertainty in some circumstances. However, once a dynamic downscaling approach is chosen (using RCM), the extent of variability caused by using different RCMs has not been fully evaluated. For that case, there is no guideline available on how to best use RCM output for further impact analyses. Since then, some impact modelers have chosen to work with only one RCM, while others are using multi-model approaches, the so-called RCM ensembles. Obviously, it seems that the only use of the good aspects of all models will be beneficial.

Apparently, there has been significant improvement in climate modeling, particularly with respect to RCM, as they transfer the large-scale signal from GCMs to scales closer to the catchment scale [93]. While cascading climate impact simulations, uncertainties may arise due to the choice of climate model structure, emission scenario, downscaling methods, correction techniques, and hydrological modeling uncertainty [92], [94]. However, a common approach has emerged with respect to these uncertainties, and indeed, multi-model approaches that attempt to represent these uncertainties using model ensembles are now widely recommended and widely accepted [95].

This study employed future climate data from the CIMP5 CORDEX project using global warming time series from three GCM-RCM combinations of one regional model (RCA4). Accordingly, ensemble climate GCM models (MOHC-HadGEM2-ES, CCCma-CanESM2, and Ncc-NorESM-M) are employed for a single regional climate model (RCM) of RCA4 under the most recent representative concentration pathways (RCPs). Hence, water availability under climate change consequences has been examined using RCP4.5 and RCP8.5 scenarios. To this study, the three (3) ensembles of the GCM climate model were averaged to produce a single precipitation and temperature time series over the catchment. The reason for choosing the two representative concentration scenarios is that the RCP4.5 emission scenario is due to their range

of location in the middle of the IPCC, with a CO_2 concentration of about 650 ppm by 2100, while the RCP8.5 scenario is in the top range of the IPCC, with a CO2 concentration of about 1370 ppm by the end of 2100. And also, in most climate research works, scientists and modelers use these scenarios.

For climate change data processing the following steps were utilized.

- The first step was utilized the downloaded simulated daily maximum and minimum temperatures and daily amounts of precipitation from CORDEX project (Coordinated Regional Climate Downscaling Experiment) at spatial grid resolution of 0.44º (~50Km) (http://esgfdata.dkrz.de/login/?next=http://esgf data.dkrz.de/search/cordex-dkrz/)
- The second step was to extract the RCM overlapping grids that fall into the study area for the Selected gauging stations from step one. Then, basin average climate model time series data were calculated using area weighted average for four grid boxes.
- The third and final step was to calculate the biases for the historical and future climate scenarios.
- Bias correction is done for daily precipitation and temperature data after all the final step of processing.

Table 5: Detail of selected models and variable derived from CORDEX-Africa as a source (https://esgf-data.dkrz.de/projects/esgf.dkrz)

Feature of selected model	Variables
Project	CORDEX
Domain	AFR-44
Institute	SMHI
Experiment	Historical, RCP 4.5 and RCP 8.5
Ensemble	r1i1p1
Variable	Pr, Tmax and Tmin daily
Time frequency	Daily
Global Climate Model (GCM)	MOHC-HadGEM2-ES, CCCma-CanESM2 and Ncc-NorESM-M
Regional Climate Model (RCM)	RCA4

Where r1i1p1, which represents realization #1, initialization I #1, and physics p#1; SMHI: Swedish Meteorological and Hydrological Institute, RCA4: Rossby Center Regional Atmospheric Model, Pr: Precipitation, Tmax: Maximum temperature and Tmin: Minimum temperature.

Table 6: Detail climate model summary

Model Name	Reference	Description
MOHC HadGEM2-ES	[96]	HadGEM2-Earth System model; high resolution global climate model; includes atmosphere, ocean ice, and land surface components
cccma-CanESM2	[97]	Canadian Earth System Model version 2; global climate model with advanced atmosphere, ocean, land, and cryosphere components
Ncc-NorESM-M	[98]	Norwegian Earth System Model- Model M; coupled atmosphere-ocean general circulation model with interactive sea ice and land ice components

Remark: all three models are considered state-of -art global climate models and are used by the Intergovernmental Panel on Climate Change (IPCC), where each model has its own strengths and weaknesses, and the best model for a particular application will depend on the specific needs of the users. It is important to use multiple models when making climate projections, as this helps to account for the uncertainties inherent in any single model.

3.7.2. Bias Correction for CORDEX Climate Data

Bias correction is an important task in climate data projection, and a procedure employs a transformation algorithm for adjusting climate model output. The underlining idea toward bias correction is to identify biases between observed and simulated historical climate variables to parameterize a bias correction algorithm that is used to correct simulated historical climate data. Since bias correction is assumed to be stationary, the corrected algorithm and its parameterization for current climate conditions are similarly valid for future conditions as well. Obviously, climate models often exhibit systematic errors or biases, which occur as a result of limited spatial resolution, simplified physical and thermodynamic processes, numerical schemes, or incomplete knowledge of climate system processes. Hence, bias correction is applied to avoid overestimation or underestimation of downscaled variables.

For this study, linear scaling and power transformation were used as bias correction methods. The linear scaling method is a bias correction of the climate data model by adjusting rainfall and temperature in the RCM simulation using multiplicative and additive factors, respectively [99]. And also, these factors aimed to develop by comparing the observed data with the corresponding historical RCM simulations. The linear scaling method corrects the biases based on the mean. For temperature, monthly systematic biases were computed for the baseline period by comparing RCP outputs with the observations [100]. The power transformation method reproduces the standard deviation, coefficient of variation (CV), wet-day frequencies, and intensities of rainfall based on observed data [101]. Thus, the daily rainfall of RCMs is changed into a corrected rainfall by fitting the CV of the corrected daily RCM rainfall with the CV of observed daily rainfall for each month. In this case of the study area, linear scaling (additive factors) was used to adjust the temperature of RCM, while power transformation was to adjust the rainfall of RCM simulation, respectively.

Mathematical Equations applied to correct future precipitation and temperature data obtained from CORDEX-RCP as follows:-

$$T(RCM\ corr, daily) = T(hist, daily) + [\overline{Tobs}) - (\overline{T\ hist}, daily)\ )] \quad (28)$$

$$p^* = aP^b\ , daily\ RCM \quad (29)$$

Where: $Tcorr$ Corrected future temperature

$\mathrm{T(hist, daily)}$ Daily RCM simulated temperature

$\overline{\mathrm{Tobs}}$ Mean daily observed temperature

$\overline{\mathrm{T\ hist}}$, daily Mean daily RCM simulated temperature

p^* Corrected future precipitation

a and b are parameters which can be estimated with the help of distribution free approach

CMhyd software is designed to work with the CORDEX data, which provides downscaled RCM data. It is obtained from https://swat.tamu.edu/software/ and used for the extraction of CORDEX-NetCDF while bias correction of precipitation, minimum and maximum temperatures

are downscaled [18]. And also used for bias correction of extracted climate data from the CORDEX model of precipitation, minimum and maximum temperature simulation for historical and future periods of analysis under different scenarios [102].

3.8. Sensitivity Analysis

Sensitivity analysis is an important concept for cross checking any hydrological simulation model. It was conducted to quantify the impact of input parameters on the output or result of the model and aim to limit the number of optimized parameters that are to be a good fit between the simulated and measured data. Apparently, the simplest method for sensitivity analysis is to vary repeatedly one parameter at a time while others are fixed, as mentioned by [103]. According to [104], sensitivity analysis aims to determine the relative ranking of which parameters most affect the output variance since input variability reduces uncertainty and provides parameter estimation guidance for the calibration step of the model. [105] States that sensitivity analysis evaluates how different parameters influence a predicted output. For this study, a sensitive analysis was performed to select the most sensitive parameters of the selected model parameters for the calibration step of the model.

3.9. HBV-Light Model Calibration and Validation

Model calibration is defined as adjusting the model parameters to match the observed data with a limited range of deviation. And also, the modification of parameter values and comparison of the predicted output of interest to measured data until a defined objective function is achieved for the same desired or expected conditions according to [46] and [46]. Calibration is an attempt to better parameterize a model to a specific set of local conditions, thereby reducing forecasting uncertainty. Calibration of the HBV light was done for the Sibilu River based on stream flow recorded at the gauge sites. In this case, calibration of the selected sensitive parameters was undertaken in different time steps. Manual (trial-and-error) was the initial step to reach some level of agreement with that of the observed flow and thereby minimize the potential range that bound the value of each parameter. In a second step, the automatic calibration method uses a Monte Carlo procedure by searching within wide parameter ranges. A total of 18 years (1985-2002) of Sibilu river stream flow was used during calibration, including a one -year warming up period. Finally, calibration was done by optimizing the model parameters in the subroutine that have a significant effect on the performance of the model.

For instance, validation is the step where the capabilities of the calibrated model in simulating acceptable results could be confirmed [106]. Hence, validation of the model was performed to test if the calibrated model for estimating the effectiveness of future potential management practices would be consistent against an independent set of measured data without making further adjustments. According to [46] and [52] it is done by comparing the predictions against observed data that was not used in the calibration procedure, using the parameters that were obtained during the calibration phase. Similarly, the Sibilu River Gauging Station from the (2003-2011) period was used for the validation processes to evaluate the model accuracy.

Table 7: General HBV-Light model performance rating for recommended statistics [107]**.**

			PBIAS (%)
Performance Measures	NSE	R^2	Stream flow
Very Good	$0.75 < NSE \leq 1.00$	$0.70 < R^2 \leq 1.00$	$PBIAS \leq \pm 10$
Good	$0.65 < NSE \leq 0.75$	$0.60 < R^2 \leq 0.70$	$\pm PBIAS < \leq \pm 15$
Satisfactory	$0.50 < NSE \leq 0.65$	$0.50 < R^2 \leq 0.60$	$\pm 15 < PBIAS \leq \pm 25$
Unsatisfactory	$NSE \leq 0.50$	$R^2 \leq 0.50$	$PBIAS > \pm 25$

3.10. Climate Change Impact Analysis

Accordingly, changes in the projected climate were estimated for a baseline period of 1985-2014 (Vbase), whereas the two interest periods span 30 years, as recommended on the World Meteorological Organization [108], which represent from the periods from 2050s (2031-2060) and the 2080s (2061-2090). Therefore, percent changes and differences (Δ) between projected climate and baseline climate were calculated for rainfall and temperature respectively, by using the following equations:

$$\Delta P_{2050s} = \frac{V_{2050s} - V_{baseP}}{V_{base}} * 100 \quad (30)$$

$$\Delta P_{2080s} = \frac{V_{2080s} - V_{baseP}}{V_{base}} * 100 \quad (31)$$

$$\Delta T_{2050s} = T_{2050s} - V_{baseT} \quad (32)$$

$$\Delta T_{2080s} = T_{2080s} - V_{baseT} \quad (33)$$

Where ΔP and ΔT refers to the percent change in mean monthly rainfall and the difference in mean monthly temperature, respectively. V 2050s and V2080s, T 2050s, and T 2080s represent the mean of all the average monthly rainfall and the mean monthly average of temperature for the baseline period, respectively [109].

3.11. Performance Evaluation of Climate Change

Thus, comparison of dynamically downscaled regional climate model outputs with that of observed climate data was evaluated for the Sibilu catchments before it was used for any projection. The statistical measures to test the performance of models are bias in %, root mean squared error (RMSE) in mmyear^{-1} correlation coefficient (corr), and coefficient of variation (CV) in % [110]. Bias measures whether the average tendency of simulated data is larger or smaller than the observed values. The lower the absolute value of the bias, the better would be the model performance. And also, root mean square error (RMSE), which is a unit of observed variable, makes its interpretation. In this case, as the value of RMSE is close to zero, it indicates better performance of the model. The correlation coefficient (corr) is used to evaluate the linear relationship between the observed and modeled rainfall amounts. [111] it is suggested that a value of 1.0 implies a perfect linear relationship between the model output and the observed data.

$$\text{Corr} = \frac{\sum_{i=1}^{n}(R_{RCM} - R_{RCM\ Mean})\,(R_{obs} - R_{obs\ Mean})}{\sqrt{\sum_{i=1}^{n}(R_{RCM} - R_{RCM\ mean})^2 \sum_{i=1}^{n}(R_{obs} - R_{obs\ Mean})^2}} \quad (34)$$

$$\text{RMSE} = \sqrt{\frac{\sum_{i=1}^{N}(R_{RCM} - R_{obs})^2}{N}} \quad (35)$$

$$PBIAS = \frac{(R_{RCM}) - R_{Obs})}{R_{Obs}} * 100 \quad (36)$$

3.11.1. HBV-Light Model Performance Evaluation Criteria

To assess the performance of the models, it is critical to compare the capacity of each performance criteria with that of a predefined value. Accordingly, three criteria were used to evaluate the performance of the models since the models have been evaluated using their performances. According to [112], the performance of a model must be evaluated on the basis of its accuracy, consistency, and adaptability. And also, assessing the performance of the hydrologic model requires subjective and or objective estimates of the closeness of the simulated behavior of the model to observations [113].

For this particular study, three statistically parameters performance criteria namely; Nash and Sutcliffe efficiency (NSE), coefficient of determination (R^2), and Percent Biases (PIBASES), were used to check the performance of the HBV-light hydrological model. Nash and Sutcliffe efficiency (NSE) was proposed by [114], and its value lies between 1.0 (perfectly fit) and -∞.). The coefficient of determination (R^2) is expressed as the squared ratio between the covariance and the multiplied standard deviation of the observed and predicted values [113].

The percent bias (PBIAS) is used to describe the tendency of the simulated data to be greater or smaller than the observed data, which is expressed as percentages. In this case, the optimal value for PBIAS is zero (0), and a low values indicate that the model simulation is satisfactory. Positive and negative value indicates a tendency of the model to underestimate and overestimate it, respectively. This test is recommended due to its ability to reveal any poor performance of the model.

$$\text{NSE}= 1 - \frac{\Sigma(Qobs-Qsim)^2}{\Sigma(Qobs-\overline{Qobs})^2} \quad (37)$$

$$R^2= \frac{(\Sigma(Qobs-\overline{Qobs})(Qsim-\overline{Qsim}))^2}{\Sigma(Qobs-\overline{Qobs})^2\Sigma(Qsim-\overline{Qsim})^2} \quad (38)$$

$$PBIAS = \frac{\Sigma(Qobs-Qsim)}{\Sigma(Qobs)} * 100 \quad (39)$$

Where;

$Qobs$ Observed discharge

$Qsim$ Simulated discharge

$\overline{Qobs}$ Mean of observed discharge

$\overline{Qsim}$ Mean of simulated discharge

PBIAS Percent bias (%)

Table 8: Summary of efficiency criteria and their empirical equation

Error! Bookmark not defined. Objective function	Definition	Value for perfect fit
Nash-Sutcliffe Efficiency (NSE)	$1 - \frac{\Sigma(Qobs-Qsim)^2}{\Sigma(Qobs-\overline{Qobs})^2}$	1
Coefficient of determination(R^2)	$\frac{(\Sigma(Qobs-\overline{Qobs})(Qsim-\overline{Qsim})^2}{\Sigma(Qobs-\overline{Qobs})^2\Sigma(Qsim-\overline{Qsim})^2}$	1
PBIAS	$PBIAS = \frac{\Sigma(Qobs-Qsim)}{\Sigma(Qobs)} * 100$	0

Finally, the performance evaluation criteria used show the overall agreement between the observed and predicted hydrographs and the model's ability to predict the time and magnitude of peak discharges and runoff volume [115]. Hence, a good agreement between the averages of simulated and observed catchment runoff volume was good for water balance. The Performance of HBV-Light was evaluated in a subjective way following the basic approach of assessing the model's efficiency by visual inspection. This enabled examining systematic behavior, over or under prediction, dynamic behavior timing, rising limbs, and recession curves of simulated and observed hydrography visually while calibrating and validating the model, including the three objective function assessment criteria. Objective assessment of the model was done by mathematical estimation since it is used as the main criteria for accepting the parameter estimates during calibrating the model manually and also for testing the transferability of parameter set values. Accordingly, the relationship between simulated and observed runoff was quantified using the following listed efficiency criteria, which are given in the table below.

4. RESULT AND DISCUSSION

4.1. Climate Projection

4.1.1. Comparison of Baseline and Climate Model Output

It is important to check the performance of the output of RCM rainfall, minimum and maximum temperature of baseline and observed climate data before directly using it for climate change impact assessment. In such a case, bias correction was done, and each historical climate data output was compared against observational data. As a result, the mean monthly rainfall, minimum and maximum temperature of the baseline, raw RCM, and historical correction of the overlapped period were compared for the catchment. Under each scenario, spatial precipitation was computed for a general analysis of precipitation over the entire catchment.

4.1.2. Rainfall

In the climate system, rainfall is the most erratic factor and important aspect of any catchment that has an impact on the water availability of the catchment either directly or in directly, which a bimodal pattern for the study area, as [42] and [45] have done their research on the Sibilu catchment. Since then, the mean annual statistically downscaled (MOHC-HadGEM2-ES, CCCma-CanESM2, and Ncc-NorESM-M model simulation output has been compared with the baseline/observed mean annual rainfall. As a result, the observed average annual rainfall was 1305.9 mm, the bias- corrected RCM about 1401.9 mm, and bias uncorrected RCM was about 1818.5 mm. For the observed and bias-corrected RCM, they show correlation to each other, whereas the bias-uncorrected RCM shows overestimation of the model simulation outputs. In a seasonal basis, maximum rainfall was shown during Kiremt season for all stations, with values of 1005.7 mm, 1213.3 mm, and 1412.9 mm for the observed, RCM bias corrected, and RCM bias uncorrected periods respectively. For all stations, the CV value of downscaled and observed rainfall was above 30%, which indicates rainfall variability was expected to be high, as referenced by [116]. And also, at the time of Kiremt season, the output of the downscaled bias uncorrected shows likely overestimates in the catchment than the observed period of each station. Thus, an adjustment of bias correction is required for further future impact research.

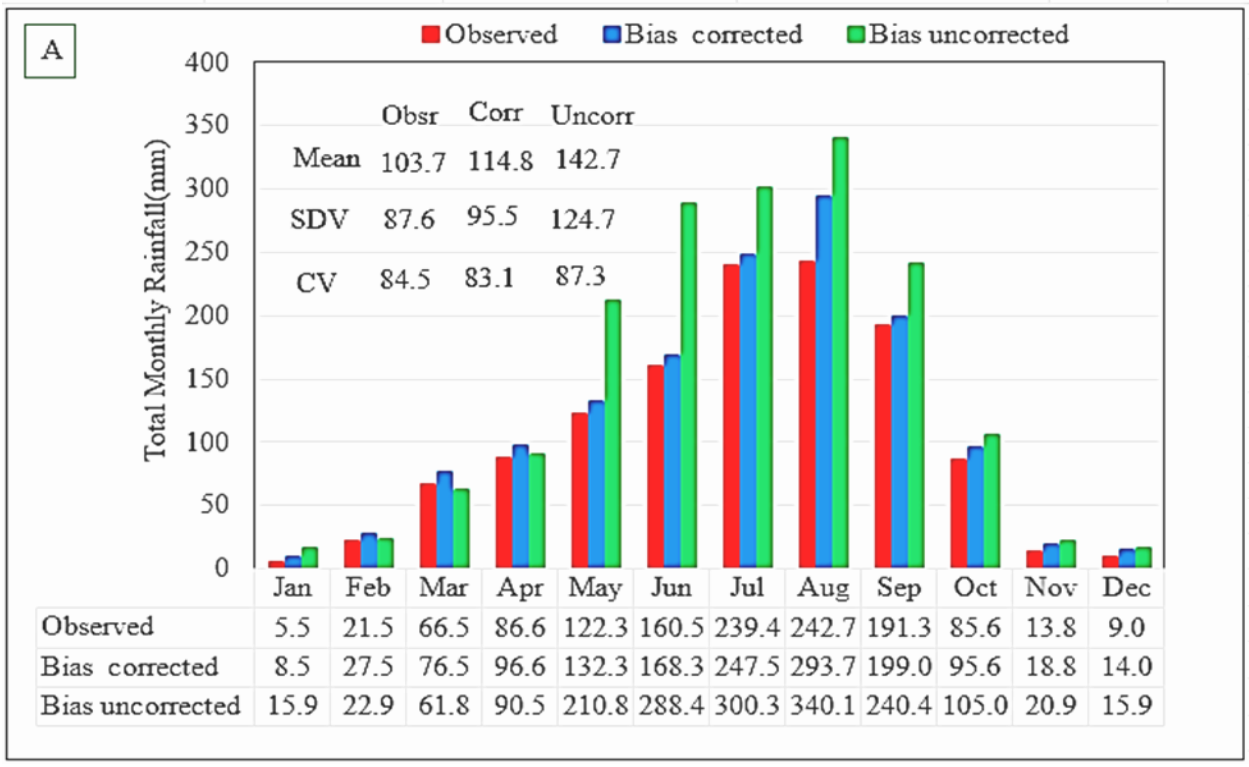

	Jan	Feb	Mar	Apr	May	Jun	Jul	Aug	Sep	Oct	Nov	Dec
Observed	5.5	21.5	66.5	86.6	122.3	160.5	239.4	242.7	191.3	85.6	13.8	9.0
Bias corrected	8.5	27.5	76.5	96.6	132.3	168.3	247.5	293.7	199.0	95.6	18.8	14.0
Bias uncorrected	15.9	22.9	61.8	90.5	210.8	288.4	300.3	340.1	240.4	105.0	20.9	15.9

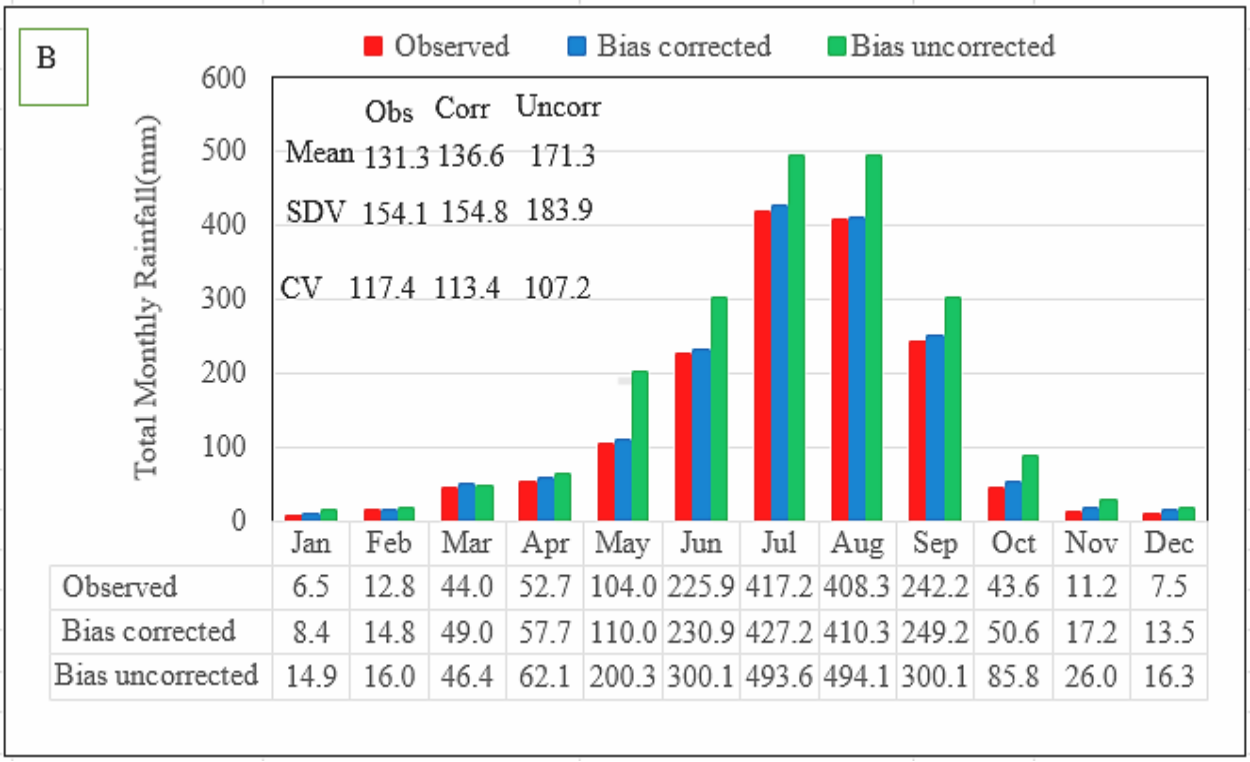

	Jan	Feb	Mar	Apr	May	Jun	Jul	Aug	Sep	Oct	Nov	Dec
Observed	6.5	12.8	44.0	52.7	104.0	225.9	417.2	408.3	242.2	43.6	11.2	7.5
Bias corrected	8.4	14.8	49.0	57.7	110.0	230.9	427.2	410.3	249.2	50.6	17.2	13.5
Bias uncorrected	14.9	16.0	46.4	62.1	200.3	300.1	493.6	494.1	300.1	85.8	26.0	16.3

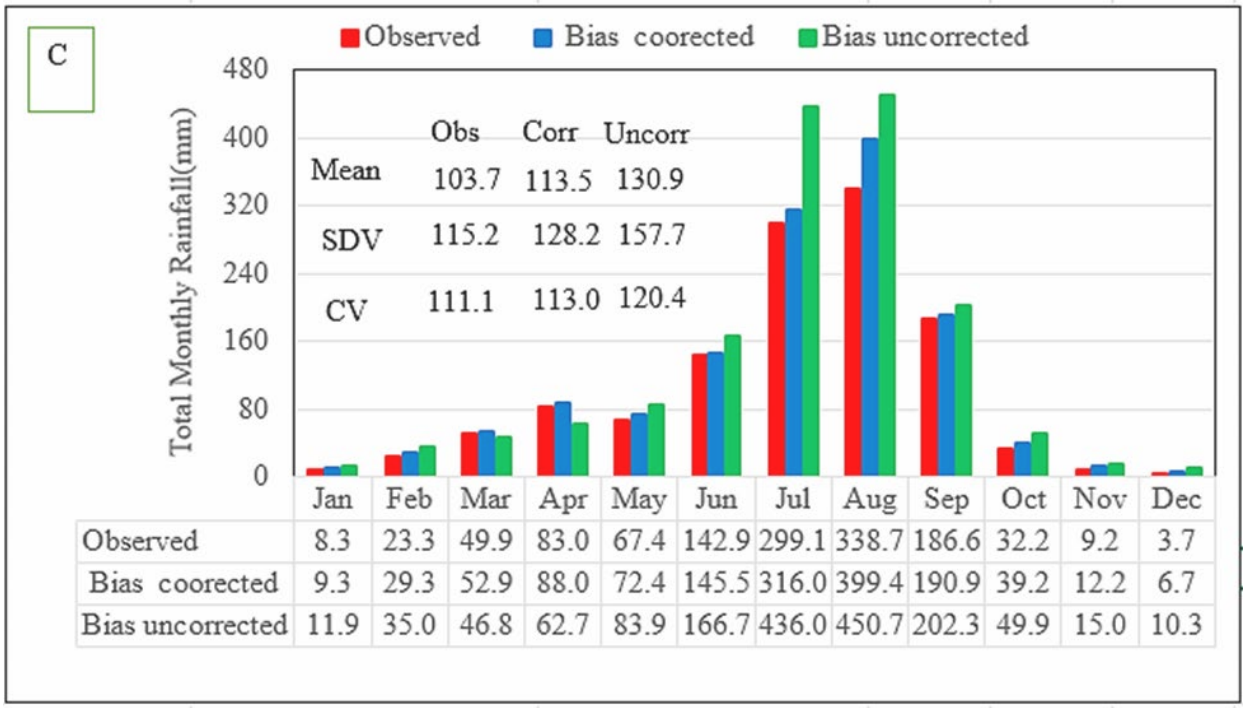

	Jan	Feb	Mar	Apr	May	Jun	Jul	Aug	Sep	Oct	Nov	Dec
Observed	8.3	23.3	49.9	83.0	67.4	142.9	299.1	338.7	186.6	32.2	9.2	3.7
Bias coorected	9.3	29.3	52.9	88.0	72.4	145.5	316.0	399.4	190.9	39.2	12.2	6.7
Bias uncorrected	11.9	35.0	46.8	62.7	83.9	166.7	436.0	450.7	202.3	49.9	15.0	10.3

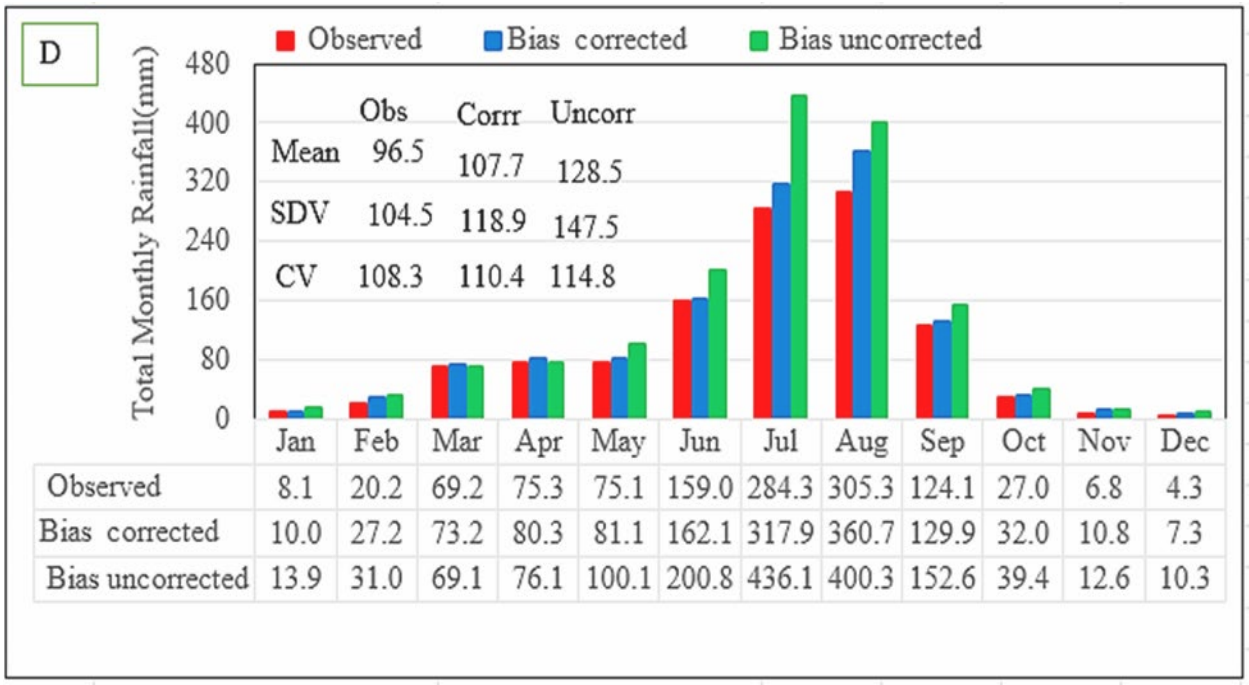

	Jan	Feb	Mar	Apr	May	Jun	Jul	Aug	Sep	Oct	Nov	Dec
Observed	8.1	20.2	69.2	75.3	75.1	159.0	284.3	305.3	124.1	27.0	6.8	4.3
Bias corrected	10.0	27.2	73.2	80.3	81.1	162.1	317.9	360.7	129.9	32.0	10.8	7.3
Bias uncorrected	13.9	31.0	69.1	76.1	100.1	200.8	436.1	400.3	152.6	39.4	12.6	10.3

Figure 17: Comparison of total monthly precipitation of observed, RCM bias Corrected, and RCM bias uncorrected (1985-2005). SDV= Standard deviation, Obs= Observed and

CV=Coefficient of variation of stations (A), Addis Ababa Observatory (B), Chanco (C) for Entoto, and (D) for Sululta, respectively.

4.1.3. Maximum Temperature

As indicated in Figure 18, the mean monthly maximum temperature of the corrected RCM during the baseline period shows, an overestimation as compared to the mean monthly observed maximum temperature for Chanco, Entoto, and Sululta and an underestimated for the Addis Ababa Observatory station. The corresponding values of observed, corrected, and uncorrected RCM for maximum temperature ranges from 16.8 ^{0}C to 25.2 ^{0}C, 16.8 ^{0}C to 25.0 ^{0}C, and 18.9 ^{0}C-25.2 ^{0}C, respectively. On a seasonal basis, the mean monthly maximum temperature of the corrected RCM shows overestimation during Bega and Belg seasons for all stations, whereas it is underestimated during Kiremt. In the study catchment, the station of Addis Ababa Observatory shows the maximum temperature observed, and Entoto, station was showing the minimum temperature as indicated in Figure 18.

4.1.4. Minimum Temperature

For the Chanco, Entoto, and Sululta stations, the mean monthly minimum temperature of the corrected RCM was overestimated during Bega season. The range of minimum temperature for observed, corrected, and uncorrected RCM are 3.9^{0}C to 12.8 ^{0}C, 4.2^{0}C to 12.6^{0}C, and 5.8^{0}C to 13.5^{0}C. On a seasonal basis, there was an overestimation of the minimum temperature during Bega, Belg, and Kiremt for all stations when compared to baseline period. In the catchment, the corrected RCM minimum temperature was overestimated for Chanco, Entoto, and Sululta whereas it was underestimated for Addis Ababa Observatory. The maximum and minimum temperatures were shown in Addis Ababa Observatory and Sululta, as observed in Figure 19. In a nutshell, there is a variation or mismatched between observed and RCM model outputs, hence bias correction was adopted for impact studies.

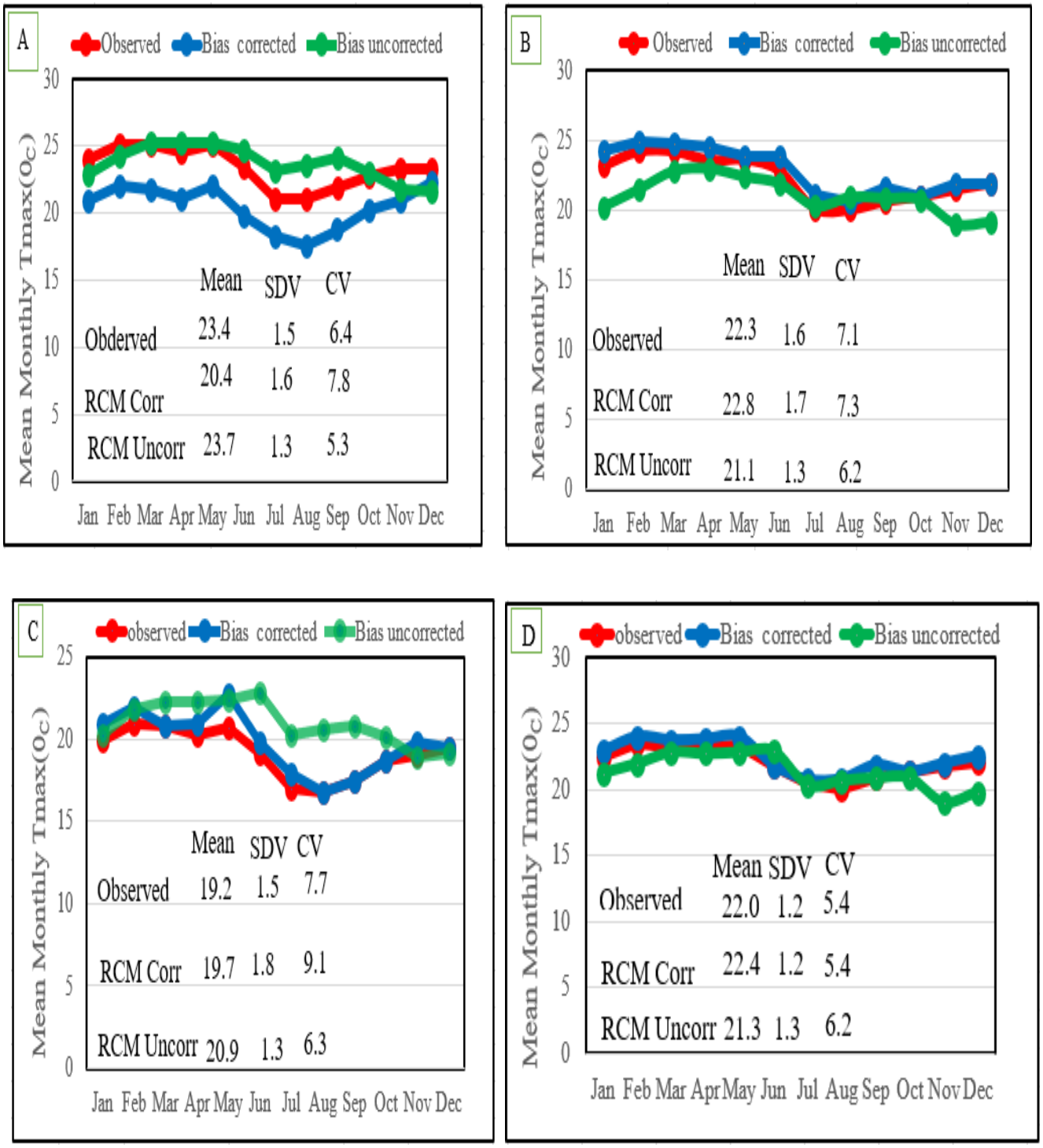

Figure 18: Comparison of mean monthly maximum temperature of observed, RCM bias Corrected, and RCM bias uncorrected (1985-2005). SDV= Standard deviation, Obsr = Observed

and CV= Coefficient of variation of stations (A), Addis Ababa Observatory (B), Chanco (C) for Entoto, and (D) for Sululta, respectively.

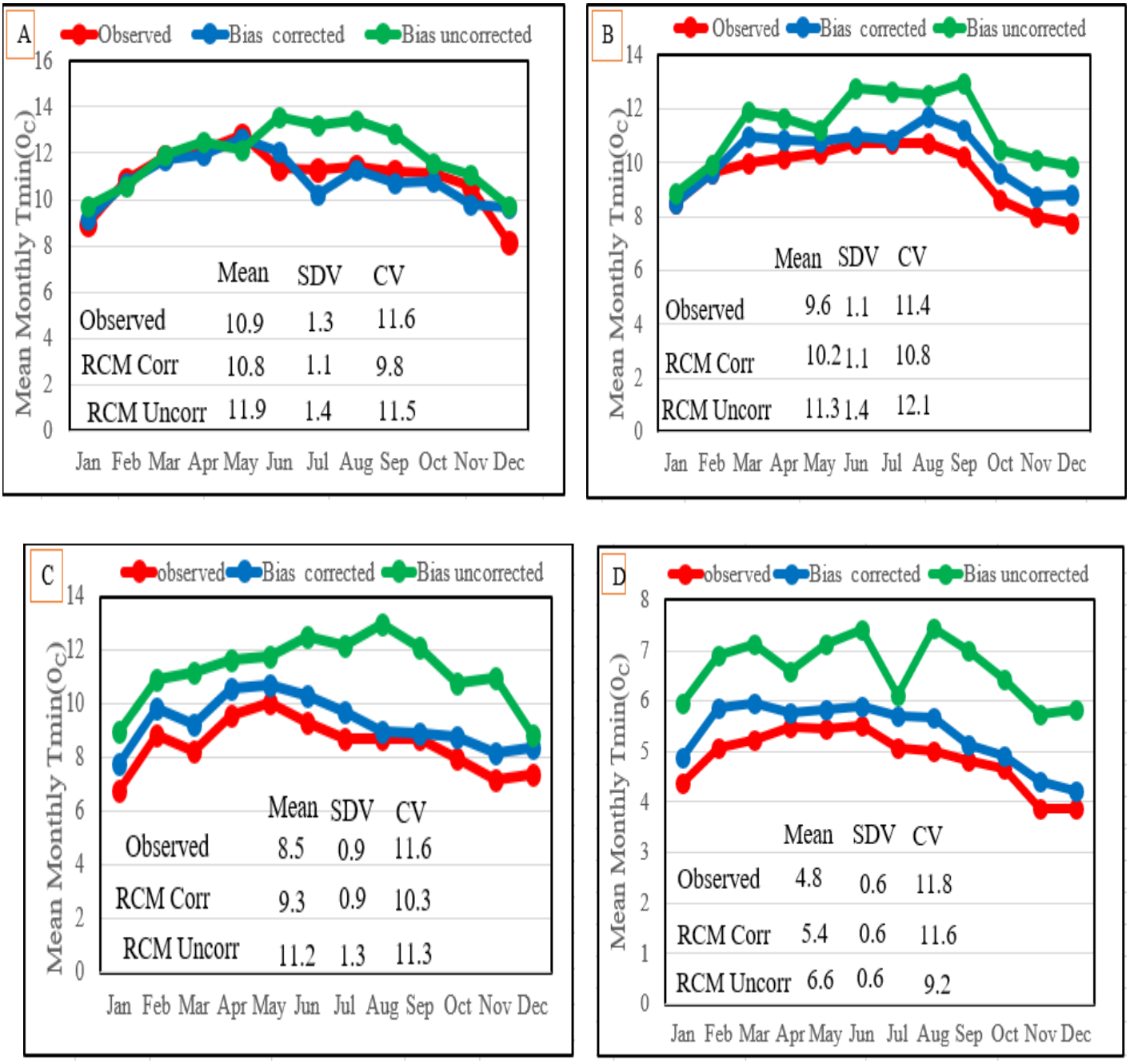

Figure 19: Comparison of mean monthly minimum temperature of observed, RCM bias Corrected, and RCM bias uncorrected (1985-2005). SDV= Standard deviation, Obsr = Observed and CV= Coefficient of variation of stations (A), Addis Ababa Observatory (B), Chanco (C) for Entoto, and (D) for Sululta, respectively.

In generally, raw RCM simulation is characterized by overestimation for both precipitation and temperatures as well.

4.2. Performance Evaluation of Climate Model

Before using climate datasets that have been downscaled either statistically or dynamically, it is important to compare the performance of the baseline data with that of the downscaled data using selected performance criteria. Hence, the mean monthly measured rainfall amount and dynamically downscaled model simulation output for the period (1985-2005) were compared, as summarized in table 12. Thus, the mean annual rainfalls obtained from the GCM/RCM (MOHC HadGEM2-ES, cccma-CanESM2, and Ncc-NorESM-M) model were compared with the corresponding observed mean annual rainfall. Accordingly, the values for observed, RCM corrected, and RCM uncorrected were found to be 1305.9 mm, 1455.4 mm, and 2206.8 mm, respectively. Having the control period 1985-2005), as table (9) revealed, the dynamically downscaled RCM model simulation shows good agreement with slight overestimation. Hence, table 8 revealed that there is very good and high agreement with PBIAS, RSME, and correlation (corr) during the control period (1985-2005), respectively. The overestimation or underestimation of the results might be due to insufficient model resolution and topography, which provide mechanical uplifting and thermal forcing to air parcels [117] and also simulation of rainfall by climate models over the Ethiopian highland was characterized by overestimation as a result of the weakness of model parameterization and cloud parameterization in high- elevation areas, as stated by [118].

In practical implications, understanding the overestimation and underestimation of precipitation, in the Sibilu catchment is a very important aspect, since our county is mainly based on rainfed. Having this concept, the overestimation of precipitation together with climate change, might lead to overuse of water resources, depleting groundwater and surface water resources and exacerbating water stress in entire catchments. Whereas, where precipitation is underestimated, leads to underuse of water resources, decreased agricultural productivity, and increased economic vulnerability, as a study supported by [119]. The same analogy holds true for temperature changes. Therefore, to address the practical implications of overestimated and underestimated precipitation, there is a need for improved climate monitoring and forecasting

tools that provide more accurate and reliable information on precipitation patterns as well as variability.

Table 9: Comparison of average monthly observed and RCM dataset of rainfall

Parameters	Annual Rainfall(mm)	PBIAS	RMSE	Correl
Observed	1305.9			
RCM Corrected	1455.4	2.9	0.0068	0.5965
RCM Uncorrected	2206.8	4.9	1.5315	0.3788

PBIAS= Percentage of Bias, Correl= Correlation coefficient, and RMSE= Root Square Mean Error.

4.3. Future Climate Projection under RCPs Scenarios

For this specific study, 0.44^0 by 0.44^0 of gridded resolution of RCM model output can be used based on RCP 4.5 and RCP 8.5 emission scenarios for the analysis. However, Future climate scenarios were downloaded and analyzed for precipitation, minimum, and maximum temperature for the Sibilu river catchment with selected RCP scenarios. Accordingly, the climate model being downloaded can be divided into two-time horizon periods of overlapped 30 years in the 2050s (2031-2060) and 2080s (2061-2090) for both RCP 4.5 and RCP 8.5 scenarios in the near term and long term, respectively. Therefore, analysis was done with respect to future changes for the selected meteorological stations of Addis Ababa Observatory, Chanco, Entoto, and Sululta with respects of changes in climate variables.

4.3.1. Projected Changes in Rainfall

Evaluation of precipitation characteristics at the catchment level is an important aspect for future changes in precipitation, mainly on a mean monthly, seasonally, and annual basis under different climate scenarios. Figure 20 presents the overall pattern of mean monthly, seasonal, and annual precipitation in the Sibilu catchment for future periods under RCP 4.5 and RCP 8.5 of the 2050s and 2080s in near and long-term scenarios, respectively. In this case, there is an increasing trend for both future projection scenarios, which is about + 17.8%, + 20.4%, + 19.8%, and 22.6% from the baseline period for RCP 4.5 (2050s), RCP 4.5 (2080s), RCP 8.5(2050s), and RCP 8.5

(2080s), respectively. As a result, the percentage increment change in mean annual rainfall for the near term was less than in the long-term in both RCP scenarios. Based on comparison, the RCP 8.5 showed a smaller increment than the RCP 4.5 since there was a higher presence of green gas concentration in the RCP 8.5 scenario, as stated by [120].

The mean annual rainfall revealed an increasing trend as compared to the base period, with maximum increases (22.6%) in 2080 for RCP8.5. Studies conducted by [52] on the upper Abbay basin concluded that annual future rainfall showed an increased trend, which is true for the study area.

On a seasonal basis, the projected mean monthly precipitation suggests an increasing and decreasing trend in both RCP scenarios. Seasonally, during the main rain season (Kiremt) starting from JJAS precipitation showed a decreasing trend by -5.8%, -1.2%, -3.7%, and -0.4% from the baseline period for RCP 4.5 (2050s), RCP 4.5 (2080s), and RCP 8.5(2080s), respectively. Likewise, on Bega dry season (ONDJ), the mean monthly precipitation showed an increasing trend for both near- term and long-term future time periods under the RCP4.5 and RCP8.5 scenarios, with a slight decrement for 2080s period under RCP8.5 by 22.0%, 27.7%, 23.9%, and 20.1% respectively. Similarly, during Belg, the beginning of the rainy season (FMAM) suggests there is an increase in the trend of mean monthly precipitation both in the near- term and long-term scenarios by amounts of 1.3%, 17.6%, 3.3% and 19.3%. As depicted in figure 20 below.

The above results are consistent with the work of [5] and [121]. As he indicated in his work, the mean monthly precipitation rainfall decreases during the main rain season (JJAS) and increases during the Bega (ONDJ) season with respect to the baseline period in all future period scenarios. Additional supportive work [122] found that, using the output of GCMs (CIRO, HadGEM2-ES, and CCSM4) models, and revealed seasonal reduction in maximum future projected precipitation during the Ethiopian rainy season which, is called “kiremt” in the Central Rift valley. Furthermore, in contrast to [122], [123] findings in the work pointed out that the monthly precipitation increasing trend during the summer season is under projected precipitation, which is not valid for the study area. Furthermore, in line with [13] findings, they pointed out that the monthly precipitation increasing is and decreasing over the Northeastern and Northwestern

lowlands of Ethiopia. In general, the projected monthly precipitation indicated a positive and negative percentage change trend in the case of seasonality through out of the entire catchment, and it is confirmed by [124]. The projected mean monthly precipitation indicated an increasing trend from January to mid to June and a decreasing trend from mid-July to November for the near term (2050) and long term (2080) in all future scenarios. In contrast, an increasing and decreasing trend for mid-April-July and mid-August – March, respectively for the long term (2080) under RCP scenarios is depicted in Figure 20 below.

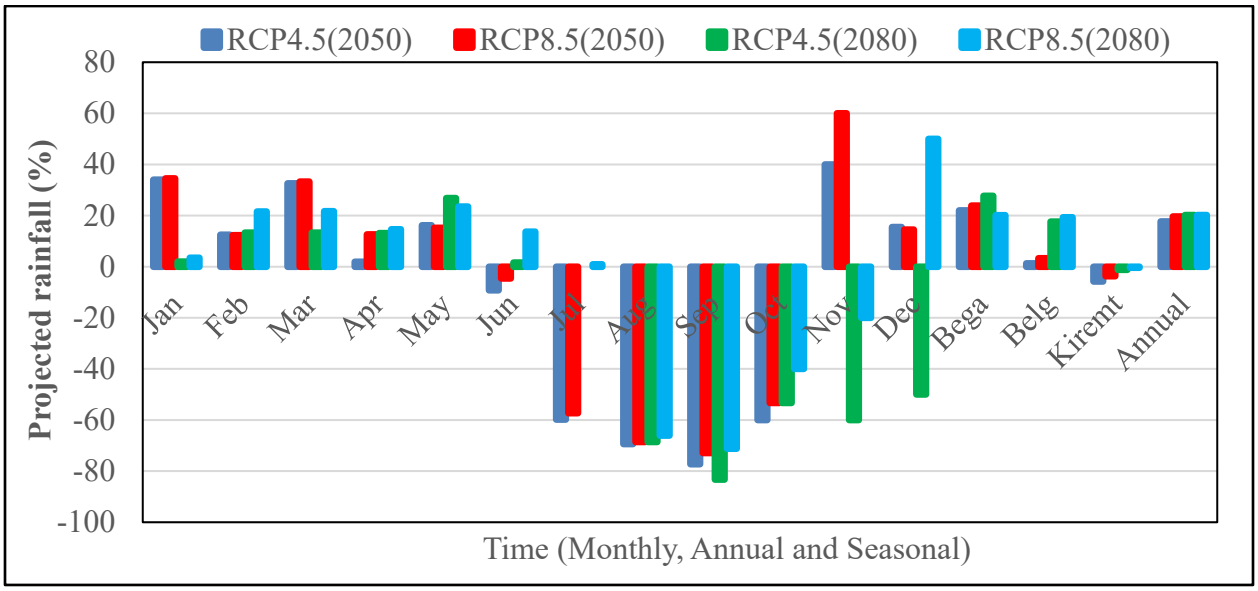

Figure 20: Projected changes of Monthly, annual, and seasonal and Rainfall for near term and long term under RCP 4.5 and RCP 8.5 scenarios, respectively.

4.3.2. Projected Changes in Maximum and Minimum Temperature

4.3.2.1. Projected Changes in Minimum temperature

Relative to the rainfall, the minimum and maximum temperature under both RCP scenarios showed an increasing trend for the near -term and long- term in all future periods. In this case, the result for the mean annual minimum temperature showed an increasing trend of 1.9 ^{0}C, 2.9 ^{0}C, 2.5 ^{0}C, and 4.5 ^{0}C under the RCP 4.5 and RCP 8.5 scenarios from the baseline period for both the near-term and long-term in all future periods, with a slight decrement in the RCP 8.5 scenario for near-term future period (2050s). On a monthly basis, there is an increase from January to June under the RCP 4.5 and RCP 8.5 scenarios for the long-term future period,

respectively. Whereas a decrement trend from June to September under RCP 4.5 and RCP 8.5 scenarios for the near -term future periods.

On a seasonal basis, Bega (ONDJ) dry season showed an increasing mean annual minimum temperature trend from the baseline period by 2.6^0C, 2.2^0C, 3.0^0C, and 3.5^0C under RCP 4.5 (2050), RCP 4.5 (2080), RCP 8.5 (2050), and RCP 8.5 (2080) scenarios, with slight decrease in RCP 4.5 (2080) in all future periods, respectively. The highest increment of minimum temperature was observed under RCP 8.5 (2080), which is about 3.5 ^{0}C.

Belg (FMAM), which is the second rain season, showed an increasing mean annual minimum temperature from the baseline period by 2.3^0C, 4.1^0C, 2.9^0C, and 5.8^0C under RCP 4.5 (2050), RCP 4.5 (2080), RCP 8.5 (2050), and RCP 8.5 (2080) scenarios for the near-term and long-term future periods, respectively but a slight decrease in the RCP 8.5 scenario for the near- term (2050) period. The highest increment of minimum temperature was observed under RCP 4.5 and RCP 8.5 for the near-term (2050) and long-term (2080) future periods, respectively. Similarly, in Summer (JJAS), which is the main rain season, showed an increasing trend of mean annual temperature from the baseline period by 0.9 ^{0}C, 2.0 ^{0}C, 1.4 ^{0}C, and 3.5 ^{0}C under RCP 4.5 (2050), RCP 4.5 (2080), RCP8.5 (2050) and RCP 8.5 (2080) in all future periods except a slight decrease in the RCP 8.5 scenario for the near- term future periods, respectively.

4.3.2.2. Projected Changes in Maximum temperature

As can be seen from Figure (22), the results of the mean annual maximum temperature showed an increasing trend from the baseline period by 1.9^0 C, 2.8 ^{0} C, 2.2 ^{0} C, and 4.1^0C under the RCP 4.5 and RCP 8.5 scenarios for both the near- term (2050) and long- term (2080) in all future periods respectively, with a slight decrease in the RCP 8.5 (2050) future time.

On a seasonal basis, Bega (ONDJ), which is the dry season, the mean annual maximum temperature revealed an increasing trend from the baseline period by 2.4^0C, 2.9^0C, 2.8^0C, and 4.0^0C under RCP 4.5 and RCP 8.5 for both the near-term (2050) and long- term (2080) in all future periods, respectively. From the result, the highest increment was observed in RCP 8.5 for a long-term (2080) time period.

In Belg (FMAM), the mean annual maximum temperature revealed that there is an increasing trend from the baseline period by 0.8 ^{0}C, 1.6 ^{0}C, 1.1 ^{0}C, and 3.9 ^{0}C under RCP 4.5 and RCP 8.5 for both near term ((2050) and long term (2080) in all future periods, respectively with a slight decrease in RCP 8.5 for near term (2050) future time. Similarly, in Summer (JJAS), the main rain season revealed an increasing trend from the baseline period by 2.5^{0}C, 2.20C, 2.80C, and 3.5^{0}C under RCP 4.5 and RCP 8.5 for both the near-term (2050) and long-term (2080), respectively. According to the result obtained, the projection of both minimum and maximum temperature from the baseline period is higher for RCP 8.5 than RCP 4.5, and that is consistent with the in line finding of [18].

In general, the temperature change projection for the Sibilu river catchment is similar to the studies conducted in different parts of the country, and hence the majority of findings exhibit an increasing trend over the Blue Nile River basin [125], [5], [126], and [127]. In a nutshell, the projected minimum and maximum temperatures for both future periods are within the range projected by [79], where the average temperature increases, ranging from 1.4 ^{0}C to 5.8 ^{0}C towards the end of this century, and also, [29] have projected that, by this century, the average temperature will rise up to about 0.3 ^{0}C-4.8 ^{0}C, which is warmer. Furthermore, [10] findings revealed an increase of a significant change in the projected average temperature by 1.6 ^{0}C over the short -term period 2021-2040 and nearly 4 ^{0}C over the long-term period 2081- 2100 for Gilgle Abbay watershed. In addition to this, in line with the finding of [128], studies conducted on the Bilate watershed in the Central Rift Valley Ethiopia revealed that there is an increasing trend of minimum temperature.

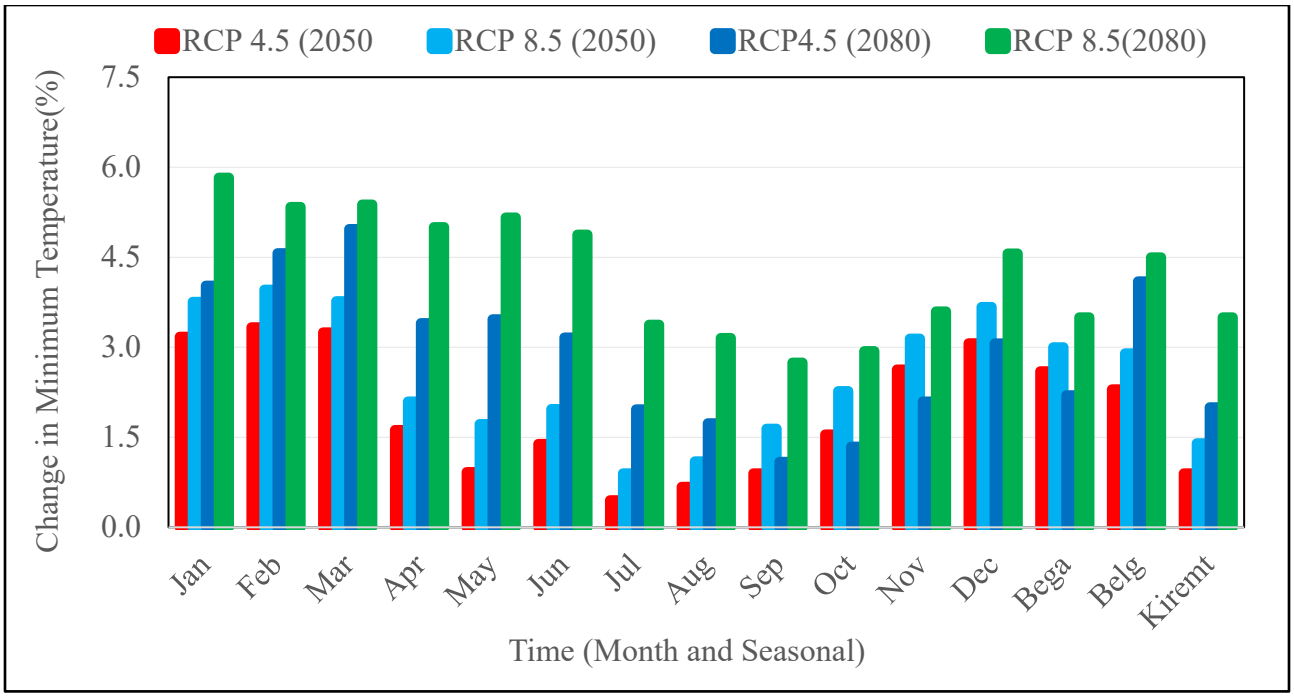

Figure 21: Projected changes of mean monthly minimum temperature for near- term (2050) and long- term (2080) under RCP 4.5 and RCP 8.5 scenarios, respectively.

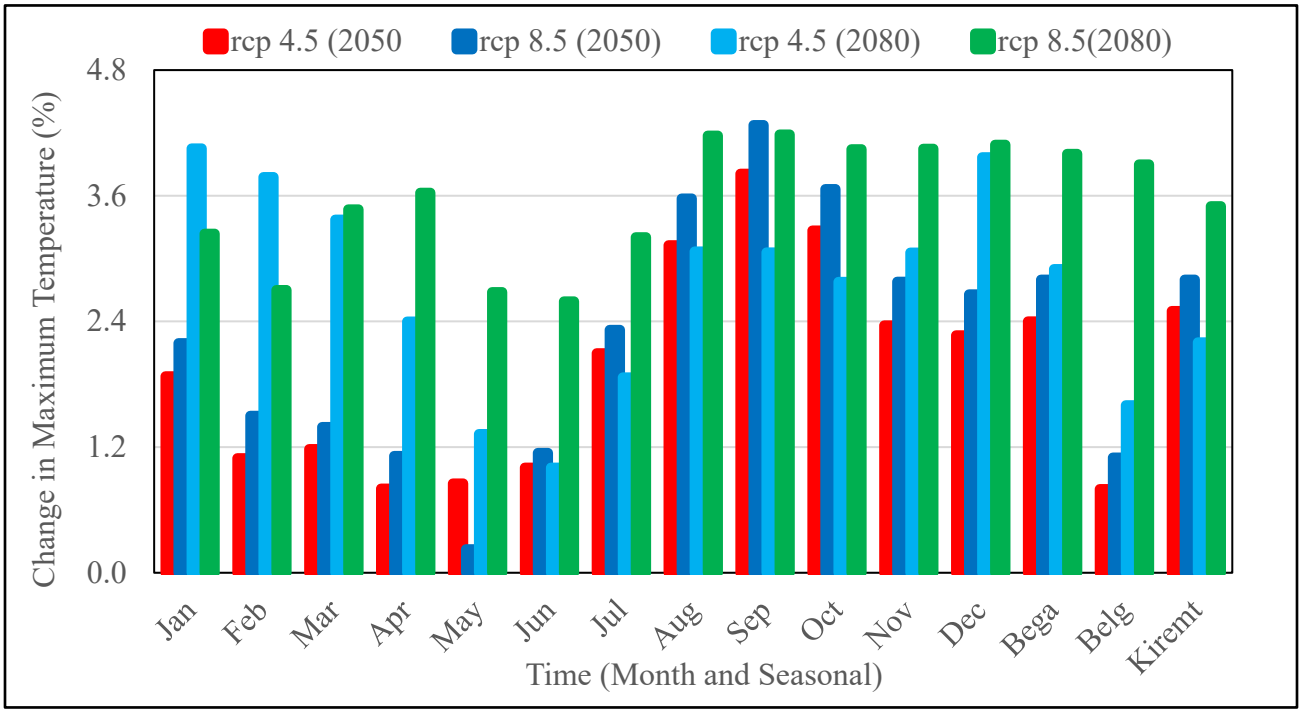

Figure 22: Projected changes of mean monthly maximum temperature for near- term (2050) and long- term (2080) under RCP 4.5 and RCP 8.5 scenarios, respectively.

In a different study, with similar concepts, results were obtained in the case of the Sibilu River catchment for the average projected minimum and maximum mean monthly temperature are harmonious with [129], [48], [5], and [29]. In the finding of [130], it was pointed out that there is a need of increasing the mean temperature by 0.8 ^{0}C in the 2020s and 1.2 ^{0}C in the 20250s in Ethiopia. And also, [129] suggested that future climate change in the Nile basin will show a high temperature change in the range of 1.0 ^{0}C -1.1^{0}C in the 2020s and 1.8 ^{0}C-2.0 ^{0}C in the 2050s the over central part of Ethiopia. Lastly, there is a need to the average temperature change in the annual and seasonal ranges until the end of the 21st century over Africa, which shows a critical warming trend. This founding is in line with [131]. As it can be seen from the result, the change in maximum temperature in dry season was higher than wet season in all future periods for both RCP4.5 and RCP8.5 scenarios in the catchments since in wet season peak temperature reduced due to rainfall, cloudy conditions, and energy use for evapotranspiration, as indicated by [125]. Overall, in all projection periods, the magnitude of the higher emission scenarios of RCP8.5 is higher than for the low emission scenarios of RCP4.5.

4.3.3. Projected Changes in potential Evapotranspiration

The projected mean annual potential evapotranspiration revealed an increasing trend in all periods from the baseline period by 6.3 %, 8.6 %, 6.7 %, and 11.4% under the RCP4.5 (2050), RCP4.5 (2080), RCP8.5 (2050), and RCP8.5 (2080) in all future periods, respectively. As a result, projected potential evapotranspiration under RCP4.5 and RCP8.5 scenarios for the long - term is higher than RCP4.5 for the near-term periods.

On a monthly basis, the model indicates an increasing and decreasing trend for average monthly potential evapotranspiration throughout the future time period for both RCP 4.5 and RCP 8.5 scenarios as compared to the baseline period. In this case, months of July to mid to November, the average monthly potential evapotranspiration increases throughout the future time period for both RCP 4.5 and RCP 8.5 scenarios as compared to the baseline period. The highest increment of potential evapotranspiration was recorded in the month of August. A decrease in the potential evapotranspiration was recorded in the months of March to June. According to figure 22, there is a monthly increase up to 0.1% to 20.7% and -2.9% to -3.2% for RCP 4.5 and also for RCP 8.5 scenarios, a monthly increase up to 0.1% to 22% and a monthly decrement up to -2.9% to -3.0%, respectively.

Based on the seasonal basis, the mean monthly evapotranspiration showed an increasing trend in Bega and Belg under RCP 4.5 and RCP 8.5 for both near-term (2050) and long-term (2080) in all future periods, with the exception of summer season, which showed significant change under RCP 4.5and RCP 8.5 for both near-term and long-term, but a need for increasing trend of potential evapotranspiration under RCP 8.5 for long-term future periods.

Bega (ONDJ), which is the dry season, revealed an increment from the baseline period by 6.4 %, 9.2%, 6.9%, and 11.9% in all future periods, with a maximum increment under RCP8.5 scenarios for both near-term and long-term periods, respectively. Belg (FMAM), the second rainy season, showed an increment of potential evapotranspiration from the baseline period by 7.1%, 8.6%, 7.5%, and 11.4%, respectively. Similarly, the Summer (JJAS) season, which is the main rainy season showed significant change under RCP 4.5 and RCP 8.5 scenarios from the baseline period by 8.1%, 9.9%, 8.6%, and 12.7% for the future period. Overall, there is a need for high potential evapotranspiration for summer the season, Bega, and Belg seasons, respectively. This result is in line with work of the [132] report, and he revealed that potential evapotranspiration in both future time periods 2031-2040 and 2091-2100 showed an increasing trend in all watersheds of the Upper Blue Nile.

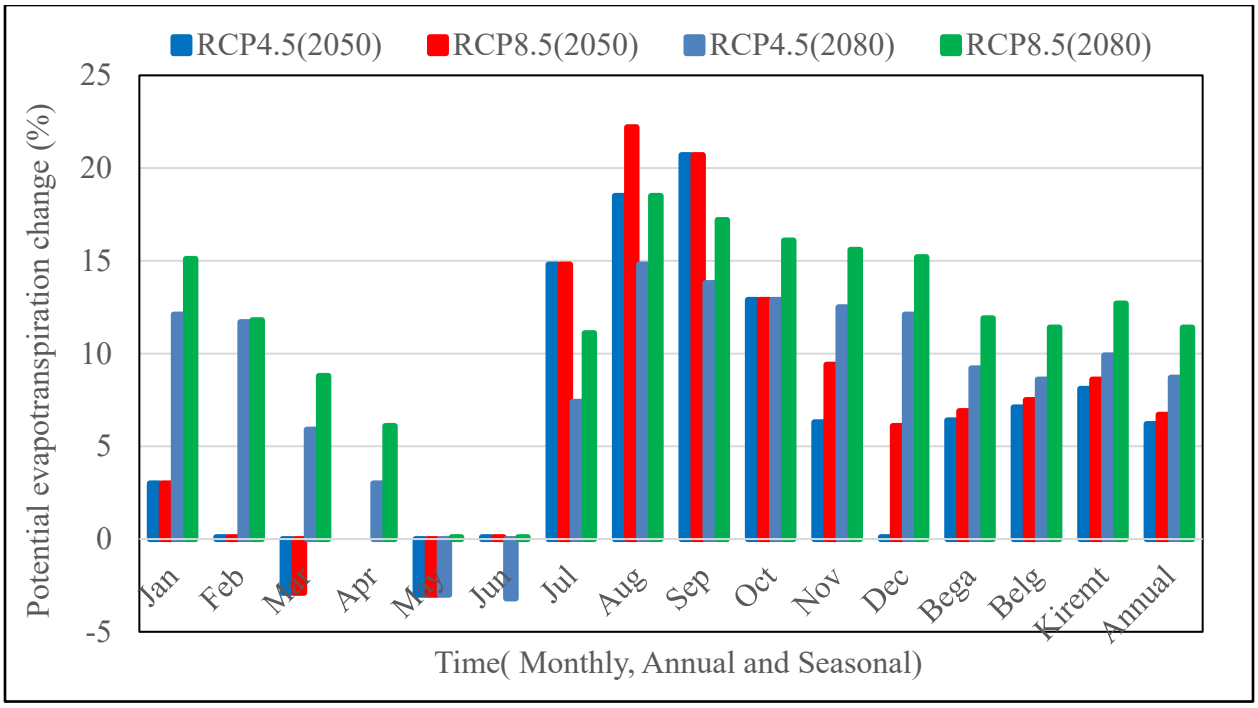

Figure 23: Projected changes of mean monthly potential evapotranspiration under RCP 4.5 and RCP 8.5 for both near-term (2050) and long-term (2080) future periods.

4.4. Calibration, Validation, and Performance Evaluation

4.4.1. HBV-Light Model Calibration

The HBV-Light model was calibrated against the stream flow of Sibilu river gauging sites, and model parameters have to be estimated through calibration. Thus, several runs have been attempted to select the most optimal parameter set that shows good agreement between observed and simulated discharge. Therefore, model calibration involves both manual and automatic adjustment of parameters that result in the best fit between observed and simulated discharge from a catchment. In fact, the HBV- Light model has 15 parameters to be calibrated. The performance of the model has been evaluated using statistical criteria's and showed good performance for daily and monthly calibration. The calibration result of stream flow for the calibration periods 1985-2002 revealed that simulated flow had goodness-of-fit with NSE= 0.88 and R^2 = 0.91, respectively. The analysis of simulated and observed flow data comparison was considered on monthly basis. The optimal calibration parameters mostly responsible for the stream flow assessment of the Sibilu river catchment are shown in (Table 10) with their fitted

values and the combination of average monthly simulated versus observed flow is presented in graphic form.

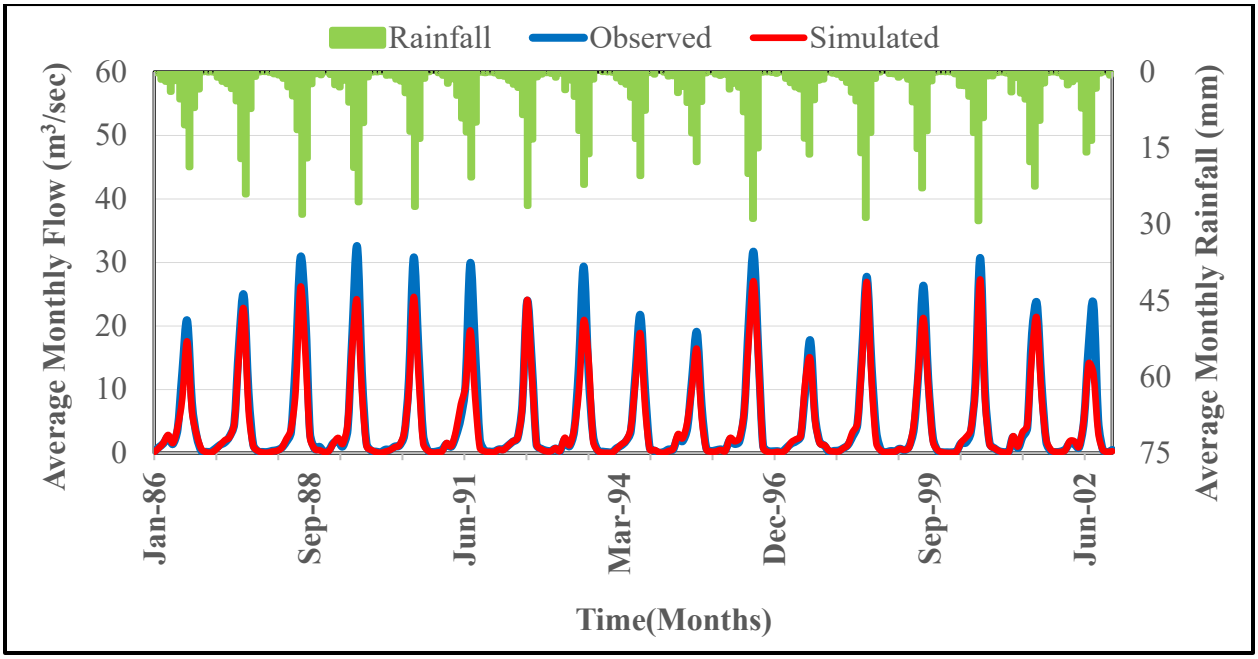

Figure 24: Average Monthly Calibration period (1986-2002) for Sibilu River Catchment

Table 10: Main calibration parameters of HBV-Light model for stream flow in Sibilu River

ID	Parameters	Unit	Descriptions	Lower value	Upper value	Fitted value
Soil Moisture Routine	FC	[mm]	Maximum soil moisture storage	50	500	65
	LP	[-]	Soil moisture above which ETR reaches ETP	0.3	1	1
	BETA	[-]	Parameter that determines the relative contribution to runoff from rain or snow melt	1	6	0.13
Response Routine	UZL	[mm]	Threshold parameter	0	100	1.5
	K0	[1/day]	Recession coefficient	0.05	0.5	0.5
	PERC	[mm/da]	Defines maximum percolation rate from the upper to the lower ground box	0.6	1	1
	K1	[1/day]	Recession coefficient	0.01	0.3	0.1
	K2	[1/day]	Recession coefficient	1	0.1	0.05
Routing Routine	MAXBAS	[day]	Triangular weighting function	0	5	1.1

From the model parameters of the HBV-Light soil moisture routine, FC was used to determine the water amount through the root zone and groundwater as recharge and model parameters; BETA determined the relative contribution to runoff from rain or snow; and LP was a parameter used to determine the relation between actual and potential evaporation. The response routine

(UZL) is a parameter used to compute runoff from the groundwater zone as the sum of linear outflow equations using the storage coefficient (Ki), depending on whether the upper groundwater zone is above the threshold parameter. K0 and K1 are response routine that governs subsurface and base flow contributions in the Sibilu river catchment. MAXBAS is Routing Routine that is used to transform runoff into simulated runoff using a triangular weighting function. Unfortunately, the stream of the Sibilu River can be categorized as flow controlled by MAXBAS rather than a storm.

4.4.2. HBV-Light Model Validation

In addition, the model was validated using an independent data set, which shows good agreement for both daily and monthly simulations without making further adjustments to sensitive parameters. In this case, a total of nine years (2003-2011) periods of data were used. In this study, the sensitive parameters that were set during the calibration period were used for validation purposes as input. Similarly, the results of the validated monthly data for the Sibilu river catchment are presented in Figure 20 and Table 10, with NSE = 0.77 and R^2 = 0.85, respectively. In nutshell, the results show that the HBV-Light model has successfully calibrated and validated the Sibilu river catchment in an acceptable range, which means it's well calibrated, its optimized model parameters are physically meaningful, and therefore, it can be used to simulate the future stream flow of the Sibilu River. The result is consistent with previous studies done over the Abbay river basin using the HBV-Light and Arc SWAT models [13], [133], [18], [134], [49], and [135], which were in acceptable ranges. Generally, from the statistical performance criteria and graphical visualization, it can be concluded that the HBV-Light hydrological model has the capacity to simulate stream flows that agree with observed values and is applicable over the Sibilu River catchment for future impact analysis.

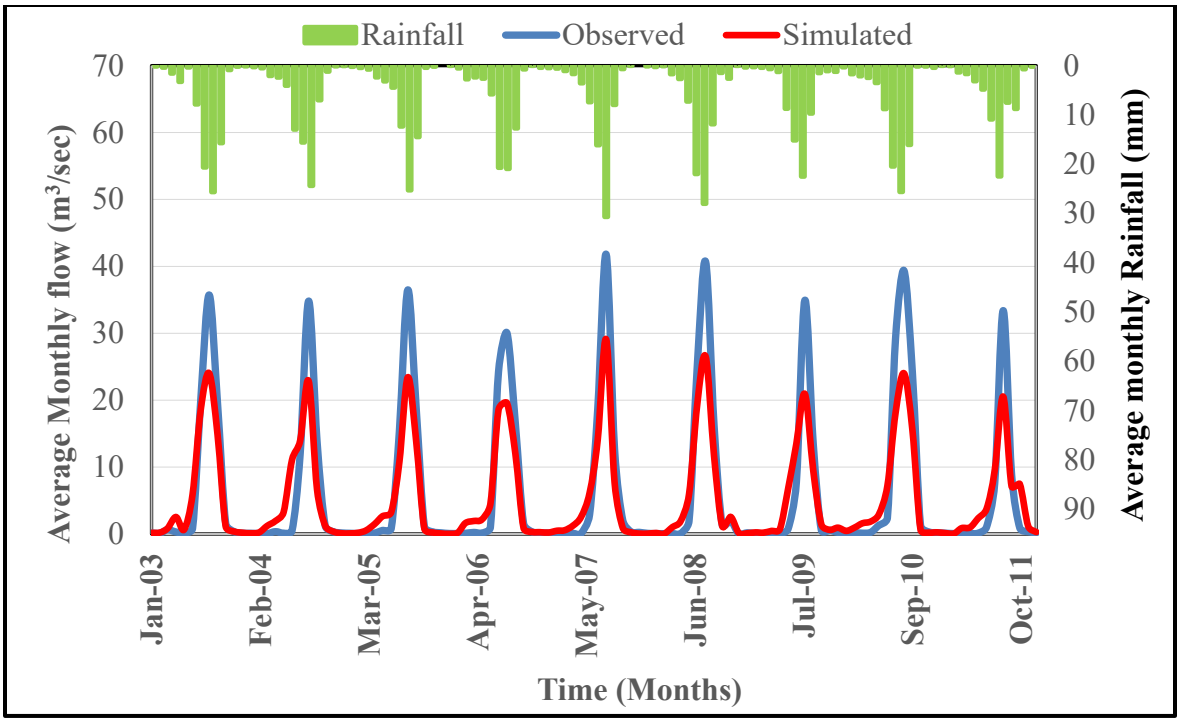

Figure 25: Average Monthly Validate period (2003-2011) for Sibilu River Catchment

4.4.3. Sensitive Analysis of HBV-Light model

The sensitivity analysis of the HBV-Light model was done to calibrate the parameters that are used to determine the influence of the model performance more than the other parameters. These were based on available measured climate and stream flow data, which aim to reduce the uncertainty, expected in future predictions. Thus, sensitivity analyses were done for the soil moisture routine, response, and routing routines. Accordingly, some parameters are found to be highly sensitive, some are low, and the rest are non-sensitive, which means the model efficiency will be constant whether the parameter value has been increased or decreased. Therefore, analysis was done by increasing and decreasing the final calibration values by $\pm 5\%, \pm 10\%, \pm 15\%, \pm 20\%, and \pm 25\%$ the result were plotted in a graph as shown in figure 26 below. From the sensitivity analysis, the triangular weighing function (MAXBAS) was the most sensitive of the calibration parameters, followed by K0, BETA, LP, and K1 in the order. Whereas, FC and maximum flow from upper to lower GW-box (PERC) show low sensitivity parameters to the model performance and lastly, Threshold parameter (UZL) and recession coefficient (K2) show non-significant to the model parameters.

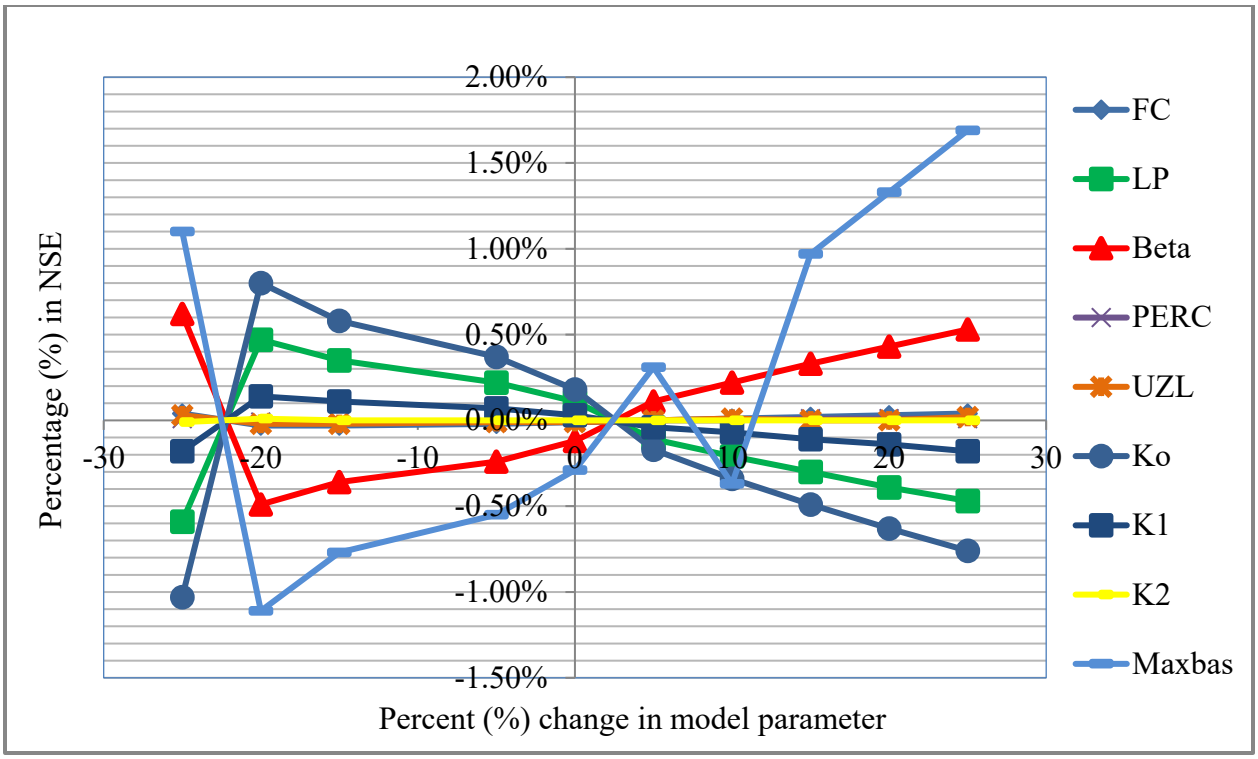

Figure 26: Sensitive of the HBV-Light model parameter

4.4.4. Model Performance Evaluation

Accordingly, the performance of the model is evaluated by the coefficient of determination (R^2) as [113], Nash-Sutcliffe efficiency as [114], and PBIAS as [136] ± 25 with results greater than 0.6 and 0.5 for R^2 and NSE, respectively, meaning that the model has performed satisfactory results as well. The model evaluation, both graphically and statistically, showed a very good agreement between the observed and simulated stream flow. In general, the model is said to be within an acceptable range of performance, and the results can be summarized in Table 10 below. PBIAS values range from +13.43 to +15.07%, which indicates positive values and implies that the model showed underestimation. Overall, the model performed satisfactorily, result falling within the tolerable ranges defined by [107].

Table 11: Summary of model performance for calibration and validation periods

Model	Mean annual flow(m^3/sec)		Performance Evaluation criteria		
HBV-Light model	Observed	Simulated	R^2	NSE	PBIAS
Calibration	1951.73	1689.54	0.91	0.88	13.43
Validation	2285.42	1940.88	0.85	0.77	15.07

4.5. Impact of Climate Change on Water Resource Availability

4.5.1. Projected changes in future flow

The projected change in average annual stream flow for two future period revealed that an increasing trend for both RCP4.5 and RCP8.5 scenarios as compared to the baseline period. Hence, the percentage increment of average annual stream flow is about 5.1% (2031-2060) and 6.3% (2061-2090) for RCP4.5 scenarios, and likely for RCP8.5 scenarios, the increment is about 8.5% (2031-2060) and 10.8% (2061-2090), as shown in figure 27. This result directly corresponded to the increment and reduction in precipitation as well as potential evapotranspiration in the Sibilu river catchment. Consequently, these situations will have an anticipated impact decreasing the stream flow for that season, but there is an increasing trend in stream flow. This result is consistent with the studies in [15] and [116] for the Borkena watershed.

On a monthly basis, the model indicates an increasing and decreasing trend for average total stream flow throughout the future periods for both RCP 4.5 and RCP 8.5 scenarios as compared to the baseline period. In the months of January to June, the average monthly total stream flow increases throughout the future periods for both RCP 4.5 and RCP 8.5 scenarios as compared to the baseline period. The highest interment stream flow was recorded in the month of June. Whereas the decrement stream flow was recorded from July to December. According to Figure 27, there is a monthly increase of up to 0.1% to 65.0% and -50.0% to -86.9% for RCP 4.5 and

also for RCP 8.5 scenarios, a monthly increase up to 2.0% to 61%, and monthly decrease up to -2.7% to -82.4%, respectively.

On a seasonal basis, in kiremt (JJAS) main rainy season, the stream flow for both RCP4.5 and RCP8.5 scenarios revealed a decreasing trend under both future periods. The projected stream flows both future periods tend to decrease by -21.7% and -15.6% for RCP 4.5 and likely for RCP 8.5 -19.7% and -12.7%, respectively. The reason for the overall decreasing trend of stream flow in the Kiremt season over all future periods is mainly due to a decrease in average annual rainfall from June to September for both RCP 4.5and RCP 8.5 scenarios. Additionally, due to the higher increment of projected maximum and minimum temperatures as wells the increasing potential evapotranspiration in the Sibilu river catchment in all future periods. Previous studies have attempted to characterize rainfall and stream flow in different parts of Ethiopia. As a result, the study by [48] in the upper Abbay basin using the HadCM3 model in the Kiremt (JJAS) season is expected to show a larger share in decreased stream flow, with a maximum reduction of -29.68% up to -25.32% in the 2080s for the A2a and B2a scenarios. Similar studies by [122] did work on the Central Rift Valley of Ethiopia using the HadGEM2-ES model, in the Kiremt season, there was a maximum reduction of -10.78%, -17.58%, and -19.23% for the periods of 2020s, 2050s, and 2080s, respectively under RCP8.5 scenarios. Studies by [137] reported that the highest stream flow reduction is seen in the Kiremt season under RCP4.5 and RCP8.5 for the reason of variation in precipitation and temperature changes. Similar studies have been performed on selected catchments of the Abbay basin (Muger sub-basin) by [132] using RegCM3 and reported that there is a reduction in Kiremt season by -1.43 to -16.66% for a period of 2031-2040 and 2090-2100. Furthermore, findings by [138] revealed that there will be a decline in both rainfall and stream flow in the wet season and an increase in the dry season in the Upper Awash River Basin.

In Belg (FMAM) second rainy season, the percentage of projected change in stream flow shows the increment in all scenarios under RCP8.5 (2050s) for future periods. In the near term (2050), the projected stream flow revealed an increment of 3.0% and 9.5% under the RCP4.5 and RCP8.5 scenarios, respectively. While, for the long-term (2080s), the stream flow increases by 5.2% and 13.6% under RCP 4.5 and RCP 8.5, respectively as compared to the baseline period. Similarly, in Bega (ONDJ), which is the dry season, the projected change in stream flow

indicates an increasing trend of 8.3% and 9.4% under RCP 4.5 and RCP 8.5 scenarios for the near-term (2050) future periods, respectively. Whereas, for the long-term (2080) future periods the stream flow is decreasing by 7.3% with a slight increment of 10.0% under RCP 4.5 and RCP 8.5 scenarios, respectively as compared to the baseline period. For a long-term (2080 future periods, the Belg and Bega seasons are expected to show a larger share of increased stream flow than the Kiremt season for both RCP 4.5 and RCP 8.5 scenarios.

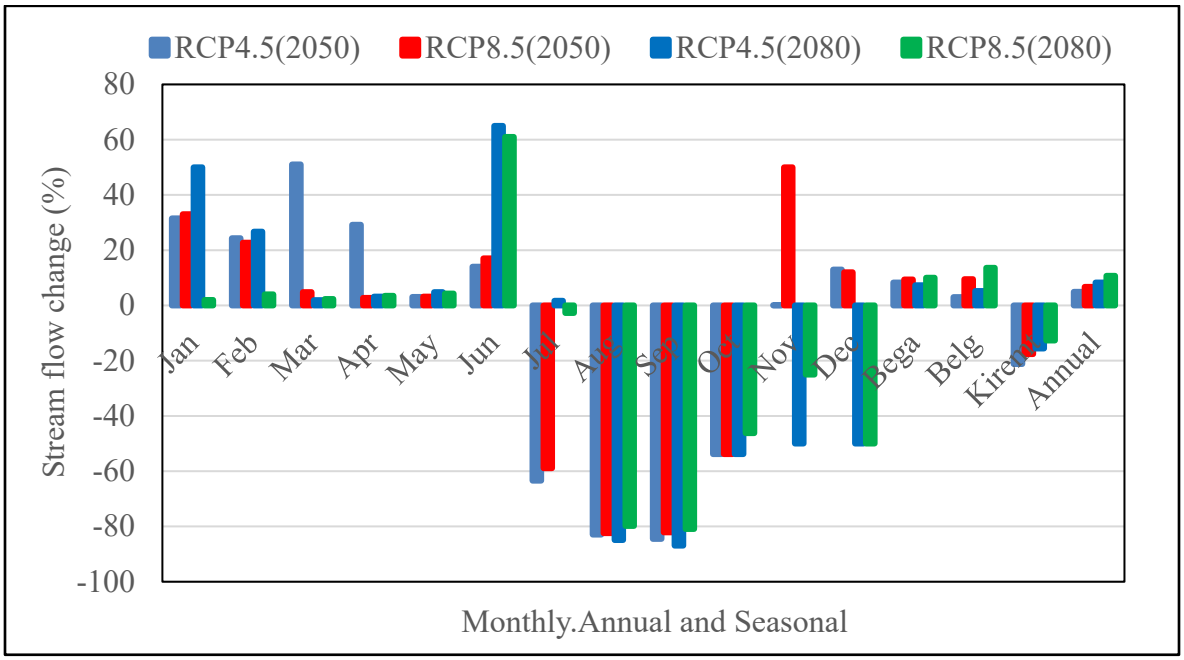

Figure 27: Percentage change in monthly, annual, and seasonal stream flow of Sibilu River catchment under both near-term and long-term from the baseline period.

4.5.2. Projected changes in future water availability

After equation (40) has been used to compute the water availability in the baseline period and future scenarios, the difference in water availability between the RCP 4.5 and RCP 8.5 scenarios for the two future periods has been used to estimate the change in water availability.

$$P - ET = Q \qquad (40)$$

Average water availability under the future periods of the 2050s and RCP 4.5 scenarios shows an increasing and decreasing trend over the Sibilu river catchment. The increment ranges from 0.1 to 7.5 mm, with the highest increase in February. Likewise, the decrement ranges from -1.5 to -

8.9 mm, with the highest decrease in the month of August. For the future periods of the 2080s and the same scenarios, water availability will increase by between 0.1 to 10.0 mm, with the highest rise in the month of June. The highest decrement occurred between -0.3 and -8.7 mm in the month of August. Similarly, for 2050s future time periods and RCP8.5 scenarios, the water availability shows an increasing and decreasing trend over the Sibilu river catchment. The increment ranges from 0.1 to 7.4 mm with the highest increase in the month of February, and the highest decrease ranged from -0.3 to -.8.8 mm in the month of August. Lastly, for 2080s future time periods under RCP8.5 scenarios, the highest increment ranged from 0.2 to 8.9 mm in month of June. The highest decrement ranges from -0.4 to -8.5 mm in the month of August.

As the result revealed under scenarios and future periods, the water availability of the Sibilu River catchment decreased during the rainy season, and hence there is a need for reduced future water availability, which is a great concern in the future, and a mitigation measurement was needed against the impact of climate change. A RCP 8.5 scenario is the worst for indication of warming the atmosphere, which has an impact on the catchment's water resource availability, in a sense. The simulated average annual water balance from baseline period and future periods change scenarios are portrayed in Table 12.

Table 12: Average simulated annual water balance for observed and future time period changes for RCP 4.5 and RCP 8.5 scenarios in the Sibilu River catchment.

Observed	P(mm)	Q(mm)	AET (mm)	PET (mm)	P (%)	Q (%)	AET (%)	PET (%)
Calibration(1985-2002)	1057.8	935.9	121.6	640.9	0	0	0	0
Future period RCP4.5								
2050s (2031-2060)	1062.2	872.3	188	938.8	0.4	-6.8	54.6	46.5
2080s (2061-2090)	817.5	704.1	113.2	693.7	-22.7	-24.8	-6.9	8.2
Future period RCP8.5								
2050s (2031-2060)	1055.0	901.5	152.9	681.7	-0.3	-3.7	25.7	6.4
2080s (2061-2090)	823.4	704.5	118.5	712.3	-22.2	-24.7	-2.5	11.1

It’s seen from the table that there is a reduction of stream flow in all future periods under RCP scenarios, whereas there is a significant increase of potential evapotranspiration. The reduction of precipitation is correspondingly related to the reduction of stream flow, and vice versa. In this case, a highly significant in potential evapotranspiration was observed in near-term periods under RCP 4.5 scenarios, which is about 46.1%.

The maximum and minimum average annual precipitation for RCP4.5 (2050) was 1062.2mm and 817.5 mm for RCP 4.5 (2080). Similarly, for RCP 8.5, the maximum and minimum average annual precipitations were 1055.0 mm and 823.4 mm under near-term and long-term future periods, respectively. Overall, future precipitation in the long-term period was under a decreasing trend when compared to the near-term for both the RCP 4.5 and RCP 8.5 scenarios. As reported by [139], the overall decrease in stream flow for future periods under RCP scenarios from near-term and long-term periods was potentially attributed the effect of climate change.

5. CONCLUSION AND RECOMMENDATION

5.1. Conclusion

The reduction in water resources is a major concern or threat in the catchment due to climate change impacts both spatially and temporarily, which corresponds to a change in water resource availability. Therefore, the study aims to assess climate change impact analysis on water resource availability in the Sibilu River catchment and changes in rainfall, temperature, water resource availability, and potential evapotranspiration were evaluated.

Accordingly, four stations were selected within and around the catchment on the basis of the length of recorded time series data, data availability, quality, and relative completeness of the data. Thirty (30) years period was taken as a baseline which started form 1985-2014. A CORDEX- Africa time domain were selected and an ensemble of climate model i.e. HadGEM2-ES, CCCma-CanESM2, and Ncc-NorESM-M) of gridded resolution 0.44^0 by 0.44^0 output was used and evaluated under two future scenarios, RCP 4.5 (low emission) and RCP 8.5 (high emission) for two future periods: near-term (2031-2060) and long-term (2061-2090) that were evaluated under one regional climate model (RCA4) and HBV-Light hydrological model. Once data was downscaled, bias correction was done in using power transformation for precipitation, and a linear scale for temperature with CMhyd tool.

Evaluation criteria like PBIAS, correlation coefficient (Correl), and root mean square error (RMSE) was used to check the performance of climate model and comparison was made between simulated and observed mean annual rainfall. Accordingly, the result revealed that there was very good agreement between simulated and observed data during the control period (1985-2005). In some cases, the downscaled mean annual rainfall and temperature in the catchment showed overestimation and underestimation due to uncertainty of climate change. The climate change impact assessment in the Sibilu River catchment showed significant variation in monthly, annual, and seasonal terms as compared to the baseline period. The HBV-Light hydrological model was used to simulate stream flow in the catchment to study the impact of climate change on water resource availability. Three model performance indicators (Nash and Sutcliff Efficiency; (NSE), Coefficient of determination; R^2 and Percentage of Bias) were used to check the performance of the model between observed and simulated. The performance evaluation of

the model confirmed that the daily simulation was in very good agreement with values of NSE = 0.88, R^2 = 0.91, and PBIAS = 13.43% for the calibration period whereas the corresponding values for the validation period NSE = 0.77, R^2 = 0.85, and PBIAS = 15.07%.

As the result indicates, the mean monthly minimum temperature would increase in the range of 1.9 ^{0}C to 2.9 ^{0}C and 2.5 ^{0}C to 4.5 ^{0}C under the RCP 4.5 and RCP 8.5 scenarios for the near-term and long-term from the baseline period, respectively. And also, the mean maximum temperatures were expected increase in the range of 1.9 ^{0}C to 2.8 ^{0}C for RCP 4.5 scenarios and 2.2 ^{0}C to 4.1 ^{0}C for RCP 8.5 scenarios from the baseline period. Overall, the projections of both minimum and maximum temperature from baseline period are higher for RCP 8.5 than RCP 4.5 scenarios.

Overall, it was found that the temperature in the future is expected to increase as it can be seen from the result. In the near-term period, the average mean seasonal maximum and minimum temperature showed a greater warming in the winter in both RCPs, whereas in the long-term period, the spring season experience warmest and the average mean seasonal maximum temperature has shown an increase during the kiremt season in both RCP scenarios. In all cases, the largest increases were observed under RCP8.5 in all future periods.

On a seasonal basis, rainfall shows an increasing and decreasing trend for both RCP scenarios. Similarly, on a monthly basis, there is an increase in some months and a decreasing trend in other months for both RCPs. However, during the main rain season, kiremt (JJAS) indicated a decreased trend, with the highest decrease up to -5.8% (2050) for the RCP 4.5 scenario and -3.7% (2050) for the RCP 8.5 scenario. In contrast, Bega (ONDJ), and Belg (FMAM) seasons showed an increasing trend in both RCPs in the future periods. Similarly, annual rainfall shows an increasing trend for both RCP 4.5 and RCP 8.5 scenarios, with the highest increment of 22.6% for long-term future time under RCP 8.5.

On a monthly basis, the future potential evapotranspiration has shown an increasing and decreasing trend for both RCP 4.5 and RCP 8.5 scenarios as compared to the base period. As a result, the average monthly potential evapotranspiration revealed that it increased from July to mid-November with a maximum increase of 22.2% in August and decreasing trend in the month of March to June with a maximum decrease of -3.2% in June. On a seasonal basis, the future potential evapotranspiration indicates an increasing trend through the future periods under both

RCP scenarios. The maximum increment of potential evapotranspiration was observed during the rainy season, reaching 12.7%, 11.9%, and 11.4% for RCP 8.5 under the long-term future periods, followed by Bega and spring compared to base period, respectively.

The predicted change in the mean annual stream revealed that an increasing trend for both RCP scenarios over the future periods, with significant changes in RCP 8.5. On a monthly basis, there is an increasing trend from January to mid-June with a maximum increases up to 65% in June. While, a decreasing trend of average monthly stream flow in the months of July to December with a maximum decrement up to -86.9% in the month of September. Kiremt, which is the rainy season, was found to have a decreasing trend throughout the future time period for both RCP scenarios with the highest decrement up to -21.7% for RCP4.5 (2050) and -19.7% for RCP8.5 (2050), respectively. In contrast, the Bega and spring seasons showed an increasing trend for both RCPs under future periods as compared to base period. In general, a significant reduction in stream flow was observed over the Sibilu river catchment for future periods since climate change had an impact on rainfall with increasing temperatures and potential evapotranspiration during major rain seasons. The findings of this study highlighted that there would be pressure on the reduction of water resource availability in the Sibilu River due to climate change, which would result in a reduction of rainfall during the rainy season, and in turn, increases during the winter season, followed by the Belg (FMAM) season.

Overall, the findings of this study revealed that there is significance variation in rainfall which is differing from previous studies mean that no significance variation in some studies in upper Abbay basin. And also, there were decrement of precipitation and air temperature in some studies. But for this study, there is an increasing of maximum temperature and minimum temperature which were an impact on future water resource. This were turn impact future flow of the Sibilu River.

5.2. Recommendation

This study evaluates climate change's effects on Sibilu River water resource availability and future conditions, offering suggestions for better alternatives and best options.

- This study provides valuable insights into the impact of changing climatic conditions on water resource availability, aiding development planners, decision-makers, and implementing agencies and other participants in planning suitable water management strategies to adapt the climate change effect for extreme events.
- The study uses a single RCM output and two emission scenarios, but it's better to compare results using various RCM outputs and scenarios to explore a wide range of climate change.
- The study area faces challenges in collecting adequate and quality data for stream flow forecasting due to discouraging tasks and questionable quality and availability, requiring attention to reliable data handling.
- As the result of the study revealed that hydroclimatic variables of the catchment are significantly impacted by climate change. For instance, during rainy season (Kiremt) stream flow of the Sibilu River typically decreased. Whereas during Bega, and Belg season it would be increased. Hence, it is important to investigate adaptation options and mitigation measures.
- Future studies should also incorporate the impact of climate change on land use and land cover since for study area use and done only changes in rainfall, maximum and minimum temperatures variables.
- An increase in maximum and minimum temperature for the study area attributed to increase potential evapotranspiration of the Sibilu River and simultaneously reduction of stream flow hence soil and water harvesting structures should be designed and planned in a proper way for implementation into the catchment.
- Lastly, climate science and climate modeling are under continuous improvement that aims to increase climate models reliability and reduce uncertainty. Hence then, climate scenario and climate impact scenario can be redefined in the future.

6. REFERENCES

[1] A. Mackay, *Climate Change 2007: Impacts, Adaptation and Vulnerability. Contribution of Working Group II to the Fourth Assessment Report of the Intergovernmental Panel on Climate Change*, vol. 37, no. 6. 2008. doi: 10.2134/jeq2008.0015br.

[2] D. Reay, C. Sabine, P. Smith, and G. Hymus, *Intergovernmental Panel on Climate Change. Fourth Assessment Report. Geneva, Switzerland: Inter-gov- ernmental Panel on Climate Change. Cambridge; UK: Cambridge University Press; 2007. Available from: www. ipcc.ch.* 2007. doi: 10.1038/446727a.

[3] M. A. Wubneh, T. A. Worku, F. T. Fikadie, T. F. Aman, and M. S. Kifelew, "Climate change impact on Lake Tana water storage, Upper Blue Nile Basin, Ethiopia," *Geocarto Int.*, vol. 37, no. 25, pp. 10278–10300, 2022, doi: 10.1080/10106049.2022.2032397.

[4] M. Azari, H. R. Moradi, B. Saghafian, and M. Faramarzi, "Climate change impacts on streamflow and sediment yield in the North of Iran," *Hydrol. Sci. J.*, vol. 61, no. 1, pp. 123–133, 2016, doi: 10.1080/02626667.2014.967695.

[5] A. K. Shaka, "Assessment of Climate Change Impacts on the Hydrology of Gilgel Abbay Catchment in Lake Tana Basin, Ethiopia," 2008.

[6] M. Nega, "Climate Change Adaptation Strategies in Ethiopia: Major Barriers and Impacts," pp. 1–10, 2022.

[7] R. C. Dorf, "Civil and Environmental Engineering," *CRC Handb. Eng. Tables*, pp. 259–324, 2020, doi: 10.1201/9780203009222-7.

[8] V. Roth, T. Lemann, G. Zeleke, and A. Teklay, "Effects of climate change on water resources in the upper Blue Nile Basin of Ethiopia," *Heliyon*, vol. 4, no. 9, p. e00771, 2018, doi: 10.1016/j.heliyon.2018.e00771.

[9] A. W. Worqlul, Y. D. Taddele, E. K. Ayana, and J. Jeong, "Impact of Climate Change on Streamflow Hydrology in Headwater Catchments of the Upper Blue Nile," 2018, doi: 10.3390/w10020120.

[10] H. S. Ayele, M. H. Li, C. P. Tung, and T. M. Liu, “Impact of climate change on runoff in the Gilgel Abbay watershed, the upper Blue Nile Basin, Ethiopia,” *Water (Switzerland)*, vol. 8, no. 9, 2016, doi: 10.3390/w8090380.

[11] A. Teklay, Y. T. Dile, D. H. Asfaw, H. K. Bayabil, and K. Sisay, “Impacts of Climate and Land Use Change on Hydrological Response in Gumara Watershed, Ethiopia,” *Ecohydrol. Hydrobiol.*, vol. 21, no. 2, pp. 315–332, 2021, doi: 10.1016/j.ecohyd.2020.12.001.

[12] T. Beyene, D. Lettenmaier, L. Angeles, and P. Kabat, “Hydrologic Impacts of Climate Change on the Nile River Basin : Implications of the 2007 IPCC Climate Scenarios,” no. December 2006, pp. 0–46, 2007, doi: 10.1007/s10584-009-9693-0.

[13] A. Basin, E. Abebe, and A. Kebede, “Assessment of Climate Change Impacts on the Water Resources of Megech River,” pp. 141–152, 2017, doi: 10.4236/ojmh.2017.72008.

[14] A. Nasr and M. Bruen, “Detection of trends in the 7-day sustained low-flow time series of Irish rivers,” *Hydrol. Sci. J.*, vol. 62, no. 6, pp. 947–959, 2017, doi: 10.1080/02626667.2016.1266361.

[15] F. F. Abera, S. Arega, and B. H. Gedamu, “Climate Change Induced Precipitation and Temperature Effects on Water Resources: the Case of Borkena Watershed in the Highlands of Wollo, Central Ethiopia,” *Water Conserv. Sci. Eng.*, vol. 5, no. 1–2, pp. 53–66, 2020, doi: 10.1007/s41101-020-00084-8.

[16] Y. B. Dibike and P. Coulibaly, “Hydrologic impact of climate change in the Saguenay watershed: Comparison of downscaling methods and hydrologic models,” *J. Hydrol.*, vol. 307, no. 1–4, pp. 145–163, 2005, doi: 10.1016/j.jhydrol.2004.10.012.

[17] W. S. Lavado Casimiro, D. Labat, J. L. Guyot, and S. Ardoin-Bardin, “Assessment of climate change impacts on the hydrology of the Peruvian Amazon-Andes basin,” *Hydrol. Process.*, vol. 25, no. 24, pp. 3721–3734, 2011, doi: 10.1002/hyp.8097.

[18] W. T. Dibaba, T. A. Demissie, and K. Miegel, “Watershed hydrological response to combined land use/land cover and climate change in highland ethiopia: Finchaa catchment,” *Water (Switzerland)*, vol. 12, no. 6, 2020, doi: 10.3390/w12061801.

[19] J. W. Gutowski *et al.*, "WCRP COordinated Regional Downscaling EXperiment (CORDEX): A diagnostic MIP for CMIP6," *Geosci. Model Dev.*, vol. 9, no. 11, pp. 4087–4095, 2016, doi: 10.5194/gmd-9-4087-2016.

[20] J. Kim *et al.*, "Evaluation of the CORDEX-Africa multi-RCM hindcast: Systematic model errors," *Clim. Dyn.*, vol. 42, no. 5–6, pp. 1189–1202, 2014, doi: 10.1007/s00382-013-1751-7.

[21] R. Laprise *et al.*, "Climate projections over CORDEX Africa domain using the fifth-generation Canadian Regional Climate Model (CRCM5)," *Clim. Dyn.*, vol. 41, no. 11–12, pp. 3219–3246, 2013, doi: 10.1007/s00382-012-1651-2.

[22] K. E. Taylor, R. J. Stouffer, and G. A. Meehl, "An overview of CMIP5 and the experiment design," *Bull. Am. Meteorol. Soc.*, vol. 93, no. 4, pp. 485–498, 2012, doi: 10.1175/BAMS-D-11-00094.1.

[23] F. Giorgi, C. Jones, and G. Asrar, "Addressing climate information needs at the regional level: the CORDEX framework," *... Organ. Bull.*, vol. 58, no. July, pp. 175–183, 2009, [Online]. Available: http://www.euro-cordex.net/uploads/media/Download_01.pdf

[24] E. Gbobaniyi *et al.*, "Climatology, annual cycle and interannual variability of precipitation and temperature in CORDEX simulations over West Africa," *Int. J. Climatol.*, vol. 34, no. 7, pp. 2241–2257, 2014, doi: 10.1002/joc.3834.

[25] L. Hernández-Díaz, R. Laprise, L. Sushama, A. Martynov, K. Winger, and B. Dugas, "Climate simulation over CORDEX Africa domain using the fifth-generation Canadian Regional Climate Model (CRCM5)," *Clim. Dyn.*, vol. 40, no. 5–6, pp. 1415–1433, 2013, doi: 10.1007/s00382-012-1387-z.

[26] D. Jacob *et al.*, "Assessing the transferability of the regional climate model REMO to different coordinated regional climate downscaling experiment (CORDEX) regions," *Atmosphere (Basel).*, vol. 3, no. 1, pp. 181–199, 2012, doi: 10.3390/atmos3010181.

[27] G. Nikulin *et al.*, "Precipitation climatology in an ensemble of CORDEX-Africa regional climate simulations," *J. Clim.*, vol. 25, no. 18, pp. 6057–6078, 2012, doi: 10.1175/JCLI-

D-11-00375.1.

[28] G. J.-Y. You and C. Ringler, “Hydro-economic modeling of climate change impacts in Ethiopia,” *IFPRI Discuss. Pap.*, vol. 960, no. April, 2010, [Online]. Available: http://www.ifpri.org/publication/hydro-economic-modeling-climate-change-impacts-ethiopia

[29] IPCC, *CLIMATE CHANGE 2013 Climate Change 2013*. 2013. [Online]. Available: https://www.researchgate.net/profile/Abha_Chhabra2/publication/271702872_Carbon_and_Other_Biogeochemical_Cycles/links/54cf9ce80cf24601c094a45e/Carbon-and-Other-Biogeochemical-Cycles.pdf

[30] R. H. Moss *et al.*, “The next generation of scenarios for climate change research and assessment,” *Nature*, vol. 463, no. 7282, pp. 747–756, 2010, doi: 10.1038/nature08823.

[31] M. G. Reniu, H. Formayer, and A. Svensson, “Evapotranspiration projections in Austria under different climate change scenarios,” *Inst. Meteorol.*, vol. Master of, no. December, p. 66, 2017.

[32] R. Work, “Summary for Policymakers,” 2000.

[33] H. Santoso, M. Idinoba, and P. Imbach, “Climate Scenarios :”.

[34] D. P. van Vuuren *et al.*, “The representative concentration pathways: An overview,” *Clim. Change*, vol. 109, no. 1, pp. 5–31, 2011, doi: 10.1007/s10584-011-0148-z.

[35] A. M. Thomson *et al.*, “RCP4.5: A pathway for stabilization of radiative forcing by 2100,” *Clim. Change*, vol. 109, no. 1, pp. 77–94, 2011, doi: 10.1007/s10584-011-0151-4.

[36] G. P. Wayne, “Representative Concentration Pathways”.

[37] K. Riahi *et al.*, “RCP 8.5-A scenario of comparatively high greenhouse gas emissions,” *Clim. Change*, vol. 109, no. 1, pp. 33–57, 2011, doi: 10.1007/s10584-011-0149-y.

[38] Y. Tan, S. M. Guzman, Z. Dong, and L. Tan, “Selection of effective GCM bias correction methods and evaluation of hydrological response under future climate scenarios,” *Climate*, vol. 8, no. 10, pp. 1–21, 2020, doi: 10.3390/cli8100108.

[39] M. Luo *et al.*, “Comparing bias correction methods used in downscaling precipitation and temperature from regional climate models: A case study from the Kaidu River Basin in Western China,” *Water (Switzerland)*, vol. 10, no. 8, 2018, doi: 10.3390/w10081046.

[40] C. Teutschbein and J. Seibert, “Bias correction of regional climate model simulations for hydrological climate-change impact studies: Review and evaluation of different methods,” *J. Hydrol.*, vol. 456–457, pp. 12–29, 2012, doi: 10.1016/j.jhydrol.2012.05.052.

[41] N. Groundwater, F. Modeling, T. H. E. Case, O. F. Sibilu, R. Catchment, and A. Basin, “ETHIOPIAN INSTITUTE OF WATER RESOURCES SCHOOL OF GRADUATE STUDIES SUSTAINABLE GROUNDWATER RESOURCE DEVELOPMENT :,” 2021.

[42] P. Evaluation and P. O. Cacthment, “\1 1 •,” no. June 2005.

[43] A. A. Science, “AKAKI-KALITY SUB CITY , ADDISS ABABA By ZEMENE MUCHE A thesis submitted to Addis Ababa science and technology University College of Architecture and Civil Engineering in partial fulfillment of Degree of Masters in Geotechnical Engineering,” 2019.

[44] Tilahun Azagegn, “Groundwater Dynamics in the Left Bank Catchments of the Middle Blue Nile and the Upper Awash River Basins,” *Ph.D. Thesis*, no. December, p. 119, 2014.

[45] T. Submitted, “A Thesis Submitted to the School of Graduate Studies of Jimma University in Partial Fulfillment of the Requirements for the Degree of Masters of Science in Hydraulic Engineering.,” 2020.

[46] R. Etefa, “Addis Ababa University Addis Ababa Institute of Technology,” *Addis Ababa Inst. Technol.*, no. December, p. 50, 2019.

[47] A. Melke, Y. Seleshi, and T. Worku, “Modeling the spatial and temporal availability of water resources potential over Abbay river basin , Ethiopia Journal of Hydrology : Regional Studies Modeling the spatial and temporal availability of water resources potential over Abbay river basin , Ethi,” *J. Hydrol. Reg. Stud.*, vol. 44, no. December, p. 101280, 2022, doi: 10.1016/j.ejrh.2022.101280.

[48] M. H. Daba, “Modelling the Impacts of Climate Change on Surface Runoff in Finchaa

Sub-basin , Ethiopia," vol. 2, no. 1, pp. 14–29, 2018, doi: 10.26855/jsfa.2018.01.002.

[49] T. M. Gemechu *et al.*, "Estimation of hydrological components under current and future climate scenarios in guder catchment, upper Abbay Basin, Ethiopia, using the swat," *Sustain.*, vol. 13, no. 17, 2021, doi: 10.3390/su13179689.

[50] A. Kebede Kassa, "Downscaling Climate Model Outputs for Estimating the Impact of Climate Change on Water Availability over the Baro-Akobo River Basin, Ethiopia," p. 103, 2013.

[51] G. Watershed, "Impacts of Climate and Land Use Change on Hydrological," *Ecohydrol. Hydrobiol.*, no. xxxx, 2020, doi: 10.1016/j.ecohyd.2020.12.001.

[52] H. M. Ibrahim, "School of Civil and Environmental Engineering," 2018.

[53] I. Masih, S. Uhlenbrook, S. Maskey, and M. D. Ahmad, "Regionalization of a conceptual rainfall-runoff model based on similarity of the flow duration curve: A case study from the semi-arid Karkheh basin, Iran," *J. Hydrol.*, vol. 391, no. 1–2, pp. 188–201, 2010, doi: 10.1016/j.jhydrol.2010.07.018.

[54] J. Cunderlik and S. P. Simonovic, "Hydrologic models for inverse climate change impact modeling," *Challenges water Resour. Eng. Chang. world*, no. June, pp. 1–9, 2007.

[55] G. Tesfaye, K. Asfaw, and B. Shimelis, "Evaluation of Climate Change Impacts on the Water Resources of Awata River Watershed," *Genale Dawa Basin South. Ethiop. Acad. Res. J. Agri. Sci. Res*, vol. 7, no. 7, pp. 414–422, 2019, doi: 10.14662/ARJASR2019.124.

[56] P. W. Gassman, M. R. Reyes, C. H. Green, and J. G. Arnold, "T s w a t : h d , a , f r d," vol. 50, no. 4, pp. 1211–1250, 2007.

[57] "S Oil and W Ater a Ssessment T Ool D Ocumentation," 2005.

[58] V. Te Chow, D. R. Maidment, L. W. Mays, and L. W. M. Ven Te Chow, David R. Maidment, "Applied Hydrology Chow 1988.pdf." pp. 1–294, 1988. [Online]. Available: http://ponce.sdsu.edu/Applied_Hydrology_Chow_1988.pdf

[59] Hydrologic Engineering Center, "Hydrologic Modeling System Technical Reference

Manual," *Hydrol. Model. Syst. HEC-HMS Tech. Ref. Man.*, no. March, p. 148, 2000.

[60] "Hydrologic Modeling System Applications Guide," no. March, 2008.

[61] H. Gao, Q. Tang, X. Shi, C. Zhu, T. Bohn, and F. Su, "Water Budget Record from Variable Infiltration Capacity (VIC) Model Algorithm Theoretical Basis Document," *Rapp. - Version 1.2*, no. Vic, p. 57, 2009.

[62] C. Res, K. Jasper, P. Calanca, D. Gyalistras, and J. Fuhrer, "Differential impacts of climate change on the hydrology of two alpine river basins," vol. 26, pp. 113–129, 2004.

[63] O. Rößler and J. Löffler, "Potentials and limitations of modelling spatio-temporal patterns of soil moisture in a high mountain catchment using WaSiM-ETH," *Hydrol. Process.*, vol. 24, no. 15, pp. 2182–2196, 2010, doi: 10.1002/hyp.7663.

[64] "The Impact of El Niño Southern Oscillation Events on Water Resource Availability in Central Sulawesi, Indonesia".

[65] S. Wagner, H. Kunstmann, A. Bárdossy, C. Conrad, and R. R. Colditz, "Water balance estimation of a poorly gauged catchment in West Africa using dynamically downscaled meteorological fields and remote sensing information," vol. 34, pp. 225–235, 2009, doi: 10.1016/j.pce.2008.04.002.

[66] H. Bormann and S. Elfert, "Advances in Geosciences Application of WaSiM-ETH model to Northern German lowland catchments : model performance in relation to catchment characteristics and sensitivity to land use change," pp. 1–10, 2010, doi: 10.5194/adgeo-27-1-2010.

[67] Z. M. Easton, S. B. Awulachew, T. S. Steenhuis, S. A. Habte, B. Zemadim, and Y. Seleshi, "Hydrological processes in the Blue Nile," pp. 84–111.

[68] R. A. Kasei, "Modelling impacts of climate change on water resources in the Volta Basin , West Africa," 2009.

[69] J. Seibert, "HBV light," *HBV Light version 2 User's Man.*, no. November, 2005.

[70] S. Bergström and S. Rapporter, "" Development and Application of a Conceptual Runoff

Model for Scandinavian Catchments Utveckling Och Tillämpning Av En Begreppsmässig Avrinningsmodell För Skandinaviska Nederbördsområden," vol. 7, 1976.

[71] S. Achleitner, M. Rinderer, and R. Kirnbauer, "Hydrological modeling in alpine catchments: Sensing the critical parameters towards an efficient model calibration," *Water Sci. Technol.*, vol. 60, no. 6, pp. 1507–1514, 2009, doi: 10.2166/wst.2009.488.

[72] R. M. Nonki, R. M. Tshimanga, and F. C. Donfack, "Journal of Hydrology : Regional Studies Performance assessment and uncertainty prediction of a daily time-step HBV-Light rainfall-runoff model for the Upper Benue River Basin , Northern Cameroon," vol. 36, no. June, 2021, doi: 10.1016/j.ejrh.2021.100849.

[73] Y. Yira, T. C. Mutsindikwa, A. Y. Bossa, J. Hounkpè, and S. Salack, "Assessing climate change impact on the hydropower potential of the Bamboi catchment (Black Volta, West Africa)," *Proc. Int. Assoc. Hydrol. Sci.*, vol. 384, no. 0123456789, pp. 349–354, 2021, doi: 10.5194/piahs-384-349-2021.

[74] P. Daliya, O. Ljungqvist, M. E. Brindle, and D. N. Lobo, *Guidelines for Guidelines*. 2020. doi: 10.1007/978-3-030-33443-7_3.

[75] A. M. Melesse, W. Abtew, and S. G. Setegn, "Nile River Basin: Ecohydrological challenges, climate change and hydropolitics," *Nile River Basin Ecohydrol. Challenges, Clim. Chang. Hydropolitics*, pp. 1–718, 2013, doi: 10.1007/978-3-319-02720-3.

[76] A. M. Mekonnen, "EVALUATION OF LAND USE PLANNING AND IMPLIMENTATION WITH RESPECT TO ENVIRONMENTAL ISSUES IN SULULTA MSc thesis in Environmental Planning and Landscape Design," 2012.

[77] S. W. Assessment, "Seasonal Weather Assessment," no. July, pp. 0–2, 2016.

[78] NAPA, "Climate change National Adapation Programme of Action of Ethiopia," *Glob. Environ. Facil.*, vol. 2, no. June, p. 96, 2007.

[79] IPCC-TGICA, "General Guidelines on the Use of Scenario Data for climate impact and adaptation assessment," *Finnish Environ. Inst.*, vol. 312, no. June, p. 66, 2007, [Online]. Available: http://www.citeulike.org/group/14742/article/8861417

[80] Gizachew G, “COLLEGE OF DEVELOPMENT STUDIES By : Gizachew Girma Advisor : Tesfaye Zeleke (PhD),” 2019.

[81] O. L. Asikoglu, “Outlier Detection in Extreme Value Series,” vol. 4, no. 5, pp. 7314–7318, 2017.

[82] “No Title,” no. December, 2016.

[83] R. G. Allen, “FAO Irrigation and Drainage Paper Crop by,” no. 56, 2006.

[84] R. G. Anderson and A. N. French, “Crop evapotranspiration,” *Agronomy*, vol. 9, no. 10, 2019, doi: 10.3390/agronomy9100614.

[85] “IMPACT OF CLIMATE CHANGE ON SURFACE WATER,” no. November, 2023.

[86] S. Trzaska and E. Schnarr, “A review of downscaling methods for climate change projections,” *United States Agency Int. Dev. by Tetra Tech ARD*, no. September, pp. 1–42, 2014.

[87] J. D. Pabon, L. O. Mearns, P. Whetton, M. H. King, L. M, and G. F, “Guidelines for Use of Climate Scenarios Developed From Regional Climate Model Experiments . Technical Report,” *Development*, no. JANUARY, p. 39, 2003, [Online]. Available: http://www.researchgate.net/publication/251994345

[88] C. Teutschbein and J. Seibert, “Regional climate models for hydrological impact studies at the catchment scale: A review of recent modeling strategies,” *Geogr. Compass*, vol. 4, no. 7, pp. 834–860, 2010, doi: 10.1111/j.1749-8198.2010.00357.x.

[89] S. M. Yimer, A. Bouanani, N. Kumar, B. Tischbein, and C. Borgemeister, “Assessment of Climate Models Performance and Associated Uncertainties in Rainfall Projection from CORDEX over the Eastern Nile Basin, Ethiopia,” *Climate*, vol. 10, no. 7, 2022, doi: 10.3390/cli10070095.

[90] C. Yoo and E. Cho, “Comparison of GCM precipitation predictions with their RMSEs and pattern correlation coefficients,” *Water (Switzerland)*, vol. 10, no. 1, 2018, doi: 10.3390/w10010028.

[91] R. Knutti, “The end of model democracy?,” *Clim. Change*, vol. 102, no. 3, pp. 395–404, 2010, doi: 10.1007/s10584-010-9800-2.

[92] Kementerian Kesehatan RI, “Profil Kesehatan Indonesia 2015,” vol. 1227, no. July, p. 496, 2018, doi: 10.1002/qj.

[93] C. Teutschbein, F. Wetterhall, and J. Seibert, “Evaluation of different downscaling techniques for hydrological climate-change impact studies at the catchment scale,” *Clim. Dyn.*, vol. 37, no. 9–10, pp. 2087–2105, 2011, doi: 10.1007/s00382-010-0979-8.

[94] H. L. Cloke, F. Wetterhall, Y. He, J. E. Freer, and F. Pappenberger, “Modelling climate impact on floods with ensemble climate projections,” *Q. J. R. Meteorol. Soc.*, vol. 139, no. 671, pp. 282–297, 2013, doi: 10.1002/qj.1998.

[95] H. J. Fowler and M. Ekström, “Multi-model ensemble estimates of climate change impacts on UK seasonal precipitation extremes,” *Int. J. Climatol.*, vol. 29, no. 3, pp. 385–416, 2009, doi: 10.1002/joc.1827.

[96] T. Hadgem, D. Team, N. Bellouin, W. J. Collins, I. D. Culverwell, and P. R. Halloran, “Model Development The HadGEM2 family of Met Office Unified Model climate configurations,” pp. 723–757, 2011, doi: 10.5194/gmd-4-723-2011.

[97] N. C. Swart *et al.*, “The Canadian Earth System Model version 5 (CanESM5 . 0 . 3),” vol. 5, pp. 4823–4873, 2019.

[98] G. Model, D. Hydrology, O. Science, S. Earth, and T. Cryosphere, “The Norwegian Earth System Model , NorESM1-M – Part 1 : Description and basic evaluation of the physical climate,” pp. 687–720, 2013, doi: 10.5194/gmd-6-687-2013.

[99] G. Lenderink, A. Buishand, and W. Van Deursen, “Estimates of future discharges of the river Rhine using two scenario methodologies: Direct versus delta approach,” *Hydrol. Earth Syst. Sci.*, vol. 11, no. 3, pp. 1145–1159, 2007, doi: 10.5194/hess-11-1145-2007.

[100] C. K. Ho, D. B. Stephenson, M. Collins, C. A. T. Ferro, and S. J. Brown, “Calibration strategies a source of additional uncertainty in climate change projections,” *Bull. Am. Meteorol. Soc.*, vol. 93, no. 1, pp. 21–26, 2012, doi: 10.1175/2011BAMS3110.1.

[101] R. Leander and T. A. Buishand, “Resampling of regional climate model output for the simulation of extreme river flows,” *J. Hydrol.*, vol. 332, no. 3–4, pp. 487–496, 2007, doi: 10.1016/j.jhydrol.2006.08.006.

[102] C. Daba Geleta and L. Gobosho, “Climate Change Induced Temperature Prediction and Bias Correction in Finchaa Watershed,” *J. Agric. Environ. Sci*, vol. 18, no. 6, pp. 324–337, 2018, doi: 10.5829/idosi.aejaes.2018.324.337.

[103] “January 2018 haramaya university, haramaya,” no. January, 2018.

[104] A. Van Griensven, A. Francos, and W. Bauwens, “Sensitivity analysis and auto-calibration of an integral dynamic model for river water quality,” *Water Sci. Technol.*, vol. 45, no. 9, pp. 325–332, 2002, doi: 10.2166/wst.2002.0271.

[105] K. L. White and I. Chaubey, “Sensitivity analysis, calibration, and validations for a multisite and multivariable SWAT model,” *J. Am. Water Resour. Assoc.*, vol. 41, no. 5, pp. 1077–1089, 2005, doi: 10.1111/j.1752-1688.2005.tb03786.x.

[106] H. J. Henriksen, L. Troldborg, P. Nyegaard, T. O. Sonnenborg, J. C. Refsgaard, and B. Madsen, “Methodology for construction, calibration and validation of a national hydrological model for Denmark,” *J. Hydrol.*, vol. 280, no. 1–4, pp. 52–71, 2003, doi: 10.1016/S0022-1694(03)00186-0.

[107] D. N. Moriasi, M. W. Gitau, N. Pai, and P. Daggupati, “Hydrologic and water quality models: Performance measures and evaluation criteria,” *Trans. ASABE*, vol. 58, no. 6, pp. 1763–1785, 2015, doi: 10.13031/trans.58.10715.

[108] WMO, “WMO Guidelines on the Calculation of Climate Normals,” *WMO-No. 1203*, no. 1203, p. 29, 2017, [Online]. Available: https://library.wmo.int/doc_num.php?explnum_id=4166

[109] R. L. Wilby and C. W. Dawson, “SDSM 4.2— A decision support tool for th e assessment of regional climate change impacts, User Manual,” *Dep. Geogr. Lancaster Univ. UK*, no. August, pp. 1–94, 2007.

[110] A. G. Mengistu, T. A. Woldesenbet, and Y. T. Dile, “Evaluation of the performance of

bias-corrected CORDEX regional climate models in reproducing Baro–Akobo basin climate," *Theor. Appl. Climatol.*, vol. 144, no. 1–2, pp. 751–767, 2021, doi: 10.1007/s00704-021-03552-w.

[111] M. A. Ayele, T. K. Lohani, K. B. Mirani, M. L. Edamo, and A. T. Ayalew, "Simulating sediment yield by SWAT and optimizing the parameters using SUFI-2 in Bilate river of Lake Abaya in Ethiopia," *World J. Eng.*, vol. 20, no. 4, pp. 681–689, 2023, doi: 10.1108/WJE-07-2021-0449.

[112] M. Goswami, K. M. O'Connor, K. P. Bhattarai, and A. Y. Shamseldin, "Assessing the performance of eight real-time updating models and procedures for the Brosna River," *Hydrol. Earth Syst. Sci.*, vol. 9, no. 4, pp. 394–411, 2005, doi: 10.5194/hess-9-394-2005.

[113] P. Krause, D. P. Boyle, and F. Bäse, "Comparison of different efficiency criteria for hydrological model assessment," *Adv. Geosci.*, vol. 5, pp. 89–97, 2005, doi: 10.5194/adgeo-5-89-2005.

[114] J. E. Nash and J. V Sutcliffe, "River Flow Forecasting Through Conceptual Models - Part I - A Discussion of Principles," *J. Hydrol.*, vol. 10, no. 1970, pp. 282–290, 1970.

[115] D. Peled, V. Pratt, and G. Holzmann, "Report documentation page," pp. 405–405, 1997, doi: 10.1090/dimacs/029/20.

[116] B. Akirso Alehu and S. Gizachew Bitana, *Assess the impacts of climate change on the patterns of rainfall, temperature, and streamow in the Abelti Watershed of Southwestern Ethiopia*. 2021. [Online]. Available: https://doi.org/10.21203/rs.3.rs-1076340/v1

[117] L. Li, W. Li, T. Ballard, G. Sun, and M. Jeuland, "CMIP5 model simulations of Ethiopian Kiremt-season precipitation: current climate and future changes," *Clim. Dyn.*, vol. 46, no. 9–10, pp. 2883–2895, 2016, doi: 10.1007/s00382-015-2737-4.

[118] T. H. Alemseged and R. Tom, "Evaluation of regional climate model simulations of rainfall over the Upper Blue Nile basin," *Atmos. Res.*, vol. 161–162, pp. 57–64, 2015, doi: 10.1016/j.atmosres.2015.03.013.

[119] S. Swain, A. K. Taloor, L. Dhal, S. Sahoo, and N. Al-Ansari, "Impact of climate change

on groundwater hydrology: a comprehensive review and current status of the Indian hydrogeology," *Appl. Water Sci.*, vol. 12, no. 6, pp. 0–25, 2022, doi: 10.1007/s13201-022-01652-0.

[120] S. Westra, L. V. Alexander, and F. W. Zwiers, "Global increasing trends in annual maximum daily precipitation," *J. Clim.*, vol. 26, no. 11, pp. 3904–3918, 2013, doi: 10.1175/JCLI-D-12-00502.1.

[121] S. Tesfaye, A. J. Raj, and G. Geberesamuel, "Assessment of Climate Change Impact on the Hydrology of Geba Catchment , Northern Ethiopia," *Am. J. Environ. Eng.*, vol. 4, no. 2, pp. 25–31, 2014, doi: 10.5923/j.ajee.20140402.02.

[122] T. Abraham, B. Abate, A. Woldemicheal, and A. Muluneh, "Impacts of Climate Change Under CMIP5 RCP Scenarios on the Hydrology of Lake Ziway Catchment, Central Rift Valley of Ethiopia," *J. Environ. Earth Sci.*, vol. 8, no. 7, pp. 81–90, 2018.

[123] A. Of *et al.*, "School of Graduate Studies School of Graduate Studies," *Thesis*, no. August, pp. 1–29, 2019.

[124] M. Gebreyes, K. Tesfaye, and B. Feleke, "Climate change adaptation-disaster risk reduction nexus: case study from Ethiopia," *Int. J. Clim. Chang. Strateg. Manag.*, vol. 9, no. 6, pp. 829–845, 2017, doi: 10.1108/IJCCSM-01-2016-0006.

[125] D. Conway, "From headwater tributaries to international river: Observing and adapting to climate variability and change in the Nile basin," *Glob. Environ. Chang.*, vol. 15, no. 2, pp. 99–114, 2005, doi: 10.1016/j.gloenvcha.2005.01.003.

[126] D. Fenta Mekonnen and M. Disse, "Analyzing the future climate change of Upper Blue Nile River basin using statistical downscaling techniques," *Hydrol. Earth Syst. Sci.*, vol. 22, no. 4, pp. 2391–2408, 2018, doi: 10.5194/hess-22-2391-2018.

[127] H. M. Bekele, "Evaluation of climate change impact on upper blue Nile Basin reservoirs," *Arba Minch Univ.*, p. 109, 2009.

[128] A. Tekle, "Assessment of climate change impact on water availability of bilate watershed, ethiopian rift valley basin," *IEEE AFRICON Conf.*, vol. 2015-Novem, no. 15, pp. 148–

157, 2015, doi: 10.1109/AFRCON.2015.7332041.

[129] D. Conway and E. L. F. Schipper, “Adaptation to climate change in Africa: Challenges and opportunities identified from Ethiopia,” *Glob. Environ. Chang.*, vol. 21, no. 1, pp. 227–237, 2011, doi: 10.1016/j.gloenvcha.2010.07.013.

[130] B. T. Kassie *et al.*, “Climate variability and change in the Central Rift Valley of Ethiopia: Challenges for rainfed crop production,” *J. Agric. Sci.*, vol. 152, no. 1, pp. 58–74, 2014, doi: 10.1017/S0021859612000986.

[131] M. Finaritra, R. Tanteliniaina, and J. Zhai, “Assessment of the Future Impact of Climate Change,” 2021.

[132] “Evaluation of Climate Change impacts on hydrology on selected catchments of Abbay Basin MSc Thesis By Haileyesus Belay June , 2011 Evaluation of Climate Change impacts on hydrology on selected catchments of Abbay Basin By,” 2011.

[133] M. Dawit, B. D. Olika, F. B. Muluneh, O. T. Leta, and M. O. Dinka, “Assessment of surface irrigation potential of the Dhidhessa River Basin, Ethiopia,” *Hydrology*, vol. 7, no. 3, pp. 1–21, 2020, doi: 10.3390/HYDROLOGY7030068.

[134] B. B. Bizuneh, M. A. Moges, B. G. Sinshaw, and M. S. Kerebih, “SWAT and HBV models’ response to streamflow estimation in the upper Blue Nile Basin, Ethiopia,” *Water-Energy Nexus*, vol. 4, pp. 41–53, 2021, doi: 10.1016/j.wen.2021.03.001.

[135] G. S. Takele, G. S. Gebre, A. G. Gebremariam, and A. N. Engida, “Hydrological modeling in the Upper Blue Nile basin using soil and water analysis tool (SWAT),” *Model. Earth Syst. Environ.*, vol. 8, no. 1, pp. 277–292, 2022, doi: 10.1007/s40808-021-01085-9.

[136] H. Yuemei, Z. Xiaoqin, S. Jianguo, and N. Jina, “Conduction between left superior pulmonary vein and left atria and atria fibrillation under cervical vagal trunk stimulation,” *Colomb. Med.*, vol. 39, no. 3, pp. 227–234, 2008.

[137] M. G. Alemu, M. A. Wubneh, and T. A. Worku, “Impact of climate change on hydrological response of Mojo river catchment, Awash river basin, Ethiopia,” *Geocarto*

Int., vol. 0, no. 0, p. 000, 2022, doi: 10.1080/10106049.2022.2152497.

[138] N. C. Emiru *et al.*, “Impact of Climate Change on the Hydrology of the Upper Awash River Basin , Ethiopia,” 2022.

[139] T. G. Gebremicael, Y. A. Mohamed, P. V. Zaag, and E. Y. Hagos, “Temporal and spatial changes of rainfall and streamflow in the Upper Tekezē-Atbara river basin, Ethiopia,” *Hydrol. Earth Syst. Sci.*, vol. 21, no. 4, pp. 2127–2142, 2017, doi: 10.5194/hess-21-2127-2017.

7. APPENDIX

7.1. Appendix Table

Table I. Average annual climate data of observed, RCM bias corrected and bias uncorrected rainfall of Addis Ababa Observatory station.

Month	Jan	Feb	Mar	Apr	May	Jun	Jul	Aug	Sep	Oct	Nov	Dec
Observed	5.5	21.5	66.5	86.6	122.3	160.5	239.4	242.7	191.3	85.6	13.8	9.0
Corr rainfall	8.5	27.5	76.5	96.6	132.3	168.3	247.5	293.7	199.0	95.6	18.8	14.0
Uncorr rainfall	15.9	22.9	61.8	90.5	210.8	288.4	300.3	340.1	240.4	105.0	20.9	15.9

Observed	24.0	25.0	25.2	24.5	25.2	23.4	21.1	21.1	21.8	22.7	23.2	23.3
Corr Tmax	20.9	22.1	21.7	21.0	22.0	19.8	18.2	17.5	18.7	20.2	20.9	22.3
Uncorr Tmax	22.9	24.3	25.2	25.2	25.2	24.7	23.2	23.6	24.1	23.1	21.7	21.7

Observed	9.0	10.9	11.9	12.1	12.8	11.4	11.3	11.4	11.2	11.1	10.6	8.2
Corr Tmin	9.1	10.7	11.7	11.9	12.6	12.1	10.2	11.3	10.7	10.8	9.8	9.7
Uncorr Tmin	9.7	10.6	12.0	12.5	12.1	13.5	13.2	13.4	12.9	11.6	11.0	9.7

Table II. Average Annual climate data of observed, future bias corrected and bias uncorrected of Chanco station

Month	Jan	Feb	Mar	Apr	May	Jun	Jul	Aug	Sep	Oct	Nov	Dec
Observed	6.5	12.8	44.0	52.7	104.0	225.9	417.2	408.3	242.2	43.6	11.2	7.5
Corr rainfall	8.4	14.8	49.0	57.7	110.0	230.9	427.2	410.3	249.2	50.6	17.2	13.5
Uncorr rainfall	14.9	16.0	46.4	62.1	200.3	300.1	493.6	494.1	300.1	85.8	26.0	16.3

Observed	23.2	24.3	24.3	23.6	23.7	22.9	20.1	20.0	20.6	21.0	21.5	21.9
Corr Tmax	24.2	25.0	24.8	24.6	23.9	23.9	21.1	20.6	21.6	21.0	21.9	21.9
Uncorr Tmax	20.3	21.5	22.8	23.0	22.4	21.9	20.3	20.9	20.9	20.8	19.0	19.2

Observed	8.5	9.6	10.0	10.2	10.4	10.7	10.7	10.7	10.2	8.6	8.0	7.8
Corr Tmin	8.5	9.6	11.0	10.9	10.8	11.0	10.9	11.7	11.2	9.6	8.7	8.8
Uncorr Tmin	8.9	9.9	11.9	11.6	11.2	12.8	12.6	12.5	13.0	10.5	10.2	9.9

Table III. Average annual climate data of observed, future bias corrected and bias uncorrected of Entoto station

Month	Jan	Feb	Mar	Apr	May	Jun	Jul	Aug	Sep	Oct	Nov	Dec
Observed	8.3	23.3	49.9	83.0	67.4	142.9	299.1	338.7	186.6	32.2	9.2	3.7
Corr rainfall	9.3	29.3	52.9	88.0	72.4	145.5	316.0	399.4	190.9	39.2	12.2	6.7
Uncorr rainfall	11.9	35.0	46.8	62.7	83.9	166.7	436.0	450.7	202.3	49.9	15.0	10.3

Observed	19.9	20.9	20.8	20.3	20.7	19.1	16.9	16.8	17.4	18.6	19.1	19.5
Corr Tmax	20.9	21.9	20.8	20.9	22.7	19.8	17.9	16.8	17.4	18.6	19.8	19.4
Uncorr Tmax	20.3	21.8	22.3	22.3	22.3	22.9	20.2	20.6	20.8	20.1	18.9	19.1

Observed	6.8	8.8	8.3	9.6	10.0	9.3	8.7	8.7	8.7	8.0	7.2	7.4
Corr Tmin	7.8	9.8	9.3	10.6	10.7	10.3	9.7	9.0	8.9	8.8	8.2	8.4
Uncorr Tmin	9.0	10.9	11.2	11.7	11.8	12.5	12.2	13.0	12.1	10.8	11.0	8.9

Table IV. Average annual climate data of observed, future bias corrected and bias uncorrected of Sululta station

Month	Jan	Feb	Mar	Apr	May	Jun	Jul	Aug	Sep	Oct	Nov	Dec
Observed	8.1	20.2	69.2	75.3	75.1	159.0	284.3	305.3	124.1	27.0	6.8	4.3
Corr rainfall	10.0	27.2	73.2	80.3	81.1	162.1	317.9	360.7	129.9	32.0	10.8	7.3
Uncorr rainfall	13.9	31.0	69.1	76.1	100.1	200.8	436.1	400.3	152.6	39.4	12.6	10.3

Observed	22.6	23.5	23.2	23.2	23.4	21.8	20.4	20.1	20.8	21.4	21.7	22.0
Corr Tmax	22.9	24.0	23.7	23.8	24.0	21.8	20.7	20.8	21.8	21.4	22.0	22.5
Uncorr Tmax	21.3	22.0	22.8	22.7	22.8	22.9	20.3	20.7	20.9	20.9	19.0	19.8

Observed	4.4	5.1	5.2	5.5	5.4	5.5	5.1	5.0	4.8	4.7	3.9	3.9
Corr Tmin	4.9	5.9	6.0	5.8	5.8	5.9	5.7	5.7	5.1	4.9	4.4	4.2
Uncorr Tmin	6.0	6.9	7.1	6.6	7.1	7.4	6.1	7.4	7.0	6.4	5.8	5.8

Table V. predicted Average monthly rainfall for RCP4.5 and RCP8.5 scenarios

Month	Jan	Feb	Mar	Apr	May	Jun	Jul	Aug	Sep	Oct	Nov	Dec
Observed rainfall	0.2	0.6	1.5	2.6	2.9	6.5	11.7	12.1	6.6	1.5	0.5	0.2
RCP4.5 rainfall (2050)	7.0	8.1	6.4	5.7	7.6	5.9	4.7	3.7	1.5	0.6	0.7	3.3
RCP4.5 rainfall (2080)	0.6	1.4	3.5	6.0	10.7	16.7	11.7	3.8	1.1	0.7	0.2	0.1
RCP8.5 rainfall (2050)	7.1	8.0	6.5	5.9	7.3	6.2	5.0	3.8	1.8	0.7	0.8	3.1
RCP8.5 rainfall (2080)	0.9	1.9	3.7	6.4	9.7	15.4	11.8	4.1	1.9	0.9	0.4	0.3

Table VI. : Predicted average monthly potential evapotranspiration

Month	Jan	Feb	Mar	Apr	May	Jun	Jul	Aug	Sep	Oct	Nov	Dec
RCP4.5 (2050)	3.0	0.1	-2.9	0.0	-3.0	0.1	14.8	18.5	20.7	12.9	6.3	0.1
RCP8.5 (2050)	3.0	0.1	-2.9	0.0	-3.0	0.1	14.8	22.2	20.7	12.9	9.4	6.1
RCP4.5 (2080)	12.1	11.7	5.9	3.0	-3.0	-3.2	7.4	14.8	13.8	12.9	12.5	12.1
RCP8.5 (2080)	15.1	11.8	8.8	6.1	0.1	0.1	11.1	18.5	17.2	16.1	15.6	15.2

Table VII. Mean monthly observed discharge (m3/sec) of Sibilu River near Chanco gauged station.

Year	Jan	Feb	Mar	Apr	May	Jun	Jul	Aug	Sep	Oct	Nov	Dec	Annual
1985	0.3	0.7	1.1	1.4	1.9	2.8	13.6	35.3	16.7	2.1	1.0	0.3	77.1
1986	0.2	0.9	1.5	2.6	1.4	3.8	12.8	20.9	8.0	2.7	0.3	0.2	55.3
1987	0.2	0.7	1.3	1.7	2.6	4.6	17.0	24.9	9.5	1.3	0.3	0.2	64.3
1988	0.2	0.4	0.5	0.8	1.8	3.4	14.6	30.8	22.0	3.2	0.6	1.0	79.1
1989	0.1	0.5	1.6	1.8	1.1	3.7	18.7	32.5	12.8	1.5	0.4	0.2	74.9
1990	0.2	0.6	0.5	1.0	1.2	2.8	11.7	30.8	16.2	2.9	0.4	0.2	68.3
1991	0.3	0.5	1.4	1.0	2.8	5.6	10.8	29.9	16.4	2.2	0.4	0.3	71.5
1992	0.2	0.6	0.6	1.2	1.8	2.4	7.6	23.9	14.2	1.3	0.7	0.4	54.9
1993	0.3	0.7	0.3	2.1	1.1	3.5	13.7	29.4	12.8	2.7	0.4	0.2	67.2
1994	0.2	0.1	0.8	1.2	1.9	3.5	12.6	21.8	10.0	0.8	0.4	0.1	53.2
1995	0.2	0.6	0.5	2.5	1.9	4.0	11.7	19.0	7.5	0.7	0.3	0.4	49.4
1996	0.6	0.5	2.1	1.4	1.8	6.3	21.1	31.7	15.6	1.1	0.3	0.3	82.9
1997	0.3	0.2	0.8	1.5	1.9	2.7	10.0	17.7	5.8	1.8	1.2	0.2	44.1
1998	0.3	0.4	0.7	1.3	2.6	4.5	15.8	27.8	13.7	3.4	0.4	0.2	71.1
1999	0.3	0.3	0.7	0.4	1.1	3.9	13.3	26.4	11.7	2.5	0.3	0.1	61.1
2000	0.1	0.1	0.3	1.6	1.7	3.2	10.9	30.7	9.9	1.5	0.8	0.3	61.2
2001	0.2	0.2	2.5	0.8	2.6	4.0	18.8	23.7	10.9	1.7	0.3	0.2	65.8
2002	0.2	0.6	1.6	1.4	0.9	5.1	16.7	23.5	5.2	0.5	0.1	0.5	56.4
2003	0.1	0.1	0.6	0.3	0.1	0.8	19.9	35.7	19.5	1.6	0.4	0.1	79.3
2004	0.1	0.1	0.0	0.4	0.1	0.5	12.0	34.8	13.9	1.3	0.3	0.2	63.6
2005	0.1	0.1	0.1	0.1	0.5	0.8	15.3	36.5	18.8	1.1	0.3	0.2	73.9
2006	0.1	0.1	0.1	0.2	0.2	1.0	24.3	30.0	16.4	1.6	0.3	0.2	74.6
2007	0.1	0.1	0.1	0.1	0.1	2.9	18.7	41.8	12.6	2.1	0.3	0.2	79.2
2008	0.1	0.1	0.1	0.1	0.1	1.9	24.9	40.7	16.3	1.4	2.0	0.1	87.6
2009	0.2	0.1	0.1	0.1	0.1	0.8	7.7	34.9	13.5	0.5	0.6	0.2	58.8
2010	0.2	0.2	0.1	0.3	1.3	2.4	29.3	39.4	24.1	1.3	0.3	0.2	99.0
2011	0.1	0.1	0.1	0.1	0.1	1.1	7.6	33.4	8.9	0.9	0.4	0.2	52.9
Average	**0.2**	**0.4**	**0.7**	**1.0**	**1.3**	**3.0**	**15.2**	**29.9**	**13.4**	**1.7**	**0.5**	**0.2**	**1826.7**

Table VIII. Predicted future Mean monthly stream flow under RCP4.5 and RCP8.5

Month	Jan	Feb	Mar	Apr	May	Jun	Jul	Aug	Sep	Oct	Nov	Dec
RCP4.5(2050)	31.5	24.3	51.0	29.2	3.1	14.0	-63.4	-82.9	-84.5	-53.8	0.1	13.0
RCP8.5(2050)	33.0	22.7	4.8	2.7	3.2	17.0	-58.9	-82.4	-82.1	-53.8	50.0	12.0
RCP4.5(2080)	50.0	26.7	1.9	3.2	4.8	65.0	1.7	-84.9	-86.9	-53.8	-50.0	-50.0
RCP8.5(2080)	2.0	4.0	2.3	3.5	4.3	61.0	-2.7	-79.8	-80.9	-46.2	-25.0	-50.0

Table IX: Grubbs-Beck (G-B) outlier test for Addis Ababa Observatory station rainfall

Year	K= AMP	LnK	Mean of LnK	St.divattion.S LnK
1985	43.2	3.77	3.81	0.18
1986	49.3	3.90	3.81	0.18
1987	56.8	4.04	3.81	0.18
1988	35.5	3.57	3.81	0.18
1989	49.2	3.90	3.81	0.18
1990	39.6	3.68	3.81	0.18
1991	47.3	3.86	3.81	0.18
1992	41.3	3.72	3.81	0.18
1993	57.0	4.04	3.81	0.18
1994	61.9	4.13	3.81	0.18
1995	37.4	3.62	3.81	0.18
1996	46.3	3.84	3.81	0.18
1997	37.6	3.63	3.81	0.18
1998	46.2	3.83	3.81	0.18
1999	46.3	3.84	3.81	0.18
2000	67.0	4.20	3.81	0.18
2001	54.9	4.01	3.81	0.18
2002	51.4	3.94	3.81	0.18
2003	38.9	3.66	3.81	0.18
2004	46.2	3.83	3.81	0.18
2005	42.5	3.75	3.81	0.18
2006	42.8	3.76	3.81	0.18
2007	48.1	3.87	3.81	0.18
2008	46.8	3.85	3.81	0.18
2009	43.3	3.77	3.81	0.18
2010	44.6	3.80	3.81	0.18
2011	41.9	3.74	3.81	0.18
2012	50.4	3.92	3.81	0.18
2013	30.1	3.40	3.81	0.18
2014	33.1	3.50	3.81	0.18

Table X: Grubbs- Beck (G-B) outlier test for Chanco station rainfall

Year	K= AMP	LnK	Mean of LnK	St. deviation LnK
1985	45.3	3.81	3.77	0.36
1986	53.5	3.98	3.77	0.36
1987	43.4	3.77	3.77	0.36
1988	43.3	3.81	3.77	0.36
1989	30.0	3.40	3.77	0.36
1990	14.2	2.65	3.77	0.36
1991	32.4	3.48	3.77	0.36
1992	32.4	3.48	3.77	0.36
1993	55.3	4.01	3.77	0.36
1994	44.5	3.79	3.77	0.36
1995	57.8	4.06	3.77	0.36
1996	66.1	4.19	3.77	0.36
1997	59.4	4.08	3.77	0.36
1998	44.2	3.79	3.77	0.36
1999	43.6	3.77	3.77	0.36
2000	49.5	3.90	3.77	0.36
2001	30.2	3.41	3.77	0.36
2002	44.5	3.80	3.77	0.36
2003	37.5	3.62	3.77	0.36
2004	37.5	3.62	3.77	0.36
2005	59.2	4.08	3.77	0.36
2006	41.5	3.73	3.77	0.36
2007	43.7	3.78	3.77	0.36
2008	35.7	3.58	3.77	0.36
2009	36.5	3.60	3.77	0.36
2010	46.5	3.84	3.77	0.36
2011	65.1	4.18	3.77	0.36
2012	23.0	4.18	3.77	0.36
2013	30.0	3.40	3.77	0.36
2014	35.5	3.57	3.77	0.36

Table XI: Grubbs- Beck (G-B) outlier test for Entoto station rainfall

Year	K= AMP	LnK	Mean of LnK	St. deviation LnK
1985	34.0	3.53	3.80	0.23
1986	65.9	4.19	3.80	0.23
1987	69.4	4.24	3.80	0.23
1988	26.0	3.26	3.80	0.23
1989	41.3	3.72	3.80	0.23
1990	47.3	3.86	3.80	0.23
1991	47.2	3.85	3.80	0.23
1992	43.7	3.78	3.80	0.23
1993	45.1	3.81	3.80	0.23
1994	59.9	4.09	3.80	0.23
1995	48.9	3.89	3.80	0.23
1996	41.3	3.72	3.80	0.23
1997	56.3	4.03	3.80	0.23
1998	39.2	3.67	3.80	0.23
1999	38.7	3.66	3.80	0.23
2000	56.8	4.04	3.80	0.23
2001	66.5	4.20	3.80	0.23
2002	33.4	3.51	3.80	0.23
2003	36.7	3.60	3.80	0.23
2004	38.7	3.66	3.80	0.23
2005	46.5	3.84	3.80	0.23
2006	48.9	3.89	3.80	0.23
2007	33.9	3.52	3.80	0.23
2008	52.0	3.95	3.80	0.23
2009	37.9	3.63	3.80	0.23
2010	47.2	3.85	3.80	0.23
2011	50.1	3.91	3.80	0.23
2012	51.0	3.93	3.80	0.23
2013	31.9	3.46	3.80	0.23
2014	40.6	3.70	3.80	0.23

Table XII: Grubbs- Beck (G-B) outlier test for Sululta station rainfall

Year	K= AMP	LnK	Mean of LnK	St.divattion.S LnK
1985	43.3	3.77	3.73	0.23
1986	54.0	3.99	3.73	0.23
1987	50.2	3.92	3.73	0.23
1988	54.0	3.99	3.73	0.23
1989	25.3	3.23	3.73	0.23
1990	28.5	3.35	3.73	0.23
1991	42.4	3.75	3.73	0.23
1992	28.4	3.35	3.73	0.23
1993	28.0	3.33	3.73	0.23
1994	52.4	3.96	3.73	0.23
1995	34.8	3.55	3.73	0.23
1996	52.3	3.96	3.73	0.23
1997	28.9	3.36	3.73	0.23
1998	41.8	3.73	3.73	0.23
1999	51.5	3.94	3.73	0.23
2000	50.6	3.92	3.73	0.23
2001	51.6	3.94	3.73	0.23
2002	41.0	3.71	3.73	0.23
2003	36.5	3.60	3.73	0.23
2004	35.1	3.56	3.73	0.23
2005	43.1	3.76	3.73	0.23
2006	52.7	3.96	3.73	0.23
2007	50.5	3.92	3.73	0.23
2008	41.0	3.71	3.73	0.23
2009	48.8	3.89	3.73	0.23
2010	46.4	3.84	3.73	0.23
2011	38.8	3.66	3.73	0.23
2012	42.6	3.75	3.73	0.23
2013	37.4	3.62	3.73	0.23
2014	49.2	3.90	3.73	0.23

7.2. Appendix Figure

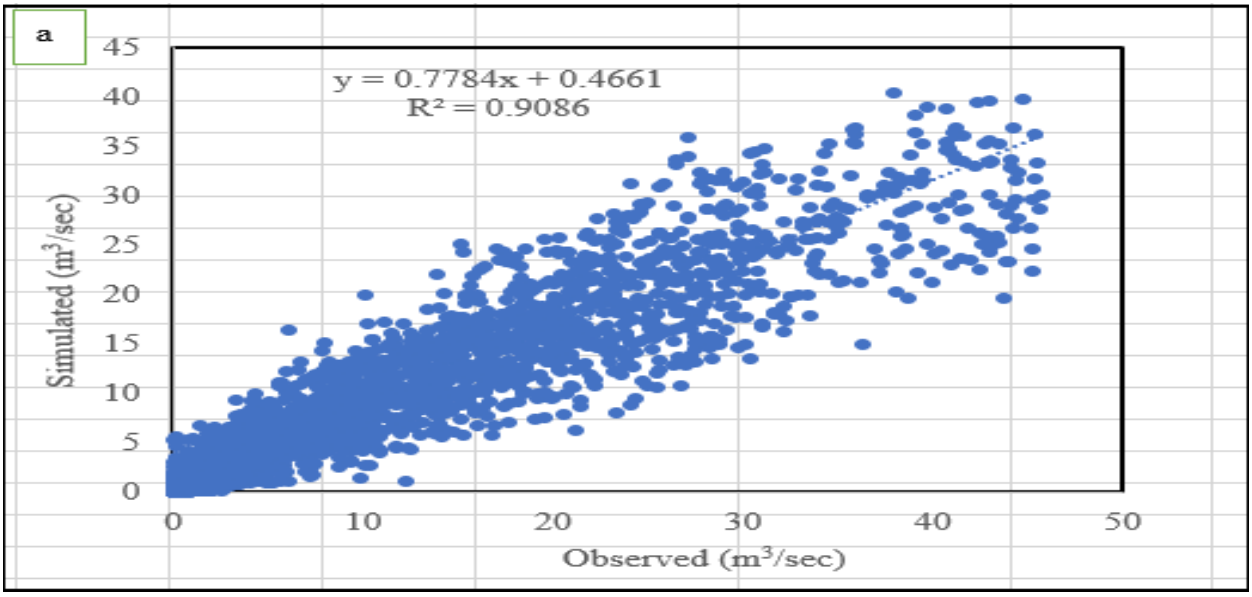

Appendix figure I. Scatter plot of observed and simulated monthly flow for calibration period (1985-2002)

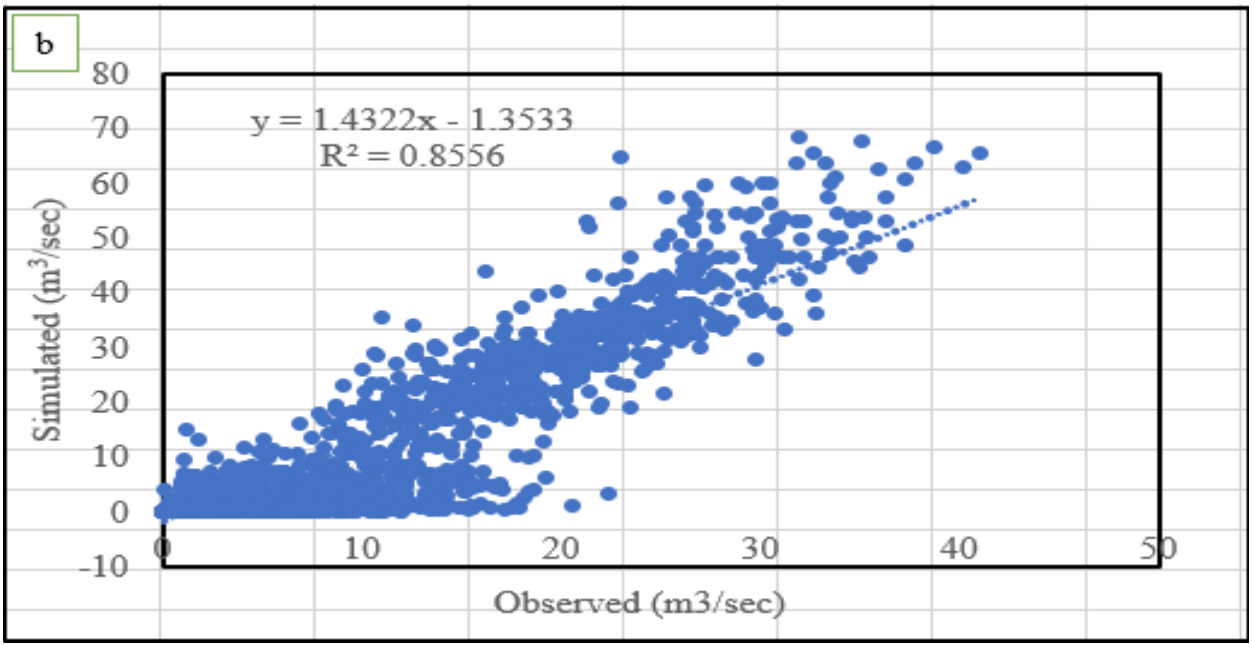

Appendix figure II. Scatter plot of observed and simulated monthly flow for validation period (2003-2011)